A phenomics-based dynamic model of growth and yield to simulate hundreds of maize hybrids in the diversity of European environments

Sébastien Lacube

A phenomics-based dynamic model of growth and yield to simulate hundreds of maize hybrids in the diversity of European environments

---

Un modèle dynamique de croissance et rendement basé sur la phénomique pour simuler la variabilité de centaines d'hybrides de maïs dans la diversité des environnements Européens

Présentée par Sébastien LACUBE
Le 15 Décembre 2017

Sous la direction de François TARDIEU et Boris PARENT

Devant le jury composé de

Franck EWERT	Professor Doctor, University of Bonn	**Rapporteur**
Gustavo A. SLAFER LAGO	Research Professor, Universitat de Lleida	**Rapporteur**
Delphine LUQUET	Chercheur, CIRAD MOntpellier	**Examinateur**
Romain BARILLOT	Chargé de recherche, INRA Lusignan	**Examinateur**
John Roy Porter	Professor Doctor, University of Copenhagen	**Examinateur**
Boris PARENT	Chargé de recherche, INRA Montpellier	**Examinateur,Encadrant**
François TARDIEU	Directeur de recherche, INRA Montpellier	**Directeur de thèse**

UNIVERSITÉ DE MONTPELLIER

Montpellier SupAgro

Résumé

Sous contrainte hydrique, les plantes limitent leur transpiration en diminuant leur croissance foliaire, économisant ainsi l'eau pour la fin du cycle de culture. Une forte variabilité génétique a été observée chez le maïs pour les processus impliqués dans cette réponse. Le compromis entre transpiration et photosynthèse implique qu'une forte plasticité n'est pas toujours avantageuse car elle diminue aussi l'accumulation de biomasse et le rendement. Un génotype qui maximise la production dans un environnement sec n'est donc pas le meilleur dans un autre environnement sec. Le but de cette thèse était de prédire quelles combinaisons de traits reliés à la croissance foliaire aboutissent aux meilleurs rendements dans différents environnements européens. Pour cela, (i) j'ai montré que les contrôles environnementaux et génétiques diffèrent entre l'élongation et l'élargissement foliaires, et établi/testé les équations décrivant ces contrôles. (ii) J'ai développé un modèle de croissance foliaire, en restant parcimonieux en paramètres et en veillant à ce que les paramètres soient mesurables en plateformes de phénotypage. (iii) J'ai développé un cadre de simulation qui inclut 36 ans de conditions climatiques et les pratiques agricoles dans 59 sites de culture du maïs en Europe, ainsi que la paramétré 254 hybrides de maïs qui maximisent la diversité génétique. (iv) Ce cadre d'analyse a été utilisé pour prédire la durée de cycle optimale dans chacun des environnements étudiés, sous les conditions climatiques présentes et futures. (v) J'ai utilisé le cadre de simulation et ces durées de cycle adaptées pour déterminer les meilleurs idéotypes de croissance foliaire adaptés aux différent scenarios environnementaux. Les résultats montrent que les variétés sensibles sont adaptées à l'Europe du sud en condition non-irriguées alors que l'opposé est adapté au nord ou en condition irriguée. Cependant, les meilleures combinaisons de paramètres déterminées dans un espace phénotypique non contraint n'étaient pas disponible dans la diversité génétique observée. Cette thèse fournit aux sélectionneurs des éléments sur les combinaisons de traits qui fournissent un avantage comparatif dans chaque environnement ainsi que le contour des possibles dans la diversité génétique observée.

Mots- clés : croissance foliaire ; maïs (*Zea Mays L.*); modèle de culture APSIM; idéotype; espace phénotypique

Abstract

Under soil water deficit, plants limit transpiration by decreasing leaf area to save water for the end of the crop cycle. A large genetic diversity has been observed in maize for the processes involved in this response. Because of the trade-off between transpiration and photosynthesis, a high plasticity is not always beneficial because it also reduces biomass accumulation and grain yield. The genotype that maximises production in one dry environment therefore does not always perform the best in another dry environment. The aim of this thesis was to predict which combination of trait values related to leaf growth would be beneficial in the diversity of European environments. For this purpose, (i) I have shown that genetic and environmental controls differ between leaf elongation and widening, and established/tested the equations that describe these controls. (ii) I have developed a model of leaf development and expansion, with a particular attention to the parsimony for parameter number and to the possibility of measuring parameter values in phenotyping platforms. (iii) I have developed a simulation framework including 36 years of environmental conditions and management practices of 59 European fields, together with the parameterisation of 254 maize hybrids maximising the maize genetic diversity. (iv) This framework has been used to simulate the optimum crop cycle duration for each site and management practice in current and future conditions. (v) The simulation framework and the adapted cycle duration were then used to determine ideotypes of leaf growth adapted to the different environmental scenarios. Results indicate that sensitive hybrids perform better in southern Europe under rainfed conditions while less-sensitive genotypes perform better in northern Europe or in irrigated fields. However, the best combinations of parameters determined in an unconstrained phenotypic space were not available in the observed genetic diversity. Overall, this study provides elements on where and when a combination of trait values can give a comparative advantage on yield, together with the boundary of possibilities within the current genetic diversity.

Key-words: leaf growth; maize (*Zea Mays L.*); crop model APSIM; ideotype; phenotypic space

Remerciements

Table of contents

Introduction

General context

Maize (*Zea mays L.*) is one of the most important crop worldwide with the 2nd harvested area (1.85 million hectares for a production of more than one billion tons) after wheat and before rice (FAOSTAT, 2014 and 2013[1]). In Europe, it reaches 25% of crop area, 37% of the grain production (FAOSTAT, 2014[1]) and is therefore one of the most important European agricultural products. Maize production is mostly used as feed for livestock, starch production, ethanol production or directly for human consumption. The origins of cultivated maize began around 9000 years ago (7000 BC) in the highlands of Mexico (Tenaillon and Charcosset, 2011) from domestication of a wild grass (téosinte) by native Americans. From there, it spread through the American continent and it is believed that it has been introduced in Europe after Christopher Columbus's first and second trip to the Americas at the end of the 15th century The first maize hybrids were developed around the 1930s, in the context of modern crop breeding that allowed a steady rise of yield over years after that (Tenaillon and Charcosset, 2011). One can still foresee major problems for maize production in a near future. Food demand will largely depend on population rise. Experts estimate an addition of another 3 billion persons in the 2050s to reach 10 billion (UN, 2015[2]). Moreover, the growth in wealth from past developing country such as China should increase meat consumption (Godfray et al., 2010) which will in turn increase the demand for livestock feed such as maize. To meet those future needs, crop production should at least double in the future (Fedoroff et al., 2010). This is in spite of the fact that climate change concerns are rising, with higher temperatures and lower precipitations in summer in southern maize growing areas (Olesen et al., 2011) implying higher risks of yield loss. Finally, policies pressure to decrease water and soil pollution imply that future agriculture would use less agricultural inputs (Tanentzap et al., 2015).

Yield increase will largely depend on the breeding of new cultivars adapted to the diversity of European environments and market requirements (Jeuffroy et al., 2014). Genetic progress and plant breeding focuses on increasing harvested plant production (either grain yield or biomass production for silage). Methods usually involve the selection and breeding of a trait of interest, through conventional or molecular breeding, and experiments to test and select genotypes in contrasted environments to assess their potential effectiveness. Currently, most of the experiments for cultivar selection use networks of field experiments to assess the suitability of a cultivar to target population of environments. In many countries, resulting varieties are then tested for receiving approval in networks of experiments over a few years, thereby considering a small fraction of the climatic variability for each target environment. A new possibility for testing more environments is to use crop modelling and in silico analyses to simulate crop behaviour in a higher number of environmental scenarios (Hammer et al., 2002), for both current and future climatic conditions. This can provide potential pathways of crop improvement by analysing traits giving comparative advantages in contrasted environmental scenarios (Messina et al., 2009). *My thesis aims at providing new elements in this effort.*

Maize is an annual crop and monoecious specie of the *Poaceae* family. It is usually sown in early spring (April or May in the northern hemisphere), to avoid frost early in the plant season (Janda et

---

al., 2003). When environmental conditions are dry, as in southern Europe, and when water is available and economical strategies permit it, maize is usually grown under irrigated conditions. In more humid environments, as in Northern Europe, it is possible to grow maize under rainfed conditions. However, a large proportion of cultivated maize suffers temporal water deficits, and this proportion will likely increase in the future (see above). Leaf growth is impacted by changes in soil water status and evaporative demand (Chenu et al., 2008). When subjected to scarce water resources, plant limit their transpiration via several mechanisms to avoid further water loss. First plant limits transpiration by decreasing leaf area. Second, when plant water status decreases due to evaporative demand or soil water deficit, a combination of hydraulic and chemical signals induces stomatal closure (Tardieu et al., 2015). This leads to decreasing plant transpiration, thereby maintaining leaf water potential at higher values (Tardieu et al., 2000), but in turn reduce photosynthesis and future biomass accumulation. There is therefore a trade-off between biomass accumulation and stress avoidance via limiting transpiration (Tardieu and Tuberosa, 2010). Studies of the sensitivity of leaf growth to soil water status and evaporative demand showed genotype specific responses for these parameters (Salah and Tardieu, 1996; Reymond et al., 2003). The diversity of responses can therefore have opposite effects depending on the drought scenario. For example, sensitive genotypes which strongly decrease leaf expansion under drought can save water for later stages of the crop cycle such as grain filling in case of severe stress, but this strategy is not beneficial in most of environmental scenarios involving milder water deficit because it decreases light interception (Chenu et al., 2009). The genotype that could maximise production in one environment is therefore not the best one in other environments, highlighting a high genotype by environment interaction on these traits (Tardieu, 2012). An efficient way to tackle with these trade-offs to maximise production is to perform simulations over long temporal series, aiming at predicting, in each studied site, the optimum between water saving and carbon capture via the control of leaf growth. *The main aim of my thesis was to develop a model that tackles the genetic variability of leaf growth and development in response to environmental conditions, thereby allowing the simulation of leaf area, transpiration and biomass accumulation in a range of environmental scenarios.*

Crop models to predict the impact of the genetic variability

According to *Sinclair & Seligman (1995,)* crop models are "computerized simulations of dynamic crop systems". They are mathematical frameworks to simulate the growth and development of the crop and its response to management and environmental factors. Model formalisms were developed to simulate complex and integrative traits such as leaf area, biomass accumulation or water use of the plant. Such formalisms can capture the dynamics of plant growth and development, and its interaction with the environment and management, to bring an integrated perspective of the influence of environment (E), genetics (G), management (M) and their respective interactions (GxExM) on traits of interest (Tardieu, 2003; Hammer et al., 2006).

The first crop models where developed in an academic context. The interest quickly grew and crop management was taken into account to answer specific agronomical requirements with models like GOSSYM *(Whisler et al., 1986)*, CERES (Timsina and Humphreys, 2006), APSIM (Keating et al., 2003) or CROPGRO (Jones et al., 2003). These models were designed for specific crops as opposed to more generic models like STICS (Brisson et al., 1998), EPIC (Kiniry et al., 1995) or CROPSYST (Stöckle et al., 2003). As climate change concerns are rising, crop models have been used to simulate crop development in projected climatic conditions, studying the potential impact of climate change on agriculture in a specific period. While management and environmental responses have been largely studied in the last decades, the genetic part has received less attention. Indeed, because crop models

have been developed for the above uses and not for studying the impact of the genetic variability on yield, most of these models consider plant parameters as being constant for the whole species.

However, a crop model with genetic input could potentially indicate which combination of trait values would be beneficial in such or such environmental scenario. This necessitates combining crop models with genetic parameters and measurements of the genetic variability (Parent and Tardieu, 2014). This is only possible if the models have the capacity to simulate genetic by environment interactions (i.e.: response of plant to specific environmental conditions using genotypic parameters). If the model design is convenient, it can be used to analyse the sensitivity of a given trait to environmental variables by analysing end of season as well as intermediate variables, guiding breeders to investigate on specific processes. *Hoogenboom et al. (2004)* classified crop models in six different levels according to genetic details in crop simulation, from generic models without any reference to species (level 1), to models including gene regulators and metabolites actions on genes (level 6). For example, in the APSIM model, plant species only differ by the shapes and thresholds of their response functions to environmental conditions (Keating et al., 2003). This category of model (including genetic differences defined by cultivar-specific parameters) is situated at the third level in the classification and is the last step before the incorporation of complex genetic ("gene-to-phenotype") parameters into the crop model itself. Parameters of these models can be either generic (the same for all simulated species), species-dependent (different for each specie) or variety/genotype specific (different for all species and genotypes). Different approaches can be used for parameter estimation, either through calibration by using optimisation algorithm on specific environmental scenarios, or by direct measurement. The first approach uses computer simulations to evaluate the set of parameters that minimize the differences between model simulation and measured data (Guérif and Duke, 2000) while the second approach aims at calculating parameters values that (i) describe cultivar specific responses derived from experiments and (ii) are measurable in phenotyping facilities (Parent and Tardieu, 2014).

For decades, measuring genetic parameters on a large number of genotypes was not possible and most models used common parameters within each species and these parameters were most often optimised. The development of phenotyping platform (Tardieu et al., 2017) now allows measuring several traits such as leaf expansion and responses to the environment at high throughput, on hundreds of genotypes. Raw data can then be analysed to define crop or cultivar specific parameters that can be used in crop models. As an example, the phyllochron (reciprocal of the slope of the linear model describing leaf appearance rate as a function of thermal time) is a variable that is easily calculated based on experimental data and that is used in crop model as a base to define leaf area dynamic during the vegetative phase. Because phenotyping platform can be environmentally controlled, they allow the measurements of complex traits describing the plant responses to environmental variables (such as light, evaporative demand or soil water deficit). Measurements and analysis of data from phenotyping platforms can therefore provide the right framework to develop new formalisms linked to measured genetic traits. *In my thesis, we have finally used three categories of parameters: (i) parameters that can be measured/calculated, (ii) parameters that are optimised and (iii) parameters whose values are specific to the specie and not the genotype, and that will stay constant within each species. As a result, an important part of the calibration work was to sort out which parameters belong to each section (measured / optimised / fixed).*

If the model has been developed to include genetic diversity and if parameters are measured for a high number of genotypes and explore the genetic variability of traits of interest, one could simulate plant production of several genotypes in different environmental scenarios. It can be used to determine the best genotype or the best set of parameters that maximises yield in target

environmental conditions. This procedure of exploring the traits of interest and their potential adaptation through crop modelling is called '*ideotyping*' (Casadebaig et al., 2011; Asseng et al., 2014; Rötter et al., 2015) and can indicate potential crop improvements by summarising the traits more suitable in each specific environment (Jeuffroy et al., 2014; Perego et al., 2014).

In this context, the definition of the phenotypic space of parameters (the ensemble of possible combinations of trait values), becomes of great importance if results aim at being used by breeders. Studying correlations between parameter values allows the bounding of the possible parameter combinations, and highlight potential trade-offs between traits (Townsend et al., 2017).While exploring a range of parameter values, this *a priori* information on the phenotypic space can therefore indicate if an ideotype of interest could be attainable by breeding regarding physiological and physical constraints (Yin et al., 2003).

Elements on the vegetative development of maize

The maize cycle is characterized by three main phases, namely the vegetative phase until all leaves have completed their growth, flowering time during which reproductive organs rapidly grow and grain filling during which the ear grows until maturity (Fig. 0.1, A). The development of the root system essentially occurs during the vegetative and flowering periods. In European material in which flowering time is independent of photoperiod, the duration of each of these three phases occurs during a period of time that essentially depends on the temperature of the plant meristems. The latter can be approximated by air temperature, in such a way that each maize line or hybrid can be characterized by the duration of each phase, calculated in time corrected for temperature, named thermal time hereafter (°C d). My thesis essentially involves the vegetative phase.

The vegetative phase consists of a rapid leaf and root growths, which allow maximising intercepted radiation, water capture and biomass production. Leaves are initiated on the meristematic zone at regular intervals of thermal time, resulting in a series of leaves of different ages located at different ranks, with most recent leaves at highest positions on the stem. Because the meristem is hidden by older leaves, leaf initiation cannot be observed directly unless the plant is dissected. Leaves then appear sequentially when their tips become visible above older leaves that are organized as a whorl (Fig. 0.1, B). After floral initiation, leaf initiation ends and male inflorescence develops. Typically, floral initiation on the meristem occurs at the middle of the vegetative phase, when half of the final number of leaves is visible (e.g. 9 visible leaves for a plant that has 18 leaves in total). Internodes then elongate, in such a way that leaves are located at different heights on the stem.

Once a leaf is initiated, tissue expansion and cell division take place in a zone located at the base of the leaf, from its insertion point to few centimetres beyond it (Fig. 0.1 C, Nelissen et al., 2016) so that the appeared part of the leaf is mature and does not grow but is pushed by earlier tissues that expand inside the whorl (Ben-Haj-Salah and Tardieu, 1995). In optimal growth conditions, this expansion can be separated into two phases : (i) a first phase of exponential leaf elongation rate, happening before leaf emergence from the whorl , and (ii) a second, phase characterised by a linear expansion of the leaf with thermal time (Muller et al., 2001). The end of leaf elongation occurs with the ligule appearance, as a small collar at the junction of the leaf sheath and laminae (Stewart and Dwyer, 1994).

The ear is initiated one phyllochron after floral transition, a few leaf ranks above the midsection of the plant. It grows during the second half of the vegetative period, whereas the initiation of ovaries and silks occur during the last phyllochrons before male flowering (Anthesis). The latter occurs one to

two phyllochrons after appearance of the last leaf. Female flowering (silking) occurs a few days later, with a anthesis silking interval (ASI) that has a major impact on abortion rate (Bolanos and Edmeades, 1996). ASI tends to increase with water deficit, and has tended to decrease with generations of selection (Bolanos and Edmeades, 1996). Hybrids released in the 1970s had an ASI of typically 5-8 days, whereas modern hybrids present nearly synchronous anthesis and silking. The number of grains on an ear is closely related to the amount of biomass accumulated by the plant (plant growth rate) around flowering (Andrade et al., 1999), and the type and intensity of stresses encountered by the crop around and before flowering. Abortion rate is closely related to the timing and rate of silk growth (Oury et al., 2016).
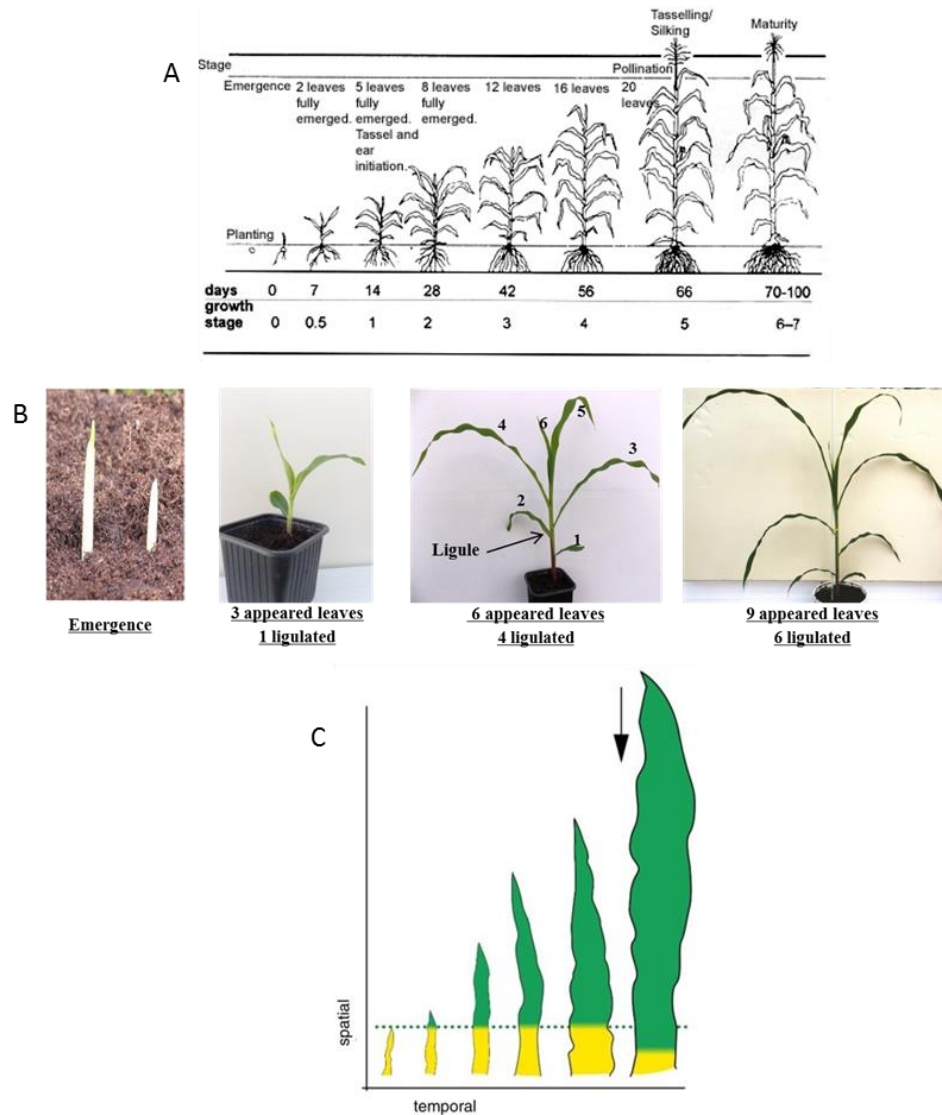
Figure 0.1: Phenological stages and leaf elongation in maize.
(A)   Phenological stages as divided into a vegetative, reproductive and grain filling phase until maturity (Clarrie Beckingham, 2007) Accessible at :
http://www.dpi.nsw.gov.au/agriculture/horticulture/vegetables/commodity-growing-guides/sweet-corn
(B)   Phenological stages during the vegetative phase are based on the observation of appeared and ligulated leaves. Stages are labelled as « stage (n) leaves » counting the number of leaves starting from the lowermost visible.
(C)   Schematic overview of the growth of dicot and monocot leaves. The yellow color indicates the cells that are actively dividing. The arrows indicate the end of the exponential growth (Nelissen et al., 2016)

Overview of the approach used in this thesis

This thesis aims at (i) analysing the genetic variability of leaf growth and of its dynamic responses to environmental condition, (ii) assessing the consequences of the resulting differences in leaf area on yield in environmental scenarios over Europe. The model itself and its parameterisation for a large maize genetic diversity were not available at the beginning of my thesis, so I have used an approach summarised in Figure 0.1.

A module of leaf growth and development for individual leaves was previously developed in APSIM and worked as a proof of concept in Chenu et al., 2008, 2009. However, this module worked only for virtual genotypes with a common number of leaves, with no link with the diversity of phenology and final leaf number. In addition, leaf widening was considered constant for all genotypes and not responding to environmental conditions. Finally, the number of involved parameters was too high to allow their measurement for a large number of genotypes. In the first part of my thesis, I have therefore analysed the responses of leaf elongation and widening to environmental conditions such as light, evaporative demand and soil water deficit (Chapter 1).

This has resulted in a new model of leaf development, leaf expansion and sensitivities to environmental conditions, which can be used for a large number of maize hybrids in many environmental conditions, and for parameters can be measurable in an phenotyping platform such as *PhenoArch* in LEPSE (Phenotyping facilities MP3, INRA-LEPSE, Montpellier, France[3])(Chapter 2).

I then included this module in a framework of simulation for which I have calculated parameter values for 254 maize hybrids previously analysed in the field and in phenotyping platforms (European Project DROPS and national project Amaizing). I have developed tools to simulate these genotypes in sites covering the European area in which maize is grown, for different irrigation scenarios. Other parameters not measured in this thesis (not related to plant growth and development) were either kept constant or optimised based on field experiments carried out in the DROPS project. Management practices (sowing density, fertilisation, etc…), phenology and yield were collected from available databases in order to test and validate the model. This has resulted in a simulation framework of 59 sites covering the European maize growing area, with three watering scenarios, together with the parameterisation of 254 maize hybrids from the DROPS panel (Chapter 3).

Testing genotypes not adapted for cycle duration to each site would result in non-realistic outputs in which yield can be very low due to reasons that are far from those linked to leaf expansion and sensitivities to environmental conditions. Indeed, a genotype whose cycle duration would be too short would flower earlier in the season compared to those grown by farmer in the considered region. Simulated yield would therefore be lower than those observed in farmer's fields in the considered region due to low intercepted radiation. In the same way, a genotype with too long cycle duration would start grain filling in autumn, a situation that is avoided by farmers who choose genotypes early enough to avoid the risks of senescence before the end of grain filling or of the impossibility to harvest because of wet conditions. I have therefore contributed to a study aiming at predicting the best ideotypes for crop cycle duration in present and future conditions, and its impact on yield (Chapter 4). This study used the model and the simulation framework that I have developed.

The first four Chapters of my thesis therefore aimed at developing a framework for the analysis of the impact of the genetic diversity of leaf expansion and development on final yield in various

---

[3] https://www6.montpellier.inra.fr/lepse/M3P/plateforme-PHENOARCH
https://www6.montpellier.inra.fr/lepse/M3P/plateforme-PHENODYN

environmental conditions over Europe, with (i) a model of leaf development and expansion adapted to a large genetic diversity, (ii) the parameterisation for 254 maize hybrids, (iii) a simulation framework of 59 European sites and (iv) an adapted crop cycle duration depending on site and irrigation strategy.

Using these tools, I have simulated in chapter 5 the consequence on yield of the set of parameter values that I observed in the 254 hybrids. A particular effort was made to define the phenotypic space, either taken as non constrained by relationship between parameter values, or constrained as observed in the 254 hybrids. This chapter shows the large impact on yield of the maize genetic diversity on parameters linked to leaf expansion. Ideotypes depended on latitude and environmental conditions and the model was able to simulate observed Genotype by Environment Interactions.
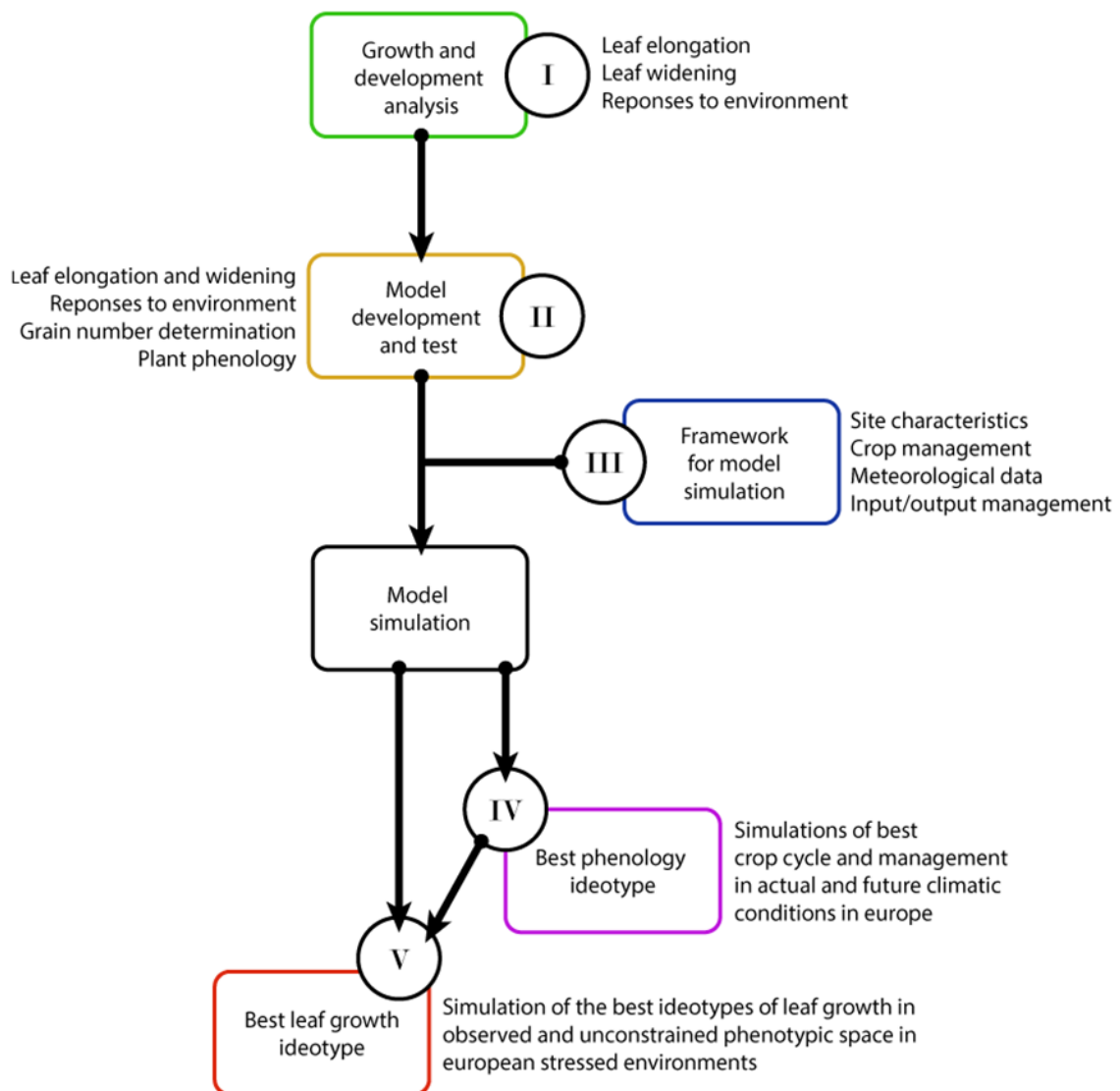
Figure 0.1: Illustration of the approach of the thesis. Roman numbers and colors refer to the five different chapters.

Chapter 1 (Fig. 0.1; I): Distinct controls of leaf widening and elongation by light and evaporative demand in maize

In this chapter, I have studied the dynamic responses of leaf widening and elongation to environmental conditions such as light, evaporative demand and soil water deficit. This work was based on several datasets of dynamics experiments in the field and in phenotyping platform to estimate potential effects of environmental variables on each of the two dimension of leaf expansion. I did not perform all experiments presented in this chapter, but I re-analysed all these datasets. Leaf elongation and widening were studied with contrasted conditions of evaporative demand and light. Results showed that leaf elongation was mostly sensitive to the evaporative demand while leaf widening was mostly sensitive to intercepted radiation. This has led to the development of formalisms that allowed simulation of individual leaf expansion and widening, through phases of leaf development. These formalisms were then used to calculate final leaf dimensions in a network of sites around Europe and compared to available measurements for a reference genotype. Because the model predicted well the final dimensions, I studied datasets of leaf width and length that I measured in the field and in the phenotyping platform PhenoArch for a set of 254 genotypes (DROPS panel) to perform genetic analyses on both variables. Overall, this work showed that leaf widening and elongation had distinct physiological and genetic controls. This chapter resulted in a paper published during my PhD thesis (Lacube et al., 2017).

Chapter 2 (Fig. 0.1; II) : A model of leaf development, leaf expansion and grain number to study the impact of the genetic variability of leaf growth on maize yield in contrasting environmental scenarios.

The second chapter presents the development of a leaf growth module that included formalisms developed in Chapter 1, adapted to a large genetic diversity of final leaf number and crop cycle duration and with parameter easily measurable in phenotyping platforms. The initial APSIM model is based on a canopy growth (big leaf) and only includes a rate of leaf initiation and appearance used for the determination of maximum number of leaf in relation with photoperiod. A first effort has consisted in including individual leaf expansion and responses to environmental conditions, by using experimental data that allowed me to parameterise a model of leaf growth and development, simulating the elongation of the leaf through thermal time and its responses to soil water deficit and evaporative demand. Several problems remained after this step. Phenology and crop cycle duration were common to all genotypes and therefore not adapted to simulate genotypes on a gradient of latitude over Europe. Secondly, leaf widening was constant and results from Chapter 1 had to be included. Finally, the resulting number of parameters was too high and difficult to measure in phenotyping platforms. Therefore, I redesigned most of the formalisms with simplifications based on experimental datasets. Formalisms regarding leaf elongation and widening, developed in Chapter 1, where implemented in the model, and parameters were estimated from several existing experiments for a panel of genotype in the phenotypic platforms PhenoArch and PhenoDyn in LEPSE. The model was tested on measured data over a network of field experiments.

Chapter 3 (Fig. 0.1; III): Simulation framework to study the impact of genetic variability of leaf expansion processes on maize yield over European environmental scenarios.

I needed to develop a framework of simulation, including the development of programming tools to perform large number of simulations in an automatized way with the APSIM model, the parameterisation of sites in Europe, and further minor developments on the model to be able to simulate genotypic variability on plant crop cycle. The development and test of the modelling framework were adapted from previous works of the APSIM Team of Toowoomba (CSIRO, Australia), with whom I have worked in close collaborations during the first years of my PhD period.

Chapter 4 (Fig. 0.1; IV): Future European maize production may be maintained if farmers adapt crop cycle duration.

In order to test he genetic diversity of leaf growth in the 59 sites, I needed an adapted phenology and crop cycle duration for each site and management practice. I have therefore contributed to this work aiming at testing the impact on yield of current and future adaptation of crop cycle duration. In this work, we have estimated the best adapted phenology in the European grid of environments. Simulations were performed on a set of 59 sites across Europe in fully irrigated, rainfed and irrigated conditions, in 36 years of current and future climatic conditions.

Chapter 5 (Fig. 0.1; V): Simulation of leaf growth ideotypes over Europe in water stress conditions.

In chapter 5, the same network of sites was used for the simulation of 254 hybrids of the DROPS panel (parameterised in chapter 2), in the same three water conditions of Chapter 4. The genotypic parameters representing genotypes were the parameters describing leaf potential growth, leaf elongation sensitivity to soil water deficit (linked to sensitivity of leaf growth to vapour pressure deficit), and the sensitivity of leaf widening to plant intercepted radiation. The other genotypic parameters in the model remained constant between genotypes, and the values used where those of the best adapted phenology in each site in fully irrigated conditions defined from Chapter 4. Two approaches were considered. A first approach considered an unconstrained phenotypic space defined by a grid of values considering all combinations of the three considered parameters. A second approach considered sets of observed values in a panel of 254 maize parameterised in Chapter 1,2 and 3. Both approaches resulted in contrasting ideotypes in different drought scenarios, with conservative genotypes resulting in higher yields in southern region under rainfed conditions and genotypes maximising the use of resources showing comparative advantages in northern Europe and in irrigated fields. However, the best combinations of parameters determined in the unconstrained phenotypic space were not available in the observed genetic diversity.

References

Andrade FH, Vega C, Uhart S, Cirilo A, Cantarero M, Valentinuz O (1999) Kernel Number Determination in Maize. Crop Science **39:** 453-459

Asseng S, Ewert F, Martre P, Rötter RP, Lobell DB, Cammarano D, Kimball BA, Ottman MJ, Wall GW, White JW, Reynolds MP, Alderman PD, Prasad PVV, Aggarwal PK, Anothai J, Basso B, Biernath C, Challinor AJ, De Sanctis G, Doltra J, Fereres E, Garcia-Vila M, Gayler S, Hoogenboom G, Hunt LA, Izaurralde RC, Jabloun M, Jones CD, Kersebaum KC, Koehler AK, Müller C, Naresh Kumar S, Nendel C, O'Leary G, Olesen JE, Palosuo T, Priesack E, Eyshi Rezaei E, Ruane AC, Semenov MA, Shcherbak I, Stöckle C, Stratonovitch P, Streck T, Supit I, Tao F, Thorburn PJ, Waha K, Wang E, Wallach D, Wolf J, Zhao Z, Zhu Y (2014) Rising temperatures reduce global wheat production. Nature Climate Change **5:** 143-147

Ben-Haj-Salah H, Tardieu F (1995) Temperature affects expansion rate of maize leaves without change in spatial distribution of cell length (analysis of the coordination between cell division and cell expansion). Plant Physiology **109:** 861-870

Bolanos J, Edmeades G (1996) The importance of the anthesis-silking interval in breeding for drought tolerance in tropical maize. Field Crops Research **48:** 65-80

Brisson N, Mary B, Ripoche D, Jeuffroy MH, Ruget F, Nicoullaud B, Gate P, Devienne-Barret F, Antonioletti R, Durr C, Richard G, Beaudoin N, Recous S, Tayot X, Plenet D, Cellier P, Machet J-M, Meynard JM, Delécolle R (1998) STICS: a generic model for the simulation of crops and their water and nitrogen balances. I. Theory and parameterization applied to wheat and corn. Agronomie **18:** 311-346

Casadebaig P, Guilioni L, Lecoeur J, Christophe A, Champolivier L, Debaeke P (2011) SUNFLO, a model to simulate genotype-specific performance of the sunflower crop in contrasting environments. Agricultural and Forest Meteorology **151:** 163-178

Chenu K, Chapman SC, Hammer GL, McLean G, Salah HB, Tardieu F (2008) Short-term responses of leaf growth rate to water deficit scale up to whole-plant and crop levels: an integrated modelling approach in maize. Plant Cell Environ **31:** 378-391

Fedoroff NV, Battisti DS, Beachy RN, Cooper PJM, Fischhoff DA, Hodges CN, Knauf VC, Lobell D, Mazur BJ, Molden D, Reynolds MP, Ronald PC, Rosegrant MW, Sanchez PA, Vonshak A, Zhu JK (2010) Radically Rethinking Agriculture for the 21st Century. Science (New York, N.Y.) **327:** 833-834

Godfray HCJ, Beddington JR, Crute IR, Haddad L, Lawrence D, Muir JF, Pretty J, Robinson S, Thomas SM, Toulmin C (2010) Food Security: The Challenge of Feeding 9 Billion People. Science **327:** 812-818

Guérif M, Duke CL (2000) Adjustment procedures of a crop model to the site specific characteristics of soil and crop using remote sensing data assimilation. Agriculture, Ecosystems & Environment **81:** 57-69

Hammer G, Cooper M, Tardieu F, Welch S, Walsh B, van Eeuwijk F, Chapman S, Podlich D (2006) Models for navigating biological complexity in breeding improved crop plants. Trends in Plant Science **11:** 587-593

Hammer GL, Kropff MJ, Sinclair TR, Porter JR (2002) Future contributions of crop modelling—from heuristics and supporting decision making to understanding genetic regulation and aiding crop improvement. European Journal of Agronomy **18:** 15-31

Janda T, Szalai G, Rios-Gonzalez K, Veisz O, Páldi E (2003) Comparative study of frost tolerance and antioxidant activity in cereals. Plant Science **164:** 301-306

Jeuffroy M-H, Casadebaig P, Debaeke P, Loyce C, Meynard J-M (2014) Agronomic model uses to predict cultivar performance in various environments and cropping systems. A review. Agronomy for Sustainable Development **34:** 121-137

Jones JW, Hoogenboom G, Porter CH, Boote KJ, Batchelor WD, Hunt LA, Wilkens PW, Singh U, Gijsman AJ, Ritchie JT (2003) The DSSAT cropping system model. European Journal of Agronomy **18:** 235-265

Keating BA, Carberry PS, Hammer GL, Probert ME, Robertson MJ, Holzworth D, Huth NI, Hargreaves JNG, Meinke H, Hochman Z, McLean G, Verburg K, Snow V, Dimes JP, Silburn M, Wang E, Brown S, Bristow KL, Asseng S, Chapman S, McCown RL, Freebairn DM, Smith CJ (2003) An overview of APSIM, a model designed for farming systems simulation. European Journal of Agronomy **18:** 267-288

Kiniry JR, Williams JR, Major DJ, Izaurralde RC, Gassman PW, Morrison M, Bergentine R, Zentner RP (1995) EPIC model parameters for cereal, oilseed, and forage crops in the northern Great Plains region. Canadian Journal of Plant Science **75:** 679-688

Lacube S, Fournier C, Palaffre C, Millet EJ, Tardieu F, Parent B (2017) Distinct controls of leaf widening and elongation by light and evaporative demand in maize. Plant, Cell & Environment**:** n/a-n/a

Messina C, Hammer G, Dong Z, Podlich D, Cooper M (2009) Modelling crop improvement in a GXEXM framework via gene-trail-phenotype relationships.

Muller B, Reymond M, Tardieu F (2001) The elongation rate at the base of a maize leaf shows an invariant pattern during both the steady-state elongation and the establishment of the elongation zone. Journal of Experimental Botany **52:** 1259-1268

Nelissen H, Gonzalez N, Inzé D (2016) Leaf growth in dicots and monocots: so different yet so alike. Current Opinion in Plant Biology **33:** 72-76

Olesen JE, Trnka M, Kersebaum KC, Skjelvåg AO, Seguin B, Peltonen-Sainio P, Rossi F, Kozyra J, Micale F (2011) Impacts and adaptation of European crop production systems to climate change. European Journal of Agronomy **34:** 96-112

Oury V, Caldeira CF, Prodhomme D, Pichon J-P, Gibon Y, Tardieu F, Turc O (2016) Is change in ovary carbon status a cause or a consequence of maize ovary abortion in water deficit during flowering? Plant Physiology

Parent B, Tardieu F (2014) Can current crop models be used in the phenotyping era for predicting the genetic variability of yield of plants subjected to drought or high temperature? J Exp Bot **65:** 6179-6189

Perego A, Sanna M, Giussani A, Chiodini ME, Fumagalli M, Pilu SR, Bindi M, Moriondo M, Acutis M (2014) Designing a high-yielding maize ideotype for a changing climate in Lombardy plain (northern Italy). Sci Total Environ **499:** 497-509

Reymond M, Muller B, Leonardi A, Charcosset A, Tardieu F (2003) Combining quantitative trait Loci analysis and an ecophysiological model to analyze the genetic variability of the responses of maize leaf growth to temperature and water deficit. Plant Physiol **131:** 664-675

Rötter RP, Tao F, Höhn JG, Palosuo T (2015) Use of crop simulation modelling to aid ideotype design of future cereal cultivars. Journal of Experimental Botany **66:** 3463-3476

Salah HBH, Tardieu F (1996) Quantitative analysis of the combined effects of temperature, evaporative demand and light on leaf elongation rate in well-watered field and laboratory-grown maize plants. Journal of Experimental Botany **47:** 1689-1698

Stewart D, Dwyer L (1994) Appearance time, expansion rate and expansion duration for leaves of field-grown maize (Zea mays L.). Canadian Journal of Plant Science **74:** 31-36

Stöckle CO, Donatelli M, Nelson R (2003) CropSyst, a cropping systems simulation model. European Journal of Agronomy **18:** 289-307

Tanentzap AJ, Lamb A, Walker S, Farmer A (2015) Resolving Conflicts between Agriculture and the Natural Environment. PLoS Biology **13:** e1002242

Tardieu F (2003) Virtual plants: modelling as a tool for the genomics of tolerance to water deficit. Trends in Plant Science **8:** 9-14

Tardieu F (2012) Any trait or trait-related allele can confer drought tolerance: just design the right drought scenario. Journal of Experimental Botany **63:** 25-31

Tardieu F, Cabrera-Bosquet L, Pridmore T, Bennett M (2017) Plant Phenomics, From Sensors to Knowledge. Current Biology **27:** R770-R783

Tardieu F, Reymond M, Hamard P, Granier C, Muller B (2000) Spatial distributions of expansion rate, cell division rate and cell size in maize leaves: a synthesis of the effects of soil water status, evaporative demand and temperature. Journal of Experimental Botany **51:** 1505-1514

Tardieu F, Simonneau T, Parent B (2015) Modelling the coordination of the controls of stomatal aperture, transpiration, leaf growth, and abscisic acid: update and extension of the Tardieu–Davies model. Journal of Experimental Botany **66:** 2227-2237

Tardieu F, Tuberosa R (2010) Dissection and modelling of abiotic stress tolerance in plants. Curr Opin Plant Biol **13:** 206-212

Tenaillon MI, Charcosset A (2011) A European perspective on maize history. Comptes Rendus Biologies **334:** 221-228

Timsina J, Humphreys E (2006) Performance of CERES-Rice and CERES-Wheat models in rice–wheat systems: A review. Agricultural Systems **90:** 5-31

Townsend TJ, Roy J, Wilson P, Tucker GA, Sparkes DL (2017) Food and bioenergy: Exploring ideotype traits of a dual-purpose wheat cultivar. Field Crops Research **201:** 210-221

Whisler FD, Acock B, Baker DN, Fye RE, Hodges HF, Lambert JR, Lemmon HE, McKinion JM, Reddy VR (1986) Crop Simulation Models in Agronomic Systems. *In* NC Brady, ed, Advances in Agronomy, Vol 40. Academic Press, pp 141-208

Yin X, Stam P, Kropff MJ, Schapendonk AHCM (2003) Crop Modeling, QTL Mapping, and Their Complementary Role in Plant Breeding Joint contrib. from Plant Res. Int. and the C.T. de Wit Graduate School for Prod. Ecol. and Resour. Conserv. Agronomy Journal **95:** 90-98

Chapter 1: Distinct controls of leaf widening and elongation by light and evaporative demand in maize

The first chapter of this thesis has been published in Plant, Cell & Environment. It aims at studying the environmental effects affecting leaf elongation and widening in maize. For this purpose, I have exploited existing datasets from field and phenotyping platform experiments and dissected the dynamic response of leaf elongation to evaporative demand and leaf widening to light in contrasted environments.

As a result, I have developed formalisms aiming at the simulation of leaf elongation and widening, and have tested it on measurements of leaf width and length performed over a network of fields around Europe. Those formalisms are further described in chapter 2, and used in subsequent chapters for leaf growth simulation.

Distinct controls of leaf widening and elongation by light and evaporative demand in maize

Sebastien Lacube[1], Christian Fournier[1], Carine Palaffre[2], Emilie J. Millet[1], François Tardieu[1] & Boris Parent[1]

[1] INRA, UMR759 LEPSE, F-34060 Montpellier, France

[2] INRA, UE 0394, SMH Maïs, Centre de recherche de Bordeaux Aquitaine, 40390 Saint-Martin-De-Hinx, France

Abstract

Leaf expansion depends on both carbon and water availabilities. In cereals, most of experimental effort has focused on leaf elongation, with essentially hydraulic effects. We have tested if evaporative demand and light could have distinct effects on leaf elongation and widening, and if short term effects could translate into final leaf dimensions. For that, we have monitored leaf widening and elongation in a field experiment with temporary shading, and in a platform experiment with 15-min temporal resolution and contrasting evaporative demands. Leaf widening showed a strong (positive) sensitivity to whole-plant intercepted light and no response to evaporative demand. Leaf elongation was (negatively) sensitive to evaporative demand, without effect of intercepted light *per se*. We have successfully tested resulting equations to predict leaf length and width in an external dataset of 15 field and 6 platform experiments. These effects also applied to a panel of 251 maize hybrids. Leaf length and width presented quantitative trait loci (QTLs) whose allelic effects largely differed between both dimensions but were consistent in the field and the platform, with high QTLxEnvironment interaction. It is therefore worthwhile to identify the genetic and environmental controls of leaf width and leaf length for prediction of plant leaf area.

Introduction

Leaf area affects the amount of light intercepted by plants, but also their transpiration. In case of drought or heat constraints, reducing leaf area reduces photosynthesis but allows plants to save water for later stages of the crop cycle without risking the over-heating that often accompanies stomatal closure (Guilioni *et al.*, 2008). The understanding of genetic and environmental controls of leaf expansion is therefore central for assessing the trade-off between transpiration and carbon assimilation. For example, a comparison of crop models has shown that the quality of yield prediction by crop models is to a large extent linked to the quality of the modelling of plant leaf area (Martre *et al.*, 2015).

Light and water affect leaf expansion in both monocotyledonous and dicotyledonous species. In the latter, in which leaves expand in two dimensions, light and water affect leaf expansion with markedly different periods of sensitivity within a leaf (Granier & Tardieu, 1999a, b). Young expanding leaves are affected by light through carbon starvation, whilst older expanding leaves are more affected by water via hydraulic limitations (Pantin, Simonneau & Muller, 2012, Pantin *et al.*, 2011). In monocotyledonous leaves, which essentially grow in one dimension, leaf elongation responds to soil water deficit, evaporative demand and temperature in maize, wheat and rice (Ben Haj Salah & Tardieu, 1997, Mahdid *et al.*, 2011, Parent *et al.*, 2010). Light has no direct effect on leaf length (Ben Haj Salah & Tardieu, 1996, Bos, Tijani-Eniola & Struik, 2000), whereas it affects leaf width (Bos, Tijani-Eniola & Struik, 2000, Sonohat & Bonhomme, 1998). However, the effect of light on leaf growth of monocotyledons via changes in leaf width has been the object of few studies. For example, entering "leaf elongation" and "leaf widening" in *The Web of Science*® (https://webofknowledge.com/) results in 3203 and 63 hits, respectively.

The hypothesis of separate controls for leaf elongation and widening of monocotyledons leaves is supported by several observations. First, final leaf width and length are largely uncorrelated in bi-parental populations (Wei *et al.*, 2016, Yang C. *et al.*, 2016) resulting in few overlapping QTLs in maize (Tian *et al.*, 2011) and wheat (Yang DL. *et al.*, 2016). Second, leaf elongation and widening occur at different places in the leaf meristematic zone (Maurice, Gastal & Durand, 1997, Muller *et al.*, 2007). Third, environmental variables that control length and width may differ. Differential effects on leaf length and leaf width have been observed in response to plant density in maize (Sonohat & Bonhomme, 1998). Furthermore, leaf width variations have been shown to closely match the decrease in light interception per plant with plant density (Fournier, Andrieu & Sohbi, 2001), whereas leaf length may respond positively or negatively to increased density depending on leaf rank (Song *et al.*, 2016, Sonohat & Bonhomme, 1998). This suggests independent effects of light and water limitations.

The above paragraphs suggest a need for the reassessment of the respective roles of carbon and water supplies on leaf expansion in monocotyledons, by distinguishing their respective effects on leaf elongation and widening. This may have a large impact on (i) the modelling of environmental effects, because the response of leaf expansion would not be the consequence of a unique sensitivity to environmental conditions but the combination of the sensitivities of leaf widening and elongation; (ii) in the simulation of the genetic variability of plant leaf area, because leaf length and width may have distinct genetic controls and their sensitivities to light or water may largely differ independently in panels of genotypes.

In this study, we have first identified, via a specific experiment, the phenological phases during which leaf widening and elongation occur. We have then analysed the dynamic responses of leaf widening and elongation to light and evaporative demand in two experiments. We have finally tested to what extent the equations derived from dynamic analyses allow simulation of leaf length and width in 15 field experiments in Europe and 6 experiments in controlled environment. A genetic analysis performed in 251 maize hybrids in the field and in controlled environment is also presented to support the hypothesis of separate genetic controls for leaf length and width in response to light and evaporative demand.

Material and methods

Calculation of Intercepted radiation in the platform and in the field

In all field experiments, the amount of light intercepted by canopies was simulated by using the crop model APSIM-maize (Hammer *et al.*, 2010) previously parameterised for the genotype B73 (Harrison *et al.*, 2014). Briefly, this model uses the Beer-Lambert approach, calculating intercepted light from the leaf area index and an extinction coefficient. We used for that daily meteorological data, sowing date and sowing density, maintaining optimal water and nitrogen conditions during simulations. The amount of light intercepted by individual plants was then calculated by using plant density.

In platform experiments, the amount of light intercepted by each plant was estimated as in Cabrera-Bosquet *et al.* (2016). Briefly, 3D plant architectures (point cloud with resolution = 0.512 cm^3) were obtained from binarized RBG images with a space carving algorithm (Kutulakos & Seitz, 2000). These 3D plants were used to reconstruct the 3D maize canopy in the platform during the whole experiment. Intercepted light was calculated by using the RATP model (Sinoquet *et al.*, 2001).

Timing of leaf elongation and widening

An experiment was performed in Mauguio (France, near Montpellier, SI Table S1) with the hybrid Déa at a density of 10 plants m^{-2} irrigated twice a week. Incident radiation was measured every 15 minutes (LI-190SB, Li-Cor, Lincoln, USA), together with air humidity and temperature (HMP35A Vaisala Oy, Helsinki, Finlande; SI Table S1 and SI Table S3). Leaf appearance rate was measured in a set of 10 plants by scoring phenological stages every second day over the whole experiment. Destructive plant measurements were carried out on 10 plants every second day. Sampled plants were chosen to represent the median of phenological stage over the whole field. For each plant, width and length of each leaf were measured after plant dissection, thereby allowing measurement of leaves enclosed in the whorl. This was performed with a ruler when leaves were more than 4-mm long, and with image analysis connected to a binocular lens (Bioscan-Optimas V 4.10, Edmonds, WA) otherwise.

Daily mean values of leaf length and maximum width were used to estimate the increase in width and length over time. To compare chronological patterns of leaf width and length on the same scale, data were first normalized by the maximum width or length. A curve was then fitted on time courses with a local regression model ('loess' function in R, − span = 0.6). Thermal time was calculated as in the APSIM model (Hammer *et al.*, 2010).

Dynamic response of leaf elongation rate to environmental conditions

Three plants of the hybrid Déa were grown under well-watered conditions in a soil 40/60% (v/v) of clay and organic compost (SI. Table S1.3), in the greenhouse of the phenotyping platform *PhenoDyn*

(Montpellier, France - *https://www6.montpellier.inra.fr/lepse/M3P* - SI.Table S1.2). The photoperiod was 14 hours day and 10 hours night with additional light used between 7h to 20h when light was below 450 W.m^{-2}. Air temperature oscillated naturally during the day but was kept above 15°C at night and below 28°C during the day (mean value of 20.4 °C), and VPD reached 3.5 kPa in some afternoons (mean value of 0.54 kPa). Air humidity, air temperature (HMP35A Vaisala Oy, Helsinki, Finland) and leaf temperature (thermocouples) were measured every 15 minutes. Leaf elongation rate (LER) was measured every 15 min with rotating displacement transducers (RDTs 60-1045 Full Smart Position Sensor; Spectrol Electronics, Ltd, Wiltshire, England) as in Sadok *et al.* (2007). Plants were maintained at a soil water potential higher than -0.05 MPa via automatic irrigation. LER of leaf 6 was measured from leaf 6 appearance for 4 days (during stable maximum leaf elongation rate) with contrasted leaf-to-air vapour pressure deficit (VPD$_{la}$) defined as the difference between saturation at leaf temperature (estimated as in Millet *et al.,* 2016) and actual vapour pressure in the air. LER was expressed per unit of thermal time at each 15 minute time step, with thermal time calculated as in the APSIM model (Hammer *et al.* 2010). The response of LER of leaf 6 to VPD$_{la}$ was estimated by using LER and VPD$_{la}$ data at the time step of 15 min for the 3 plants from 14h to 17h, i.e. during daily peaks of vapour pressure deficit. Because the relationship was tight (see results), this resulted in an equation relating LER to VPD$_{la}$.

$$LER = a_i - VPD_{la} * b \qquad \text{(Eq. 1.1)}$$

With a_i (mm °Cd^{-1}) the potential leaf elongation rate for the considered leaf rank i in well-watered conditions and low evaporative demand, and b (mm °Cd^{-1} kPa^{-1}) the sensitivity of LER to evaporative demand (leaf-to-air vapour pressure deficit VPD$_{la}$), considered common for all leaf ranks. This equation was fitted on leaf 6 results, thereby allowing estimation of a_6 and b. The potential LER for each leaf (a_i) was inferred from a_6 for each leaf rank i by using relationship of Chenu *et al.* (2008). At each time *t* between beginning and end of leaf elongation, the lamina length of leaf rank i (L_i) was simulated as the cumulated leaf elongation rate at each time step:

$$L_i = \sum_0^t LER_i \qquad \text{(Eq. 1.2)}$$

The final leaf length was calculated at the end of leaf elongation (t = t$_{final}$).

Dynamic responses of leaf length and width to light

An experiment was performed in Grignon (France, near Paris, SI Table S1.1) with the hybrid Déa at a density of 10 plants m^{-2}. The field (deep clay loam) was fully irrigated for the whole experiment. Minimum, maximum temperatures, incident light and VPD were recorded every day. Temperature varied naturally from 0.0°C to 25.2°C with mean value of 8.8°C and VPD reached 2.6 kPa (mean value, 0.5 kPa).Three plots of 10 plants were marked at emergence for identification of phenological stages (leaf tip and ligule appearances) every second day on ten plants per plot before the onset of experimental treatments.

One plot stayed under normal light conditions during the whole experiment ("Light", daily mean value of 16.6 MJ m^{-2}). The second plot was shaded from leaf-6 emergence to the end of the experiment with a horticultural net transmitting 20% of light for all wavelengths in the visible spectrum, placed at 30 cm above plant tops ("Shaded"). The same shading nets were used for the last treatment, alternating light and shade conditions ("Alternated") by placing and removing the nets : shade from leaf 6 to leaf 10 emergence, normal light conditions from leaf 10 to leaf 14 emergence, and shade conditions afterwards. Final individual leaf area and shape were measured for all leaves of all plants at the end of stem growth by image analysis (Sinoquet, Moulia & Bonhomme, 1991).

A position-time model was established to relate each longitudinal position on the leaf to the time when the considered leaf element left the leaf growing zone because it was pushed by younger elements (Ben Haj Salah & Tardieu, 1995, Silk, 1992). Thegrowing zone is located in the first 8 cm beyond the leaf insertion point in maize (Tardieu *et al.*, 2000). Leaf elongation rate was simulated by using Eq. 1.1, for which leaf length was predicted every hour from the beginning to the end of linear leaf elongation (Eq. 1.2). The beginning of leaf linear elongation was calculated as the time when the leaf reached 8 cm, estimated for each leaf as in Chenu *et al.* (2008). A relationship could therefore be established, for each time step, between leaf length and time after beginning of leaf linear elongation. Each longitudinal position along the leaf could therefore be attributed a time after the corresponding leaf element left the leaf growing zone (see Ben Haj Salah & Tardieu, 1995). We could therefore predict at which time the width at any leaf position was produced and identify the environmental conditions at that time, and finally relate these conditions to the width at the corresponding position. This has been performed for leaves 6 to 9 in the three treatments.

At each time after beginning of linear leaf elongation, a ratio was defined for comparing leaf widths produced in the alternated treatment to those in the shade and light treatments.

$$Width\ Ratio = \frac{(W_{alternated} - W_{shade})}{(W_{light} - W_{shade})}$$

(Eq.1.3)

This ratio is equal to 0 when leaf width of plants in the alternated treatment matches that of shaded plants and 1 when it matches that of plants under full-light.

Because we observed a dynamic relationship between leaf widening and whole-plant intercepted light during the period of widening, this resulted in the equation:

$$W = W_{min,i} + k\,R_{int} \hspace{4cm} \text{(Eq. 1.4)}$$

With $W_{min,i}$ the x-intercept (minimum leaf width under low light) or the considered leaf i, and k the sensitivity to intercepted radiation, considered common for all leaves.

External dataset in the platform and the field

Fifteen field experiments were carried out in a West-East transect across Europe and one site in Chile in 2011 to 2013 (DROPS network – Millet *et al.*, 2016, SI. Table S1.1, SI. Table S1.3) with the maize hybrid B73 x UH007 (named 'B73' afterwards). Soil water status was measured every second day and maintained higher than -0.1 MPa by irrigation (SI. Table S1.3). Nitrogen and pesticides application were performed following local practices. Air temperature and humidity, wind speed and incident light were recorded every hour in each experiment. Raw measurements were first converted to common units and compared to local meteorological data to assess the dataset (Millet *et al.* 2016). Vapour pressure deficit was calculated hourly using temperature and humidity, corrected by radiation in low light conditions as in Chenu *et al.* (2008). Environmental conditions are summarised for each experiment in SI. Table S1.3. The network of field experiments showed a large variety of scenarios of temperature, vapour pressure deficit and incident light through the growing season as presented in Millet *et al.* (2016) (detail in SI. Table S1.3). In each of the 15 experiments, the final length (from ligule to leaf tip) and final width (maximum over the leaf) of leaves 8 to 11 were measured in 10 plants per experiment.

Six experiments were carried out in the phenotyping platform *PhenoArch* (Montpellier, France, Cabrera-Bosquet *et al.*, 2016; *https://www6.montpellier.inra.fr/lepse/M3P*) from 2011 to 2016, during different seasons of the year (SI. Table S1.2). Three seeds per pot of the hybrid B73 were sown

at 0.025m depth, and thinned to one plant per pot at three-leaf stage. Plants were grown in 9L PVC pots in a substrate composed of a mixture of clay and organic compost (30/70 volume). Soil water content was maintained at retention capacity in each pot by daily watering (soil water potential of - 0.05MPa). Briefly, the *PhenoArch* platform is equipped with automated weighting and watering stations, imaging stations and environmental sensors. For each plant, 13 RGB images (2056×2454 pixels) were taken every night (one from top and 12 side images with a 30° horizontal rotation). Temperature and VPD_{la} were recorded every 15 min in 8 sites of the greenhouse (SI. Table S3). Incident light was estimated at each individual plant position as in Cabrera-Bosquet *et al.* (2016) from incident light outside the greenhouse and local extinction coefficients. Daily mean temperature in the greenhouse was 18 ± 2 °C (night) and 25 ± 3°C (day), with small differences between experiments. Incident light varied between experiments, with maximum values (7.7 $MJ.m^{-2}.day^{-1}$) was measured in *spring 2016* and lowest in *Autumn 2011* (2.8 $MJ.m^{-2}\ day^{-1}$).

The B73 hybrid was grown in all experiments (from 2 to 3 replicates, SI. Table S1.2), together with other 251 hybrids (Millet *et al.* 2016) (SI.Table S1.2). In each experiment, leaf width was measured on hybrid B73 by image analysis on ligulated leaves from rank 7 to 12 for 2 to 5 plants per experiment (SI. Method S1.1). It was compared to planimeter measurements (LI-3100C Area Meter) in plants of the experiment Spr16 (R^2 = 0.93, not shown).

The dynamic relationships determined previously (Eq.1.1 and Eq.1.4) were tested in this external dataset. We have first tested over the whole dataset the relationships between final dimensions and environmental variables, considering a unique sensitivity to environmental conditions for all leaves. Environmental variables were calculated as the conditions sensed by plants during the growth of each individual leaf. The effect of leaf rank was calculated as the intercept of the relationship for each leaf. The test of the model itself consisted in simulating final leaf dimensions with the equations determined in dynamic experiments (Eq. 1 and Eq. 4) and comparing with observed values.

Genetic analyses

Experiments were performed in the field and in the platform with a panel of 251 maize hybrids (DROPS panel – Millet *et al.* 2016) obtained by crossing 251 dent lines with a common flint parent (UH007). The panel structure is further described in Millet *et al.* (2016). In the field (Saint-Martin de Hinx (France, SI.Table S1), plants were sown on 12th May at a density of 8.5 plants m[-2] with 10 plants of each genotype sown in a row and soil water status maintained at high values by irrigation. Environmental conditions and crop management were collected as above and are summarised in SI.Table S1.3. The leaf length and width of leaves 7 to 10 were measured within 3 days before flowering for three plants per hybrid. Leaf width and length were also measured in the platform experiment on the 251 genotypes (Exp. Spr16) for leaves 7 and 8.

Genotypic means were calculated for each hybrid using a mixed model based on spatial design:

$$y = Z_g \tau_g + Z_c u_c + Z_r u_r + e \tag{Eq. 1.5}$$

where y is the vector of phenotypic observations in a given experiment, τ_g is the vector of fixed genotypic effect, and u_c and u_r are vectors of random column and row effects, which are used to capture linear trends that might exist across rows and columns. The residual error *e* was assumed to follow a zero mean multivariate normal distribution, with covariance determined by autoregressive processes of order one in the row and column direction. Calculations were performed with ASReml-R (Butler *et al.*, 2009). Narrow-sense heritability was estimated with a model assuming additive SNP effects using the R-package *Heritability* (Kruijer *et al.*, 2015).

Lines were genotyped using a 50K Infinium HD Illumina array (Ganal *et al.*, 2011), and a 600K Axiom Affymetrix array (Unterseer *et al.*, 2014). The genetic analysis was performed with the single-environment method (GWAS, Genome Wide Association Study) presented in Millet *et al*. (2016) with FaST-LMM v2.07 (Lippert *et al.*, 2011) on individual traits for each experiment using the single locus mixed model:

$$Y = \mu + X\beta + G + E \tag{Eq. 1.6}$$

where Y is the vector of phenotypic values, μ the overall mean, X is the vector of SNP scores, β is the additive effect, and G and E represent random polygenic and residual effects. The variance-covariance matrix of G was determined by a genetic relatedness (or kinship) matrix, derived from all SNPs except those on the chromosome containing the SNP being tested as described in Millet *et al*. (2016) following the method of Rincent *et al.* (2014). The SNP effects β were estimated by generalized least squares, and their significance (H_0: β = 0) tested with an F-statistic. Candidate SNPs distant less than 0.1 cM were considered as belonging to a common QTL, described via the most significant SNP in the QTL and the interval between all SNPs belonging to the QTL. Co-localisations between QTLs were checked by comparing QTLs intervals and checking for overlap (defined by all SNPs contained in the QTL). Physical positions of significant SNPs were projected on the consensus genetic map for Dent genetic material (Giraud *et al.*, 2014).

Results

Different time courses for leaf elongation and widening.

The time courses of elongation and widening were analysed in a field experiment in which leaves 8 to 11 of ten plants were sampled every second day from leaf initiation to end of elongation, after dissection of the plant whorl. The increase in leaf length, defined as the distance from the leaf insertion point to the tip, was delayed compared to the increase in leaf width (Fig. 1.1). The beginning of rapid elongation (5% of final leaf length) occurred 35°Cd later than the beginning of rapid leaf widening (5% of final leaf width). Cessation of elongation (95% of final length) occurred 39°Cd after cessation of widening. This temporal pattern, presented in Fig. 1.1 for leaf 8, was also observed in leaves 6, 7, 9, 10 and 11 (SI. Fig.S1.1). In analyses presented below, the effects of environmental conditions were therefore tested during the respective periods corresponding to 5-95% of either elongation or widening.
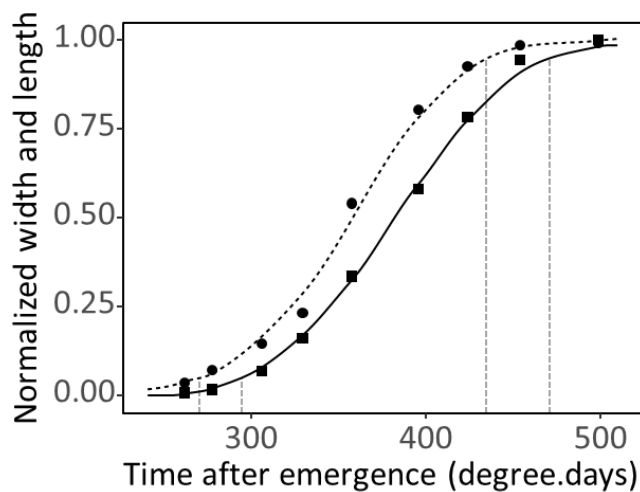
Figure 1.1 : Time courses of widening and elongation of leaf 8. Round and square dots: respectively mean of maximum leaf width and lamina length for 10 plants per date (data are normalized by maximum value). *Dashed and solid lines* are local regressions ("loess" function) for respectively width and length. Grey vertical dotted lines show 5% and 95% thermal time thresholds for each variable.

Leaf width increased with intercepted light with no effect of evaporative demand

Shading largely affected leaf width in a field experiment where plants were grown either under natural light conditions ("Light"), shaded (80% light attenuation from the appearance of leaf-6 tip onwards, "Shaded") or undergoing alternating periods of normal light and shade ("Alternated"), with shading from leaf-6 appearance to leaf-10 appearance and from leaf-14 appearance onwards (Fig.1.2, 1.3). Plants with maximum incident light had wider leaves than those permanently shaded (Fig.1.2c; SI. Fig.1.2). Shading during part of the period of leaf widening (Fig.1.3a) resulted in intermediate values (Fig.1.2c) and suggested a dynamic effect because differences between treatments changed with time (Fig.1.2a). This effect was analysed via a position-time model that allowed associating each longitudinal position on the leaf to a time after beginning of linear elongation. New cells are continuously produced in the 3-cm-long meristem close to the leaf insertion point and flow through the 8-cm-long growing zone to mature zones (Tardieu *et al.*, 2000). One can therefore assign, to each longitudinal position on the leaf (Fig.1.2a), a time after the considered cells have left the elongation zone (Eq. 1.1 and 1.2, SI. Fig.1.3). A width ratio (Eq.1.3) was defined for comparing leaf widths in the three treatments at any longitudinal position of the leaf. It equalled 100% if width were equal in 'Alternated' and 'Light' treatments and 0% if width were equal in 'Alternated' and 'Shaded' treatments (Fig. 1.3a). This was performed for leaves 7 to 9 whose development phases were shifted by 35 °Cd per leaf rank.
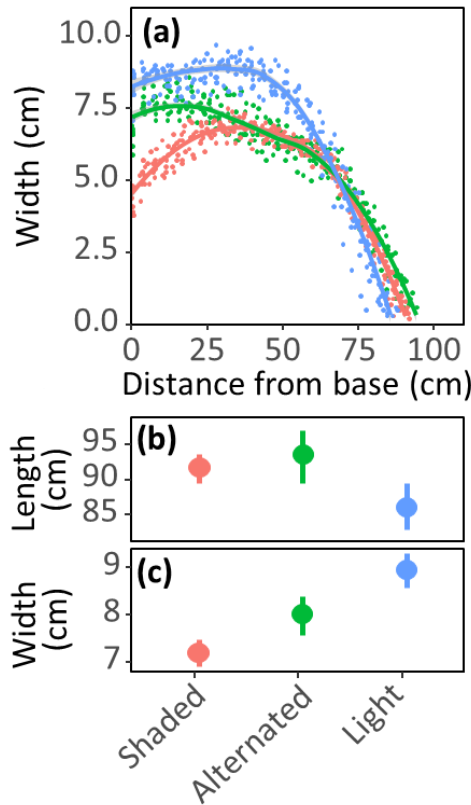
Figure 1.2 : Leaf-8 shape in 3 light treatments (a) and averaged values for maximum leaf length (b) and width (c) for 10 plants. Blue : control treatment without shade; Red: shaded plants since leaf-6 appearance; Green: alternated treatment between shade and light. **(a)** Measured leaf width at each distance from leaf base. Points: experimental data. Lines: local regression (fonction "loess", span = 0.3). **(b, c)** Averaged values and standard deviation of maximum leaf length and width.
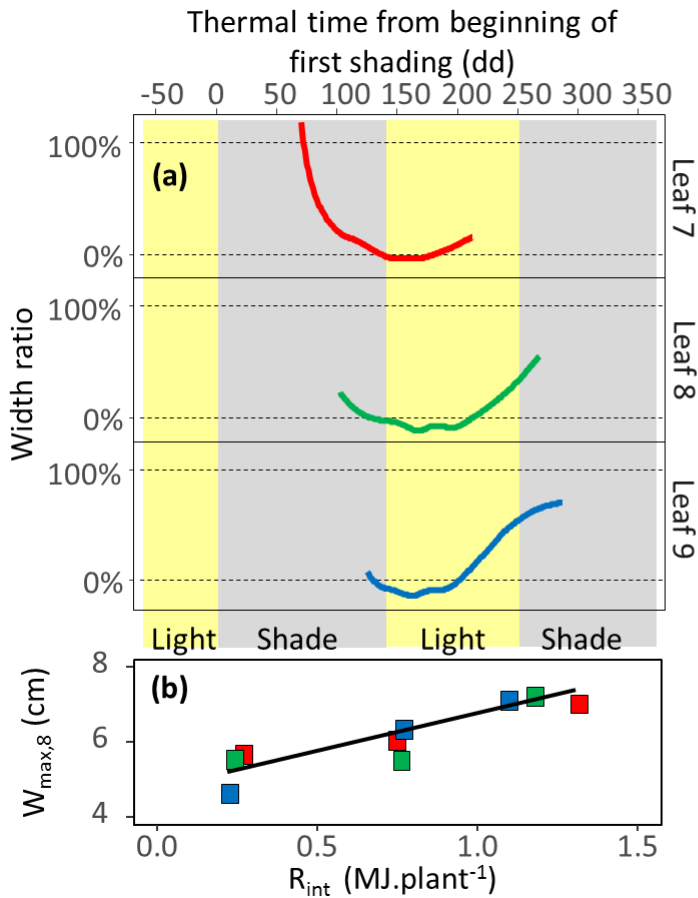
Figure 1.3 : Response of leaf widening to intercepted light. (a) Leaf widening in the alternated treatment, relative to the full-light and shaded treatments in leaves 7 to 10. On the y-axis, width values produced in the alternated treatment are normalized by the difference between control and shade treatments, and showed as a percentage. 0% displays leaf width produced in the shaded treatment (80% light reduction) while 100% displays the width produced in the control treatment (no light reduction. Width measurements are averaged from 10 plants. Width produced at a specific length is linked to thermal time (x-axis) by simulating leaf elongation rate from the beginning of leaf expansion. Only width values higher than 20% of maximum for each leaf are displayed. (b) Maximum leaf width vs. plant intercepted light (R_{int}) in the three treatments and three leaf ranks. Colours displays the different leaf numbers as in (a). Maximum leaf width of the three leaf ranks are corrected by the estimated difference between each rank and the estimated width of leaf 8 ($W_{max,8}$; see M&M for further details)

22

The width ratio of leaf 7 rapidly decreased when plants were shaded and increased after full light was restored (Fig.1. 3a). Because the beginning of leaf expansion differed for each leaf rank, leaves of different ranks underwent different timing of full-light and shading in the 'Alternated' treatment. The width of leaf 8 decreased when plants were shaded and increased under full light after a lag time. Leaf 9 started growth just before full-light, with rapid increase of the width ratio, followed by a stabilization of this ratio at the beginning of the second period of shading. Overall, the final leaf width corrected for the effect of leaf rank was closely related to the cumulated light intercepted per plant for the period with maximum widening rate (Fig.1.3b; calculated with the crop model APSIM-maize). It is noteworthy that a common calculation was adopted for intercepted light per plant in the three treatments without considering the effect of light on leaf width, to avoid circular reasoning (i.e. effect on light interception on leaf width and effect of leaf width on light interception).

The validity of the relationship between intercepted light per plant and leaf width (Fig. 1.3b; Eq.1.4) was tested in an external dataset of 15 experiments in the field and six experiments in the phenotyping platform. A large range of environmental conditions was observed (SI. Table 1.3), with lower values of intercepted light per plant and evaporative demand in the greenhouse than in the field. Leaf width was significantly higher in the field than in the greenhouse for leaves 8 to 11 (50% of mean values for each leaf rank, SI. Fig.1.4). For a given leaf rank, it was closely related to the amount of light intercepted by plants for the period elapsing from 5% to 95% final width. A common relationship between leaf width and intercepted light per plant accounted for variations in width between field experiments and for the difference between field and greenhouse (Fig. 1.4a). Leaf width was also negatively related to minimum and mean temperatures (Table 1.1), probably via the effect of temperature on the amount of light intercepted over the considered period of development. Indeed, because the latter has a constant duration in thermal time, its duration in calendar time decreased with temperature. Leaf width showed no relationship with vapour pressure deficit (Table 1.1).
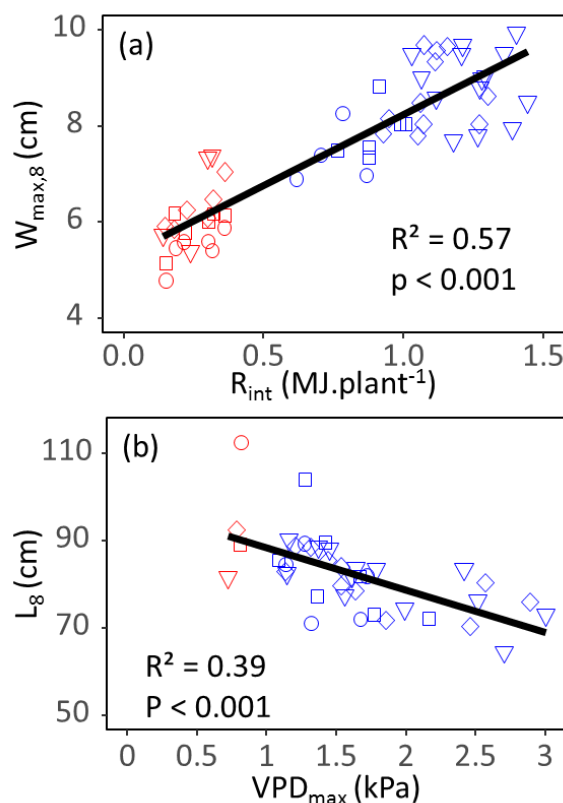
Figure 1.4 : Response of (a) maximum leaf width to plant intercepted light (R_{int}) and leaf length to maximum VPD_{la} (VPD_{max}) (b) in platform and field experiments. Blue dots : Field data. Red dots: Platform data. Shapes display leaf numbers from 8 to 11, respectively : circles, squares, diamonds and triangles. Maximum leaf width and length values of the four leaf ranks are corrected by the estimated difference between each rank and the estimated width and length of leaf 8 (L_8 and $W_{max,8}$; see M&M for further details). Black lines show the linear regressions associated with coefficient of determination and p-value.

23

	T_{max}		T_{min}		T_{mean}		VPD_{max}		VPD_{min}		VPD_{mean}		R_n	
	r	p-value	r	p-value	r	p-value	r	p-value	r	p-value	r	p-value	r	p-value
Width	0.29	0.01	-0.71	<0.001	-0.66	<0.001	0.04	0.73	-0.09	0.4	-0.02	0.83	0.82	<0.001
Length	-0.04	0.19	-0.15	0.09	0.19	0.72	-0.4	<0.001	-0.04	0.23	-0.29	<0.01	-0.09	0.67

Table 1.1 : Correlation matrix of environmental variables with leaf width and length. The coefficient of correlation (r) was calculated with the R function "corr", and corresponding p-values were calculated with the "cor.test" function. Data is summarized from leaf beginning to leaf end of expansion : daily minimum, maximum and mean temperature (T_{min}, T_{max} and T_{mean}); daily minimum, maximum and mean leaf-to-air vapour pressure deficit (VPD_{max}, VPD_{min} and VPD_{mean}); mean of daily incident light (R_n). Significant threshold was fixed at a p-value of 0.01 (p-value > 0.01 : non significant ; p-value ≤ 0.01 : significant ; p-value ≤ 0.001 : highly significant).

Leaf length decreased with evaporative demand and light

Leaf elongation was analysed in the shading experiment presented above and in one experiment in controlled environment. In the latter, the elongation rate of leaf 6 was maximum during the night, with no light and low VPD_{la}, and minimum during periods with high light and VPD_{la}. Plants reacted within minutes after changes in environmental conditions with a strong negative effect of VPD_{la} on leaf elongation rate (Fig. 1.5a,b). Leaf elongation rate measured every 15 min was closely related with VPD_{la} over the same periods (Fig. 1.5c), probably via a negative hydraulic effect decreasing leaf water potential in the leaf growing zone (Tardieu, Simonneau & Parent, 2015).
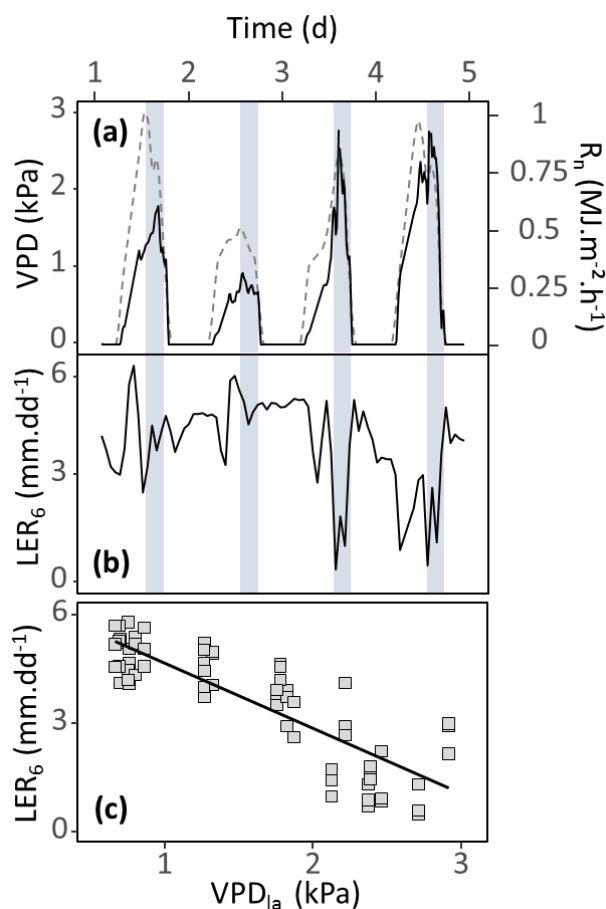
Figure 1.5. Time courses of vapour pressure deficit (VPD) (**a**, solid black line), light intensity (R_n) (**a** - dashed grey line) and leaf elongation rate of leaf 6 for three plants of the genotype B73 (**b**) during a 4 days experiment in the platform *PhenoDyn* in well-watered conditions. Data are smoothed with local regression (function loess, span = 0.02). Grey rectangles highlight the daily values of each variable between 14h and 17h, during daily peaks of VPD_{la}. (**c**) **Response of l**eaf elongation rate (raw data, non-smoothed) to VPD_{la} during highlighted periods.

Shading had opposite effects on leaf length and width in the shading experiment (Fig.1.2b,c, SI. Fig.1.2). Final leaf length of plants growing under shading was longer by 6 to 14 cm compared to those grown under full light, with intermediate values for alternated shading (Fig. 1.2b). In the platform experiment, light had a negative effect on leaf elongation rate, probably via its contribution to VPD_{la} due to leaf heating and, eventually, its effect on leaf water potential (Ben Haj Salah & Tardieu, 1996).

We have tested if the relationship between leaf elongation rate (LER) and VPD_{la} in the greenhouse (Eq. 1) may account for variations of final leaf length in 15 experiments in the field and one experiment in the platform. Final leaf length was closely related to the mean value of afternoon VPD_{la} over the period of maximum leaf elongation. The latter was calculated in each field based on the thermal times at which leaf length reached 5 and 95% of their final values according to Fig. 1.1. A clear relationship was observed between fields, which also accounted for the difference between field and greenhouse (Table 1.1 and Fig. 1.4b). Final leaf length had no relationship with intercepted light per plant or with mean temperature over the same period.

Taking into account environmental effects on leaf length and width largely improved the prediction of individual leaf area.

The results presented above resulted in Eq. 1.1 to 1.4, with parameters established in short term experiments. These equations adequately predicted leaf length and width observed in the independent dataset of field and platform experiments carried out over the whole vegetative period (Fig. 1.4) with CV of 7% and 11% for leaf length and width, respectively. The model of leaf width based on intercepted light captured a large part of the observed variance, with predictions highly improved (R^2 =0.71, CV of error = 11%) compared to the algorithm in which leaf width would be considered as proportional to leaf length (R^2 = 0.01, CV of errors = 26%). This resulted in an adequate prediction of individual leaf area in the whole field dataset (Fig. 6c, R^2=0.62, CV = 16%), compared to the model in which leaf width was calculated as a proportion of leaf length (R^2=0.04, CV = 34%).
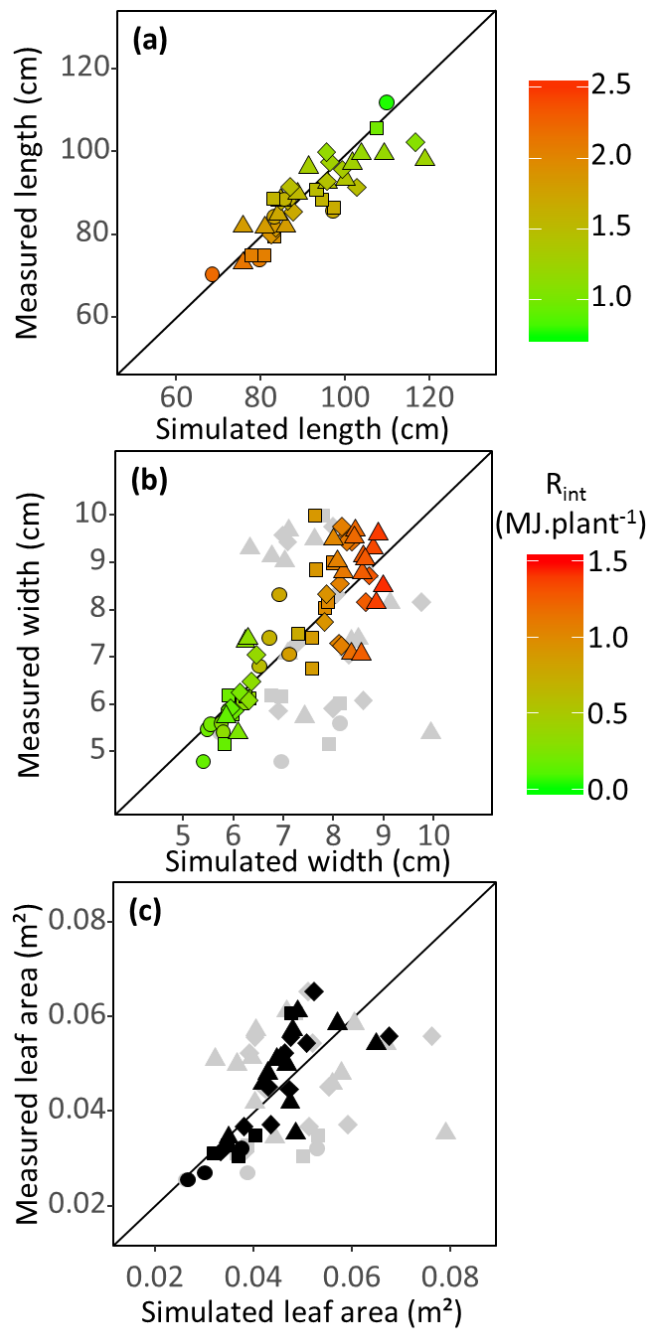
Figure 1.6 : Observed and simulated final leaf length (a), maximum leaf width (b) and leaf area (c).

Points display several leaf numbers. Circles : leaf 8 ; Squares : leaf 9 ; Diamonds : leaf 10 ; Triangles : leaf 11.

a). Observed vs. simulated final leaf length. RMSE = 6.21 cm, CV = 7%. Colours display the maximum VPD_{la} during leaf elongation (from green : low VPD_{la} to red : high VPD_{la}).

b). Grey dots: observed vs. simulated leaf width estimated by considering leaf width as a constant proportion of leaf length (mean width/ length ratio for the whole dataset). RMSE = 1.95 cm , CV = 26%.

Coloured dots: observed vs. simulated leaf width considering an effect of plant intercepted light (R_{int}) during leaf widening. Colours show mean plant intercepted light during this period (green : low ; red : high). RMSE = 0.8 cm, CV = 11%.

c). Grey dots: observed vs. simulated leaf area estimated by considering leaf width as a constant proportion of leaf length. RMSE = 0.02 m², CV = 34%.

Black dots: observed vs. simulated leaf area considering an effect of plant intercepted light during leaf widening. RMSE= 0.007m², CV = 16%.

The genetic controls of leaf length and width were largely independent, with consistent allelic effects in field and platform experiments.

Genetic analyses were performed on the mean length and width of leaves 7 and 8 in the platform and of leaves 8 to 10 in the field, in a panel of 251 maize hybrids. Heritabilities were medium to high, except for width measured in the field (Table 1.2b). The width of leaf 8 largely varied from 5.1 to 9.9 cm in the field and from 5.6 to 8.3 cm in the platform. Correlations between leaf width and leaf length were low in both platform and field experiments (R^2 = 0.001 and 0.26, Table 1.2). Measured leaves were longer and narrower in the platform than in the field (respectively +30% and -26% for leaf 8; mean value for all genotypes), consistent with the difference in intercepted light per plant and evaporative demand (Fig. 1.7). Hence, the effects studied in detail in one hybrid applied to the whole panel.
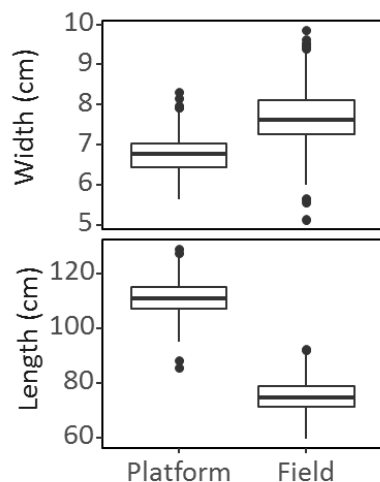
Figure 1.7 : Boxplot of measured maximum leaf width and final leaf length for leaf 8 for one platform experiment and one field experiment, for 253 maize hybrids.

(a)

		Platform		Field	
		Length	Width	Length	Width
Platform	Length	1	0.03	0.24	-0.14
	Width		1	0.06	0.42
Field	Length			1	0.51
	Width				1

(b)

	Trait	Heritability	QTLs	Prediction
Platform	Length	0.80	5	0.35
	Width	0.73	16	0.64
Field	Length	0.48	10	0.19
	Width	0.10	15	0.39

Table 1.2 : Coefficient of correlation between leaf length and width (a), narrow sense heritability, number of QTLs identified by the GWAS analysis and prediction capacity of each set of QTLs on the measured variable (b)

GWAS analysis led to the identification of twenty nine and fourteen significant QTLs in our dataset for leaf width and leaf length, respectively, either in the field or in the platform (Table 3).

We have first tested if QTLs that affected leaf length or leaf width in the field also affected the same trait in the platform and vice versa. For that, we have considered allelic effects of all QTLs in field and platform, regardless of their significance in the considered condition (by allelic effect, we mean the effect of the allele of the reference hybrid B73 vs the other allele at each QTL, expressed as a percentage of the general mean). This can be visualized in Table 1.3 (upper part) in which the allelic effects of the 15 QTLs of leaf width identified in the field are also presented for leaf width in the platform and the 15 QTLs identified for leaf width in the platform are also presented for the field. A visual inspection shows that QTLs that positively affected leaf width in one environment also positively affected it in the other one (consistent colours in Table 1.3). Allelic effects had contrasting amplitudes in the field and in the platform, so most significant QTLs in the field did not reach the threshold of significance (only one colocation of significant QTLs). However, allelic effects were clearly correlated between experiments, for instance allelic effects of QTLs of width identified in the platform were highly correlated with allelic effects of the same QTLs in the field (R^2=0.88, and R^2=0.68 for the reciprocal analysis). The same conclusion applied to QTLs of leaf length, in which the nine QTLs of leaf length identified in the field also affected leaf length in the platform, with

consistent signs of allelic effects and a high correlation (R^2=0.91, and R^2=0.91 for the reciprocal analysis). Hence, we can conclude in a largely common genetic control in the field and in the platform for both leaf width and leaf length, in spite of a high QTL x experiment interaction.

We have then tested if QTLs of leaf width also affected leaf length and vice versa. Overall, this was not the case because QTLs which had high allelic effects on leaf width had small effects on leaf length and vice versa (R^2=0.18). This can be visualized in Table 1.3 via the difference in colour and colour intensity between the left and right parts of the table. Hence, we can conclude that the genetic controls of leaf width and leaf length were largely independent.

Table 1.3 : Comparison of allelic effects of QTLs identified for leaf width or length in the platform and in the field

Variable	SNP name	Bin	Position (cM)	Effect on width (%)		Effect on length (%)	
				Field (Light = 1.4)	Platform (Light = 0.4)	Field (VPD = 2.4)	Platform (VPD = 0.8)
Field Width	S1_14810807	1.02	35.2	2.2	0.1	0.7	-0.5
	AX-90656316	1.02	53.4	2.4	0.4	0.3	-0.3
	S1_204867908	1.07	155.9	-2.3	-1.6	-1.3	0.0
	S1_205242298	1.07	156.2	2.5	1.9	0.9	0.2
	AX-91404589	2.06	128.3	2.2	1.3	0.6	0.1
	AX-91846273	2.06	129.5	2.4	1.5	0.8	0.3
	AX-90618756	2.07	159.5	2.4	1.0	0.0	0.1
	AX-90782812	2.07	160.1	2.3	1.2	0.0	-0.2
	AX-90841086	3.06	111.4	2.3	1.0	1.2	0.5
	AX-90841149	3.06	111.6	2.3	1.0	1.2	0.5
	AX-91623171	4.05	55.7	2.4	1.5	0.0	-0.4
	AX-90977036	5.08	187.1	-2.3	-0.5	0.0	1.1
	SYN19549	10.05	87.9	2.3	1.0	0.6	0.0
	S10_141613269	10.06	109.6	-2.3	-1.0	-1.2	-0.4
	AX-91194831	10.07	116.8	2.3	-0.2	0.0	-0.5
Platform Width	AX-90700654	1.06	147.8	-1.4	-2.8	0.0	-0.9
	AX-90700772	1.06	148.3	-1.0	-2.5	0.3	-1.2
	AX-91402250	1.07	156.5	-2.1	-2.7	0.1	0.1
	AX-90610562	1.08	189.7	-1.5	-3.1	-0.9	-0.5
	AX-90733206	2.02	39.1	-1.1	-2.7	0.2	0.3
	S2_11564804	2.02	39.7	1.4	2.6	-0.3	-0.6
	AX-91388874	2.02	42.8	-1.4	-2.6	0.0	0.3
	AX-90598044	2.03	59.1	0.7	2.7	0.3	-0.1
	AX-90775864	2.06	110.6	0.6	2.9	-0.2	-0.1
	AX-91541880	2.06	111.0	-0.7	-2.7	-0.3	-0.2
	PZE-102124387	2.06	111.2	-0.8	-2.7	-0.4	-0.1
	AX-90776150	2.06	111.9	-1.1	-2.7	0.1	-0.1
	AX-91542155	2.06	112.8	-0.7	-2.7	-0.3	-0.2
	AX-91412182	6.01	12.5	0.8	2.8	0.4	0.1
	S8_172254661	8.08	170.6	0.9	2.7	-0.2	0.0
Field Length	AX-91418229	1.08	200.5	1.9	0.8	1.8	0.7
	AX-90716443	1.09	207.6	-1.2	-0.3	-1.8	-1.0
	AX-90602493	4.03	41.2	-1.1	-0.6	-1.9	-0.9
	AX-90896424	4.06	63.2	-0.4	0.5	-2.0	-0.8
	AX-90547782	5.07	149.7	0.9	0.9	2.1	1.0
	S6_103026220	6.03	42.2	1.1	0.4	1.9	0.5
	S6_113779929	6.04	56.1	-0.6	-1.2	-2.0	-1.3
	PZE-108093081	8.06	129.4	0.5	-0.5	1.8	1.0
	AX-90624676	8.06	145.4	-0.7	-1.2	-1.9	-0.4
Platform Length	AX-91488109	1.06	141.9	-0.7	0.7	-0.1	2.0
	AX-91525911	2.05	95.0	1.5	2.9	-0.2	0.5
	AX-90575329	5.05	108.3	-0.1	-0.5	-0.9	-2.0
	S9_90366933	9.03	59.2	-0.1	1.1	0.2	2.0
	AX-91445646	9.05	81.6	0.3	-0.6	-0.9	-1.8

Discussion

This study reconciles the results on the effects of light interception on leaf growth in dicotyledonous and monocotyledonous species. Whereas a clear effect was shown in dicotyledonous species (Granier & Tardieu, 1999a,b, Pantin, Simonneau & Muller, 2012, Pantin *et al.*, 2011), most physiological studies on monocotyledons concluded in a strong effect of hydraulics and an absence of effect of intercepted light (Ben Haj Salah & Tardieu, 1997, Mahdid *et al.*, 2011, Parent *et al.*, 2010). This was because leaf width was not taken into account in these studies. Here, both short-term dynamic experiments and statistical analyses of a large dataset in the field and in phenotyping platform conclude in a clear effect of light interception on the growth of individual leaf area.

Leaf width and length are under different genetic and physiological controls. The lack of genetic correlation between length and width is consistent with studies on biparental populations (Wei *et al.*, 2016, Yang C. *et al.*, 2016), but this study extends them to the dent maize populations originating from breeding programmes in the USA and Europe and, potentially, to the whole maize species. We also confirm the large variability of leaf width from both genetic and environmental points of view. Within the few studies considering leaf width, most of them have shown that a larger part of variance of individual leaf area in biparental population was explained by leaf width compared to that by leaf length (Wei *et al.*, 2016, Yang C. *et al.*, 2016). This contrasts to a study in wheat (Yang DL. *et al.*, 2016), working with biparental population found that leaf width was less variable compared to leaf length. In our diversity panel, we found an even larger importance of leaf width on individual leaf area compared to that of leaf length (85% vs 15 % of explained variance). Several underlying mechanisms could explain the differences in responses of leaf elongation and widening. It has been shown that lower water status results in shorter cells in maize (Ben Haj Salah et al., 1997) but at the present time and in our knowledge, there is no evidence in favour of the hypothesis of larger cells of more cell rows due to higher intercepted radiation.

The impact of variation of leaf width in multi-environment field trials was also larger than expected. It contrasted with the results of Chenu *et al.* (2008) that did not take into account the variations of leaf width for predicting plant leaf area in Australian maize experiments, but still obtained an adequate prediction of leaf area. We can hypothesise that fields in Australia received high and relatively similar light, resulting in similar leaf widths. Conversely, the experiments presented here, which covered a large part of the European maize growing area presented large differences in light, resulting in large impacts on leaf width and area. Overall, this study to some extent reconciles the results of short-term experiments, which have focused on leaf length with essentially hydraulic effects, with those of a family of crop models that involve carbon supply in the control of leaf area. Indeed, short-term experiments found an effect of intercepted light per plant on leaf area, provided that leaf width is taken into account.

Extrapolating relationships observed at different levels of integration (temporal, spatial) was successful here although they are largely debated (Passioura, 1996, 2007, Poorter *et al.*, 2016). Indeed, many processes show trades-off between rates and duration. For instance, temperature has a large effect on leaf elongation rate of several species, but a very low effect on final length because of a total compensation of rate by duration (Parent & Tardieu, 2012). The success in the upscaling performed here probably involves that such compensations had a minor role in the effects of environmental conditions on leaf width and length. This opens the way to a dialogue between platform and field experiments for the prediction of the genetic variability of the control of leaf growth, in spite of the fact that traits largely differ between field and controlled environment (Poorter *et al.*, 2016).

A crucial question in crop modelling is whether adding complexity to the system could significantly improve simulations (Parent *et al.*, 2016). It is therefore a relevant modelling question if both leaf widening and elongation have to be considered compared to simpler formalisms. At present, in most crop models, two categories of algorithms have been proposed, giving contrasting roles for water *vs* carbon availabilities in the control of leaf growth. The first category considers that the sensitivity of leaf expansion to environmental conditions is indirect and acts through photosynthesis and carbon allocation (e.g. GECROS; Yin & van Laar, 2005). The second category considers direct empirical responses to environmental conditions, regardless of carbon availability, either at the whole-plant level (big leaf models, e.g. APSIM-maize, Hammer *et al.*, 2010) or at individual leaf level. (e.g. Chenu *et al.*, 2008, Lawless, Semenov & Jamieson, 2005, Lizaso *et al.*, 2003, 2011). All these models consider the expansion of individual leaf area as a whole, thereby implicitly considering that, in monocotyledons, differential responses of leaf widening and elongation to environmental variables do not need to be distinguished. The same implicit assumption can be found in (Chenu *et al.*, 2008, 2009) that simulated the impact of QTLs of maize leaf elongation on yield, without considering that leaf width may respond differentially to environment. By contrast, this study shows that it can be a relevant choice to consider separately leaf widening and elongation in the range of studied situations and genotypes, which caused large variations of leaf width. Because the quality of simulations of crop models are linked to the goodness of leaf area predictions (Martre *et al.*, 2015), we propose that identifying leaf widening and elongation in a plant model and therefore improving leaf area predictions could significantly improve predictions This conclusion is consistent with physiological considerations, namely that the controls of carbon-driven and hydraulic- driven mechanisms at the cellular scale, are under the control of very different genes, and translating into contrasted sensitivities of final leaf length and width to environmental conditions in different genotypes.

Acknowledgements

Author Contributions

S.L. analyzed most data

C.F. performed dynamic experiments on width

C.P supervised the field experiments for genetic analyses

E.M. analyzed data on mapping population

B.P. and F.T. planned and designed the research

B.P., S.L. and F.T. wrote the manuscript.

References

Ben Haj Salah H. & Tardieu F. (1995) Temperature affects expansion rate of maize leaves without change in spatial-distribution of cell length - analysis of the coordination between cell-division and cell expansion. *Plant Physiology*, **109**, 861-870.

Ben Haj Salah H. & Tardieu F. (1996) Quantitative analysis of the combined effects of temperature, evaporative demand and light on leaf elongation rate in well-watered field and laboratory-grown maize plants. *Journal of Experimental Botany*, **47**, 1689-1698.

Ben Haj Salah H. & Tardieu F. (1997) Control of leaf expansion rate of droughted maize plants under fluctuating evaporative demand - A superposition of hydraulic and chemical messages? *Plant Physiology*, **114**, 893-900.

Bos H.J., Tijani-Eniola H. & Struik P.C. (2000) Morphological analysis of leaf growth of maize: responses to temperature and light intensity. *Netherlands Journal of Agricultural Science*, **48**, 181-198.

Butler D.G., Cullis B.R., Gilmour A.R. & Gogel B.J. (2009) *Mixed models for S language environments. ASReml-R reference manual.* Queensland Department of Primary Industries and Fisheries.

Cabrera-Bosquet L., Fournier C., Brichet N., Welcker C., Suard B. & Tardieu F. (2016) High-throughput estimation of incident light, light interception and radiation-use efficiency of thousands of plants in a phenotyping platform. *New Phytologist*, **212**, 269-281.

Chenu K., Chapman S.C., Hammer G.L., McLean G., Salah H.B.H. & Tardieu F. (2008) Short-term responses of leaf growth rate to water deficit scale up to whole-plant and crop levels: an integrated modelling approach in maize. *Plant Cell and Environment*, **31**, 378-391.

Chenu K., Chapman S.C., Tardieu F., McLean G., Welcker C. & Hammer G.L. (2009) Simulating the Yield Impacts of Organ-Level Quantitative Trait Loci Associated with Drought Response in Maize - A 'Gene-to-Phenotype' Modeling Approach. *Genetics*, **183**, 1507–1523.

Fournier C., Andrieu B. & Sohbi Y. (2001) *Virtual plant models for studying interactions between crops and environment*.

Ganal M.W., Durstewitz G., Polley A., Berard A., Buckler E.S., Charcosset A., Clarke J.D., Graner E.M., Hansen M., Joets J., Le Paslier M.C., McMullen M.D., Montalent P., Rose M., Schon C.C., Sun Q., Walter H., Martin O.C. & Falque M. (2011) A Large Maize (Zea mays L.) SNP Genotyping Array: Development and Germplasm Genotyping, and Genetic Mapping to Compare with the B73 Reference Genome. *Plos One*, **6**.

Giraud H., Lehermeier C., Bauer E., Falque M., Segura V., Bauland C., Camisan C., Campo L., Meyer N., Ranc N., Schipprack W., Flament P., Melchinger A.E., Menz M., Moreno-Gonzalez J., Ouzunova M., Charcosset A., Schon C.C. & Moreau L. (2014) Linkage Disequilibrium with Linkage Analysis of Multiline Crosses Reveals Different Multiallelic QTL for Hybrid Performance in the Flint and Dent Heterotic Groups of Maize. *Genetics*, **198**, 1717-+.

Granier C. & Tardieu F. (1999a) Leaf expansion and cell division are affected by reducing absorbed light before but not after the decline in cell division rate in the sunflower leaf. *Plant Cell and Environment*, **22**, 1365-1376.

Granier C. & Tardieu F. (1999b) Water deficit and spatial pattern of leaf development. Variability in responses can be simulated using a simple model of leaf development. *Plant Physiology*, **119**, 609-619.

Guilioni L., Jones H.G., Leinonen I. & Lhomme J.P. (2008) On the relationships between stomatal resistance and leaf temperatures in thermography. *Agricultural and Forest Meteorology*, **148**, 1908-1912.

Hammer G.L., van Oosterom E., McLean G., Chapman S.C., Broad I., Harland P. & Muchow R.C. (2010) Adapting APSIM to model the physiology and genetics of complex adaptive traits in field crops. *Journal of Experimental Botany*, **61**, 2185-2202.

Harrison M.T., Tardieu F., Dong Z., Messina C.D. & Hammer G.L. (2014) Characterizing drought stress and trait influence on maize yield under current and future conditions. *Global Change Biology*, n/a-n/a.

Kruijer W., Boer M.P., Malosetti M., Flood P.J., Engel B., Kooke R., Keurentjes J.J.B. & van Eeuwijk F.A. (2015) Marker-Based Estimation of Heritability in Immortal Populations. *Genetics*, **199**, 379-393.

Lawless C., Semenov M.A. & Jamieson P.D. (2005) A wheat canopy model linking leaf area and phenology. *European Journal of Agronomy*, **22**, 19-32.

Lippert C., Listgarten J., Liu Y., Kadie C.M., Davidson R.I. & Heckerman D. (2011) FaST linear mixed models for genome-wide association studies. *Nature Methods*, **8**, 833-U894.

Lizaso J.I., Batchelor W.D., Westgate M.E. & Echarte L. (2003) Enhancing the ability of CERES-Maize to compute light capture. *Agricultural Systems*, **76**, 293-311.

Lizaso J.I., Boote K.J., Jones J.W., Porter C.H., Echarte L., Westgate M.E. & Sonohat G. (2011) CSM-IXIM: A New Maize Simulation Model for DSSAT Version 4.5. *Agronomy Journal*, **103**, 766-779.

Mahdid M., Kameli A., Ehlert C. & Simonneau T. (2011) Rapid changes in leaf elongation, ABA and water status during the recovery phase following application of water stress in two durum wheat varieties differing in drought tolerance. *Plant Physiology and Biochemistry*, **49**, 1077-1083.

Martre P., Wallach D., Asseng S., Ewert F., Jones J.W., Rotter R.P., Boote K.J., Ruane A.C., Thorburn P.J., Cammarano D., Hatfield J.L., Rosenzweig C., Aggarwal P.K., Angulo C., Basso B., Bertuzzi P., Biernath C., Brisson N., Challinor A.J., Doltra J., Gayler S., Goldberg R., Grant R.F., Heng L., Hooker J., Hunt L.A., Ingwersen J., Izaurralde R.C., Kersebaum K.C., Muller C., Kumar S.N., Nendel C., O'Leary G., Olesen J.E., Osborne T.M., Palosuo T., Priesack E., Ripoche D., Semenov M.A., Shcherbak I., Steduto P., Stockle C.O., Stratonovitch P., Streck T., Supit I., Tao F.L., Travasso M., Waha K., White J.W. & Wolf J. (2015) Multimodel ensembles of wheat growth: many models are better than one. *Global Change Biology*, **21**, 911-925.

Maurice I., Gastal F. & Durand J.L. (1997) Generation of form and associated mass deposition during leaf development in grasses: a kinematic approach for non-steady growth. *Annals of Botany*, **80**, 673-683.

Millet E.J., Welcker C., Kruijer W., Negro S., Coupel-Ledru A., Nicolas S.D., Laborde J., Bauland C., Praud S., Ranc N., Presterl T., Tuberosa R., Bedo Z., Draye X., Usadel B., Charcosset A., Van Eeuwijk F. & Tardieu F. (2016) Genome-Wide Analysis of Yield in Europe: Allelic Effects Vary with Drought and Heat Scenarios. *Plant Physiology*, **172**, 749-764.

Muller B., Bourdais G., Reidy B., Bencivenni C., Massonneau A., Condamine P., Rolland G., Conejero G., Rogowsky P. & Tardieu F. (2007) Association of specific expansins with growth in Maize leaves is maintained under environmental, genetic, and developmental sources of variation. *Plant Physiology*, **143**, 278-290.

Pantin F., Simonneau T. & Muller B. (2012) Coming of leaf age: control of growth by hydraulics and metabolics during leaf ontogeny. *New Phytologist*, **196**, 349-366.

Pantin F., Simonneau T., Rolland G., Dauzat M. & Muller B. (2011) Control of Leaf Expansion: A Developmental Switch from Metabolics to Hydraulics. *Plant Physiology*, **156**, 803-815.

Parent B., Suard B., Serraj R. & Tardieu F. (2010) Rice leaf growth and water potential are resilient to evaporative demand and soil water deficit once the effects of root system are neutralized. *Plant Cell and Environment*, **33**, 1256-1267.

Parent B. & Tardieu F. (2012) Temperature responses of developmental processes have not been affected by breeding in different ecological areas for 17 crop species. *New Phytologist*, **194**, 760-774.

Parent B., Vile D., Violle C. & Tardieu F. (2016) Towards parsimonious ecophysiological models that bridge ecology and agronomy. *New Phytologist*, **210**, 380-382.

Passioura J. (2007) The drought environment: physical, biological and agricultural perspectives. *Journal of Experimental Botany*, **58**, 113-117.

Passioura J.B. (1996) Simulation models: Science; snake oil, education, or engineering? *Agronomy Journal*, **88**, 690-694.

Poorter H., Fiorani F., Pieruschka R., Wojciechowski T., van der Putten W.H., Kleyer M., Schurr U. & Postma J. (2016) Pampered inside, pestered outside? Differences and similarities between plants growing in controlled conditions and in the field. *New Phytologist*, **212**, 838-855.

Rincent R., Moreau L., Monod H., Kuhn E., Melchinger A.E., Malvar R.A., Moreno-Gonzalez J., Nicolas S., Madur D., Combes V., Dumas F., Altmann T., Brunel D., Ouzunova M., Flament P., Dubreuil P., Charcosset A. & Mary-Huard T. (2014) Recovering Power in Association Mapping Panels with Variable Levels of Linkage Disequilibrium. *Genetics*, **197**, 375-387.

Silk W.K. (1992) Steady form from changing cells. *International Journal of Plant Sciences*, **153**, S49-S58.

Sinoquet H., Le Roux X., Adam B., Ameglio T. & Daudet F.A. (2001) RATP: a model for simulating the spatial distribution of radiation absorption, transpiration and photosynthesis within canopies: application to an isolated tree crown. *Plant Cell and Environment*, **24**, 395-406.

Sinoquet H., Moulia B. & Bonhomme R. (1991) Estimating the 3-dimensional geometry of a maize crop as an input of radiation models - comparison between 3-dimensional digitizing and plant profiles. *Agricultural and Forest Meteorology*, **55**, 233-249.

Song Y.H., Rui Y.K., Bedane G. & Li J.C. (2016) Morphological Characteristics of Maize Canopy Development as Affected by Increased Plant Density. *Plos One*, **11**.

Sonohat G. & Bonhomme R. (1998) Variations de structure aérienne de peuplements de maïs en fonction de la densité de semis. Implications pour la modélisation. In: *Fonctionnement des peuplements végétaux sous contraintes environnementales*, pp. 403-421. INRA Editions, Paris.

Tardieu F., Reymond M., Hamard P., Granier C. & Muller B. (2000) Spatial distributions of expansion rate, cell division rate and cell size in maize leaves: a synthesis of the effects of soil water status, evaporative demand and temperature. *Journal of Experimental Botany*, **51**, 1505-1514.

Tardieu F., Simonneau T. & Parent B. (2015) Modelling the coordination of the controls of stomatal aperture, transpiration, leaf growth, and abscisic acid: update and extension of the Tardieu-Davies model. *Journal of Experimental Botany*, **66**, 2227-2237.

Tian F., Bradbury P.J., Brown P.J., Hung H., Sun Q., Flint-Garcia S., Rocheford T.R., McMullen M.D., Holland J.B. & Buckler E.S. (2011) Genome-wide association study of leaf architecture in the maize nested association mapping population. *Nature Genetics*, **43**, 159-U113.

Unterseer S., Bauer E., Haberer G., Seidel M., Knaak C., Ouzunova M., Meitinger T., Strom T.M., Fries R., Pausch H., Bertani C., Davassi A., Mayer K.F.X. & Schon C.C. (2014) A powerful tool for genome analysis in maize: development and evaluation of the high density 600 k SNP genotyping array. *Bmc Genomics*, **15**.

Wei X.M., Wang X.B., Guo S.L., Zhou J.L., Shi Y., Wang H.T., Dou D.D., Song X.H., Li G.H., Ku L.X. & Chen Y.H. (2016) Epistatic and QTLxenvironment interaction effects on leaf area-associated traits in maize. *Plant Breeding*, **135**, 671-676.

Yang C., Tang D., Qu J., Zhang L., Chen Z. & Liu J. (2016) Genetic mapping of QTL for the sizes of eight consecutive leaves below the tassel in maize (Zea mays L.). *Theoretical and Applied Genetics*, **129**, 2191-2209.

Yang D.L., Liu Y., Cheng H.B., Chang L., Chen J.J., Chai S.X. & Li M.F. (2016) Genetic dissection of flag leaf morphology in wheat (Triticum aestivum L.) under diverse water regimes. *Bmc Genetics*, **17**.

Yin X.Y. & van Laar H.H. (2005) *Crop Systems Dynamics. An ecophysiological simulation model of genotype-by-environment interactions.* Wageningen Academic Publishers, Wageningen, The Netherlands.

Supporting Information

Supplementary figure 1.1: Time courses of widening and elongation of leaves 6 to 11 (respectively in panels a to f). Round and square dots: respectively mean of maximum leaf width and lamina length for 10 plants per date (data are normalized by maximum value). Dashed and solid lines are local regressions ("loess" function) for respectively width and length.
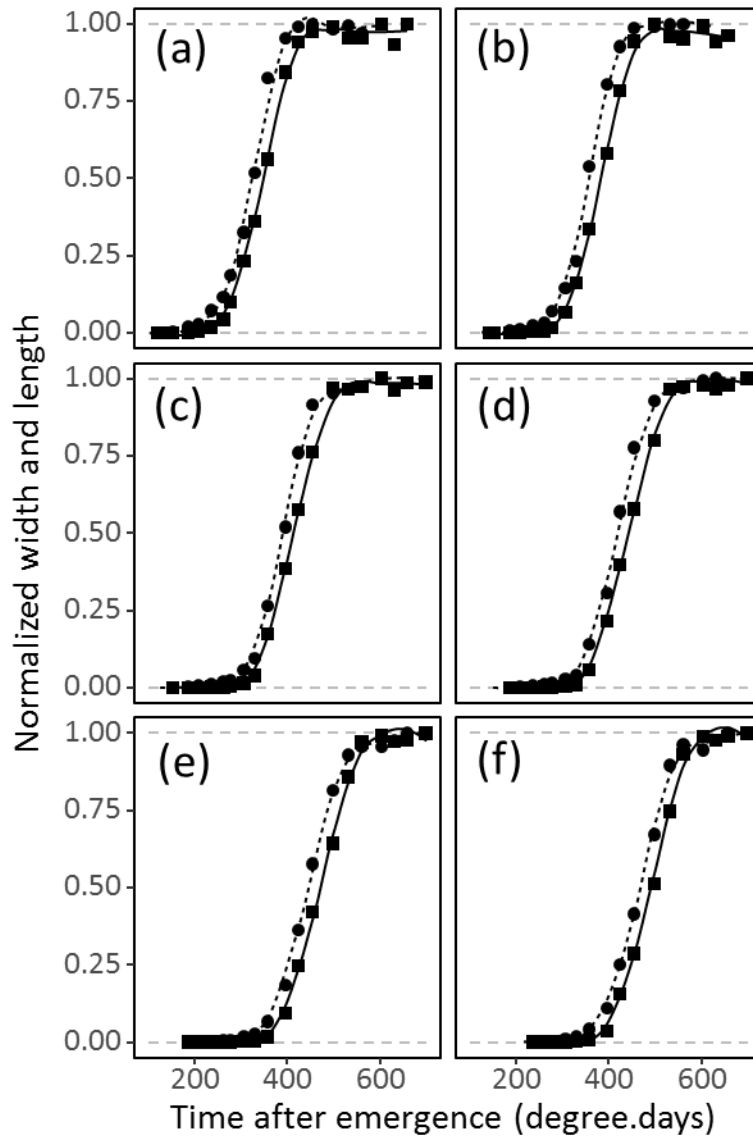
Supplementary Figure 1.2: Leaf shape for leaves 6 to 9 in 3 light treatments. Blue: control treatment without shade; Red: shaded plants since leaf-6 appearance; Green: alternated treatment between shade and light. Measured leaf width at each distance from leaf base. Points: experimental data. Lines: local regression (function "loess", span = 0.3).
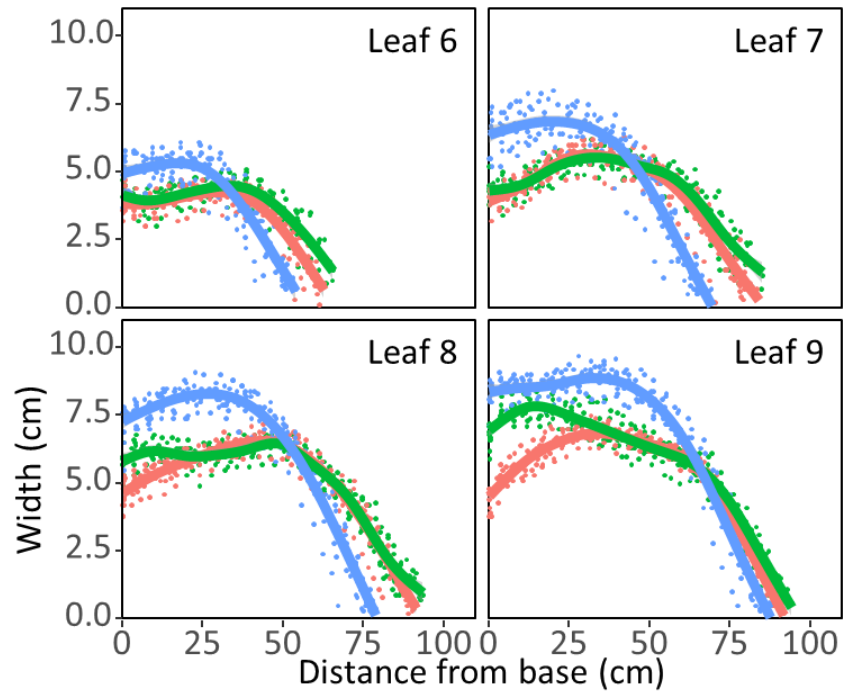
Supplementary Figure 1.3: Profiles of leaf width as a function of time of leaf widening for leaves 6 to 9 in 3 light treatments. Blue: control treatment without shade; Red: shaded plants from leaf-6 appearance; Green: alternated treatment between shade and light. Measured leaf width at each distance from leaf base. Points: experimental data. Lines: local regression (function "loess", span = 0.3). Time of leaf widening was calculated for each distance from the leaf base (Fig.2 or SI.Fig.2) from leaf elongation rate and the beginning of leaf expansion as specified in M& M.
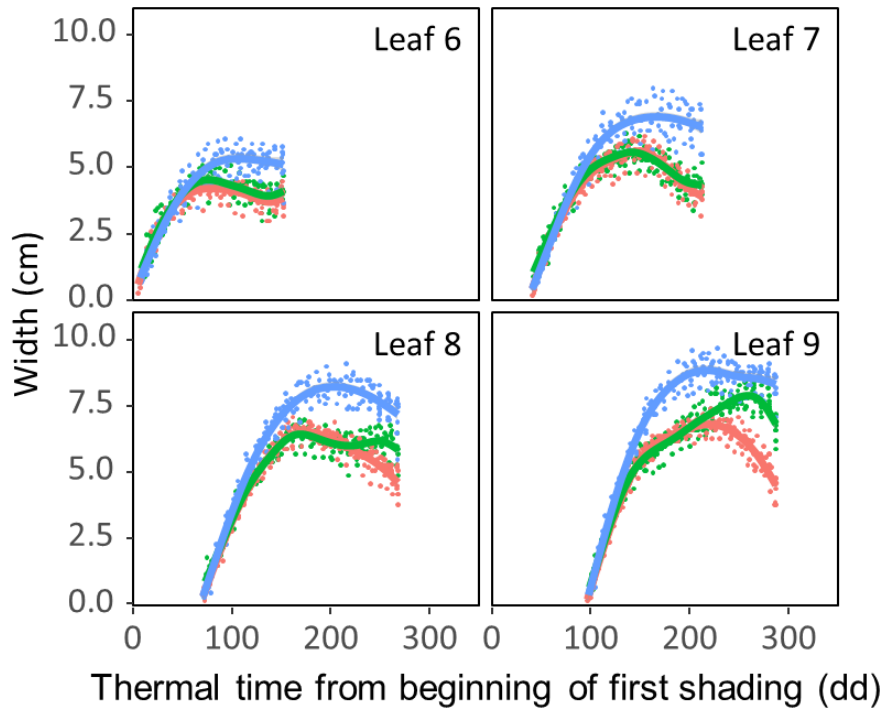
Supplementary Figure 1.4: Final maximum leaf width (a) and leaf lamina length (b) for all measured leaf ranks in several experiments in the platform and in the field. Plain lines: mean values for each leaf rank. Dashed lines: mean ± standard deviation per leaf rank. Blue lines : Field data. Red lines : Platform data.
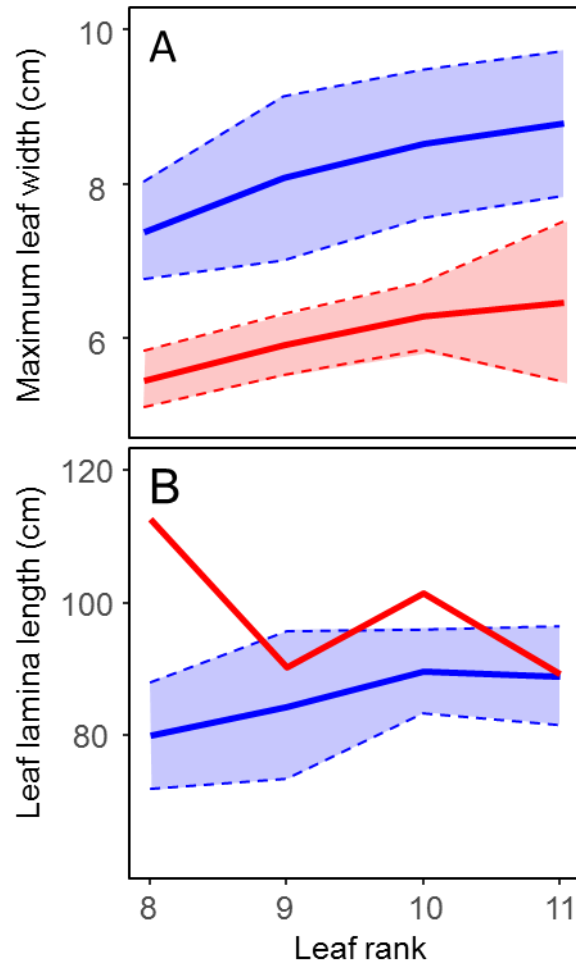
Supplementary Figure 1.5: Observed (blue dots and lines) and simulated leaf width (red dots and lines) for several leaf numbers in 21 experiments in the field and in the platform. Leaf width are estimated from leaf rank and the effect of intercepted light during the period of leaf widening.
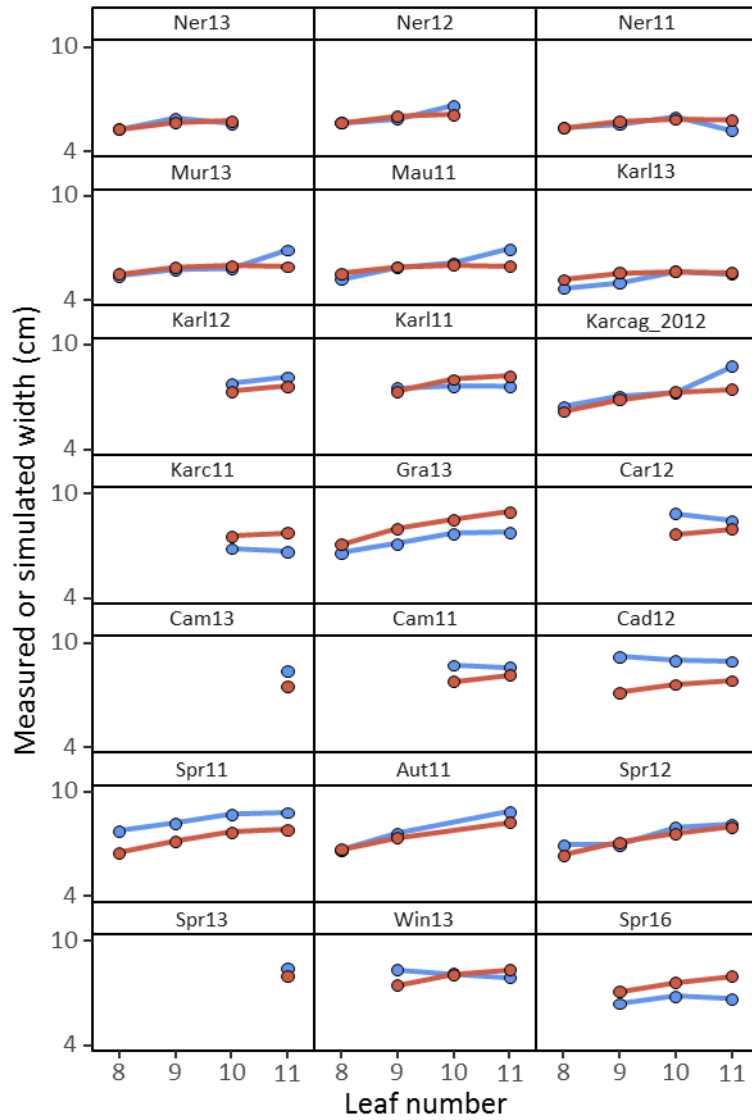
Supplementary table 1.1: Summary of all field experiments.

Location	Country	Year	ID	Genotypes	Treatments	Rep	Measurements	Leaf rank
Mauguio	France	1998	Mau98	Déa	WW	10	Length / Maximum width (2 days)	All leaves
Gruignon	Paris	1996	Gru96	Déa	Light conditions : Control / Alterned / Shadow	10	Leaf shape (harvest)	All leaves
Saint-martin de Hinx	France	2016	SdH16	DROPS panel (255 genotypes)	WW	3	Length / Maximum width (harvest)	leaf 7 to 11
Cadriano	Italy	2012	Cad12	B73	WW / WD	10	Length / Maximum width (harvest)	leaf 7 to 11
Campagnola	Italy	2011	Cam11	B73	WW / WD	10	Length / Maximum width (harvest)	leaf 7 to 11
Campagnola	Italy	2012	Cam12	B73	WW / WD	10	Length / Maximum width (harvest)	leaf 7 to 11
Campagnola	Italy	2013	Cam13	B73	WW / WD	10	Length / Maximum width (harvest)	leaf 7 to 11
Caracal	Romania	2012	Car12	B73	WW / WD	10	Length / Maximum width (harvest)	leaf 7 to 11
Gaillac	France	2012	Gai12	B73	WW / WD	10	Length / Maximum width (harvest)	leaf 7 to 11
Graneros	Chile	2013	Gra13	B73	WW / WD	10	Length / Maximum width (harvest)	leaf 7 to 11
Karcag	Hungary	2011	Karc11	B73	WW / WD	10	Length / Maximum width (harvest)	leaf 7 to 11
Karcag	Hungary	2012	Karc12	B73	WW / WD	10	Length / Maximum width (harvest)	leaf 7 to 11
Karlsruhe	Germany	2011	Karl11	B73	WW / WD	10	Length / Maximum width (harvest)	leaf 7 to 11
Karlsruhe	Germany	2012	Karl12	B73	WW / WD	10	Length / Maximum width (harvest)	leaf 7 to 11
Karlsruhe	Germany	2013	Karl13	B73	WW / WD	10	Length / Maximum width (harvest)	leaf 7 to 11
Mauguio	France	2011	Mau11	B73	WW / WD	10	Length / Maximum width (harvest)	leaf 7 to 11
Murony	Hungary	2013	Mur13	B73	WW / WD	10	Length / Maximum width (harvest)	leaf 7 to 11
Nerac	France	2011	Ner11	B73	WW / WD	10	Length / Maximum width (harvest)	leaf 7 to 11
Nerac	France	2012	Ner12	B73	WW / WD	10	Length / Maximum width (harvest)	leaf 7 to 11
Nerac	France	2013	Ner13	B73	WW / WD	10	Length / Maximum width (harvest)	leaf 7 to 11

Supplementary table 1.2: Summary of all platform experiments.

Platform	Year	ID	Genotypes	Treatments	Rep	Measurements	Leaf rank
PhenoDyn	2006	Dyn06	Déa	VPD (1/2/3 kPa)	3	Leaf elongation rate (15 minutes)	Leaf 6
PhenoArch	2016	Spr16	DROPS panel (255)	WW / WD	2	Length / Maximum width (Harvest)	leaf 7 to 11
PhenoArch	2011	Spr11	B73	WW / WD	2	Length / Maximum width (Harvest)	leaf 7 to 11
PhenoArch	2011	Aut11	B73	WW / WD	2	Length / Maximum width (Harvest)	leaf 7 to 11
PhenoArch	2012	Spr12	B73	WW / WD	3	Length / Maximum width (Harvest)	leaf 7 to 11
PhenoArch	2013	Win13	B73	WW / WD	3	Length / Maximum width (Harvest)	leaf 7 to 11
PhenoArch	2013	Spr13	B73	WW / WD	3	Length / Maximum width (Harvest)	leaf 7 to 11

Supplementary table 1.3 : Summary of environmental variables in all experiments carried out in the field and in the platform. Data are summarized from sowing to harvest for : daily minimum, maximum and mean temperature (T_{min}, T_{max} and T_{mean}); daily minimum, maximum and mean leaf-to-air vapour pressure deficit (VPD_{max}, VPD_{min} and VPD_{mean}); mean of daily amount of light (Rn).

Experiment	Location	Country	Year	ID	Latitude (°N)	Longitude (°E)	Altitude (m)	T_{max} (°C)	T_{min} (°C)	T_{mean} (°C)	VPD_{max} (kPa)	VPD_{min} (kPa)	VPD_{mean} (kPa)	R_n (MJ/m²)
Field	Cadriano	Italy	2012	Cad12	44.93	11.88	5	38.2	4.1	24.8	5.3	0.5	3.1	24.5
	Campagnola	Italy	2011	Cam11	45.17	9.53	49	37.7	8.6	22.5	4.5	0.0	2.0	20.8
	Campagnola	Italy	2012	Cam12	45.17	9.53	49	37.6	9.5	22.7	4.0	0.2	2.1	21.6
	Campagnola	Italy	2013	Cam13	45.17	9.53	49	36.2	5.7	21.3	3.7	0.0	1.7	19.4
	Caracal	Romania	2012	Car12	44.12	24.35	101	40.8	7.1	23.9	5.9	0.0	3.0	22.1
	Gaillac	France	2012	Gai12	43.89	1.99	150	40.8	2.8	20	5.4	0.2	2.1	18.4
	Graneros	Chile	2013	Gra13	-34.06	-70.73	478	33.7	1.9	18.2	6.4	0.2	2.4	26.5
	Karcag	Hungary	2011	Karc11	47.18	20.54	81	35.5	1.8	20.1	3.8	0.4	2.0	20.4
	Karcag	Hungary	2012	Karc12	47.18	20.54	81	37.7	1.3	20.6	5.8	0.8	2.8	18.8
	Karlsruhe	Germany	2011	Karl11	49.07	8.28	115	33.8	1.7	17.3	3.6	0.4	1.5	17.3
	Karlsruhe	Germany	2012	Karl12	49.07	8.28	115	35.1	2	17.1	3.5	0.2	1.4	16.8
	Karlsruhe	Germany	2013	Karl13	49.07	8.28	100	36.3	2.3	16.2	4.6	0.1	1.3	15.9
	Mauguio	France	2011	Mau11	43.61	3.98	12.7	35.3	4.2	21.1	3.5	0.1	1.6	20.7
	Murony	Hungary	2013	Mur13	46.78	21.05	85	38.2	-2.5	19.4	5.3	0.1	2.1	18.1
	Nerac	France	2011	Ner11	44.17	0.31	40	39	5.5	19.8	4.2	0.2	1.8	19.4
	Nerac	France	2012	Ner12	44.17	0.31	40	46.5	1.5	21.5	7.4	0.3	2.8	20
	Nerac	France	2013	Ner13	44.17	0.31	40	38.5	2	19	3.8	0.2	1.7	19
Platform	Montpellier	France	2011	Spr11	43.62	3.86	43	37.6	9.2	26.6	2.7	0.8	1.6	4.3
	Montpellier	France	2011	Aut11	43.62	3.86	43	36	17.1	24.7	2.1	0.7	1.4	2.8
	Montpellier	France	2012	Spr12	43.62	3.86	43	32.8	20.7	25.1	2.4	0.9	1.4	5.9
	Montpellier	France	2013	Win13	43.62	3.86	43	29	19.5	21.3	2	0.8	1.5	3.2
	Montpellier	France	2013	Spr13	43.62	3.86	43	32	17.1	23.4	2	0.5	1.3	6
	Montpellier	France	2019	Spr16	43.62	3.86	43	31.4	16	23.5	1.9	0.5	1.0	7.7

SI Method S1.1: Measurements of maximum leaf width from whole plant images in the platform *PhenoArch* (INRA Montpellier)

Measurements of maximum leaf width from whole plant images in the platform *PhenoArch* (INRA Montpellier)

Plants were imaged every 2-3 days with one top view and 12 side views (every 30°). Plant phenology (appeared and ligulated leaves) was measured at the same time.
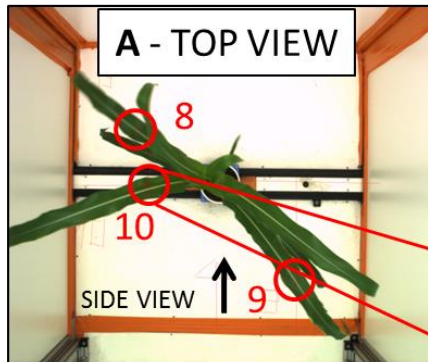
(A) Top views of plants in which mature leaf blades were fully visible were selected.
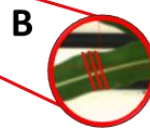
(B) Leaf maximum widths were estimated, for each individual leaf at 3 points along the first half of leaf length from the top view, with the software ImageJ.
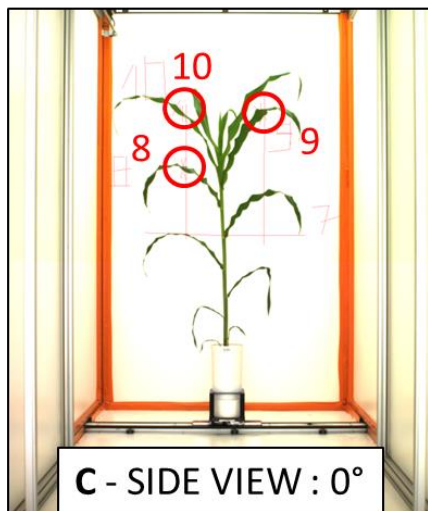
(C) For each top measurements, corresponding side images with the best angle were selected to estimate the z coordinate (height from pot surface) of measurements. This method allowed the correction of width measurements in pixels (from top view) with the distance to the camera. Corrected measured width in pixels were converted to centimeters with a camera-dependent factor.

(D) For one experiment, maximum leaf width of leaves 8 to 12 for 6 plants of the genotype B73_H were measured both by image analysis and via planimeter measurements of leaf shapes.

$R^2 = 0.93$
$y = 1.02\,x + 0.34$
RMSE= 0.3 cm
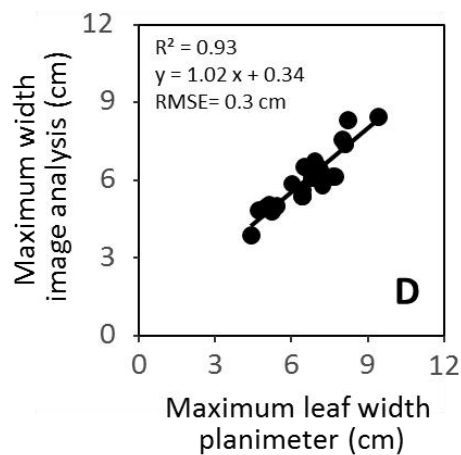
Chapter 2: A model of leaf development, leaf expansion and grain number to simulate leaf area and yield of hundreds of maize hybrids in contrasting environmental scenarios

This chapter uses the results of chapter 1 to develop a model that predicts individual leaf area for a range of genotypes and environmental conditions. Due to the recently demonstrated relationship between the sensitivities of ovary abortion rate and leaf elongation rate in plants subjected to water deficit (Oury et al., 2016), the model is extended to predict grain number. This results in a module that I have implemented and tested within the APSIM crop model. The module presented here can also work independently and will be implemented as a module in the modelling platform BioMA[4].

This chapter uses several pre-existing datasets that I have re-analysed in this thesis for either designing the model, or estimating its parameters for hundreds of genotypes, or testing the model against measured leaf dimensions or yield.

This chapter will be submitted to a scientific journal and is therefore written as a manuscript

---

[4] http://bioma.jrc.ec.europa.eu/index.htm

A model of leaf development, leaf expansion and grain number to study the impact of the genetic variability of leaf growth traits on maize yield in contrasting environmental scenarios.

Sebastien Lacube, Claude Welcker, Emilie Millet, Boris Parent and François Tardieu

INRA, UMR759 LEPSE, F-34060 Montpellier, France

Abstract

Quality of crop model prediction is often linked to the quality of simulation of leaf area. Most models generally follow the approach of simulating canopy growth as a whole, without considering individual leaves and the effect of environmental conditions affecting them. In this study, we worked on the development of a model of leaf growth and development that integrates observed genetic variability in its parameters/traits, and simulates adequately responses of genotypes to environmental conditions. Maize leaves development stages were studied with a measured dataset from two genotypes with different maximum leaf numbers and formalisms of leaf elongation and widening from chapter 1 were studied and implemented in the new module. Model development focused on linking model parameters to measurable traits in phenotyping platforms, and a particular attention was given to limit and reduce the number of genotype specific parameters and study the effect of maximum leaf number on leaf profiles. All model parameters were measured for a set of 254 genotypes from platform and field experiments, and the model was tested on (i) measurements of final leaf length and width of a reference genotype in a network of field experiment around Europe, (ii) on a final length and width on a subset of 16 genotypes in one experiment, and (iii) on the whole panel of 254 genotypes against measured data of grain number and final grain yield. The simulated values showed a good adequation with measurements for all three tests, and explained between 10 and 60% of the variability of grain yield depending on the environment. Therefore, this model has the potential of providing elements of study for leaf growth ideotypes for different regions and environmental scenarios around Europe that will be presented in chapter 4 and 5.

Introduction

Leaf expansion is central in the trade-off between light interception and plant transpiration. Indeed, reducing leaf area in case of water deficit saves water for later stages of development, but at the same time reduces the amount of intercepted light resulting in lowering biomass accumulation and yield. As a consequence, a reduction in plant leaf area can have positive or negative impacts on crop production depending on environmental scenarios (Tardieu, 2012).

The increase in leaf area over the crop cycle is the consequence of several processes that have each their own genetic and environmental controls. First, processes linked to plant development (e.g. the timing of leaf initiation or the duration of leaf expansion) respond mostly to temperature. Second, leaf elongation and widening have, in monocotyledonous leaves, separate environmental and genetic controls (Lacube et al., 2017, Chapter 1). Historical (Boyer, 1970; Saab and Sharp 1989) and more recent (Tardieu et al., 2014) studies report and quantify the implications of hydraulics and plant water status on leaf elongation. Conversely, leaf widening is probably mostly affected by intercepted light (Lacube et al., 2017 Chapter 1). Recently, the development of phenotyping platforms has allowed characterising the genetic variability for these components of leaf growth.

Combining simulation and phenotyping could be an efficient strategy to study the impacts of the genetic variability of several traits on plant performances in contrasting environmental scenarios, provided that corresponding processes are adequately taken into account in the model (Parent and Tardieu, 2014). A model can be used to compare the advantages of real or virtual genotypes in a range of environmental conditions, and define the best ideotype for a specific set of environmental conditions (Rötter et al., 2015; Gouache et al., 2017). Martre et al. (2015) define an ideotype as '*a combination of morphological and/or physiological traits, or their genetic bases, optimizing crop performance to a particular biophysical environment, crop management, and end-use*'. We shall follow this line by defining here an ideotype as a vector of parameter values that maximizes yield in a given environmental and management context, with a given crop model.

Crop models have been developed in a context of yield prediction on environmental gradients rather than in the context presented above. Indeed, most of the genetic variability can hardly be taken into account in most models (Hoogenboom et al. (2004), thereby requiring changes in model structure and formalisms (Hammer et al., 2002; Hammer et al., 2010; Parent et al., 2015). First, formalisms need to be adapted to link phenotypic traits, as measured in phenotyping platforms, to key genotypic parameters in the model (Tardieu et al, 2017). Secondly, as most crop models usually use a number of parameters larger than that which can be measured, a hierarchy is needed to define which key and independent parameters should be formalised (Casadebaig et al., 2016). Calibration is usually involved in any modelling exercise, by comparing the measured and simulated data of a model in order to re-evaluate parameters for a better estimation of output variables (Duke and Guerrif, 1999). The common procedure consists of an optimization of the vector of parameters aiming at minimizing the difference between measured and simulated variables. The vector of parameters is then validated with independent input data. High throughput phenotyping now allows measurement of precise plant-scale traits on a high number of genotypes (Parent and Tardieu, 2014). When using measured traits as genotypic parameters in the model, parameters used for the simulation can be estimated via measurements, thereby minimizing the role of parameter optimization.

A comparison of crop models has shown that the quality of yield prediction is often linked to that of the modelling of plant leaf area (Martre et al., 2015). While most phenotyping platforms have been developed to characterise leaf growth and its responses to several environmental conditions, the modelling of leaf area expansion is still viewed with the "Big Leaf approach" in most models, i.e. leaf area index (LAI) is growing as a whole, without considering individual leaves and the effects of environmental conditions affecting them. A model of leaf development and leaf expansion has been developed as an APSIM module (Chenu et al., 2008) to simulate the effect of QTL of responses of leaf elongation to soil water deficit (Chenu et al., 2009). However, this study worked as a proof-of-concept, and did not consider the genetic variability of leaf development, final number of leaves, and responses of leaf widening. In addition, the number of genotypic parameters was very high and difficult to measure in phenotyping platforms on a large number of genotypes.

In order to simulate "real genotypes" and the resulting large variability of behaviours, it is timely to develop a model of leaf area expansion that includes individual leaf elongation, widening and development together with the responses of these processes to environmental conditions and with the associated genetic variability. In this chapter, we present a model aimed at applying to maize plants presenting the existing genetic variability of plant and leaf development, and of responses to environmental conditions.

Modelling strategy

The rationale of this strategy differs from that of models aiming at optimizing the prediction of model performance (eg. Asseng et al, 2013) or of models aiming at providing the best representation of a large number of plant processes and structure (FSPM, eg. (Fournier et al., 2005)).
- Most parameters are related to measured variables in phenotyping platforms that measure either leaf elongation with a time resolution of a few minutes (Phenodyn, (Sadok et al., 2007)), or whole plant expansion at a time resolution of one day (PhenoArch, Cabrera et al, 2016). Parameters were therefore either directly measured or calculated from easily-measurable variables when they were not themselves measurable for a large number of genotypes, rather than estimated via optimisation based on yield.
- A particular attention was given to the number of parameters. Genetic correlations between parameters were investigated and considered within formalisms when necessary. This has allowed us to reduce the number of parameters but also to consider real or virtual genotypes within the natural phenotypic space, i.e. not simulating genotypes with a combination of parameters which does not exist in the natural diversity to our knowledge.
- Formalisms applied to different traits including final leaf number (linked to plant earliness).

Plant growth and development was divided into underlying processes (Fig. 2.1) developed as an independent module implemented in APSIM-maize, but which is autonomous enough to be implemented later in a modelling platform such as BioMA, thereby allowing its re-use in different crop models. For each component of the module, a similar strategy was carried out: (i) choice of formalism based on a limited number of genotypes based on detailed measurements and involving various datasets (Fig. 2.2 and Table 2.1). (ii) Parameterisation of 254 hybrids based on a limited number of field and greenhouse experiments (Fig. 2.2 and Table 2.1). (iii) Implementation of module elements with parameter values for 254 hybrids into the crop model APSIM-maize and (iv) test on independent datasets. Accuracy for intermediate dynamic variables such as leaf expansion and

development was tested on the reference hybrid of the panel (B73_H) in several fields and on 16 hybrids in one field. Then, the model was tested on yield components by simulating the 254 hybrids in field experiments carried out in the DROPS project (Table 2.1). (v) Simulations in a large range of scenarios, presented in Chapters 3-5 of this thesis (Fig. 2.2).
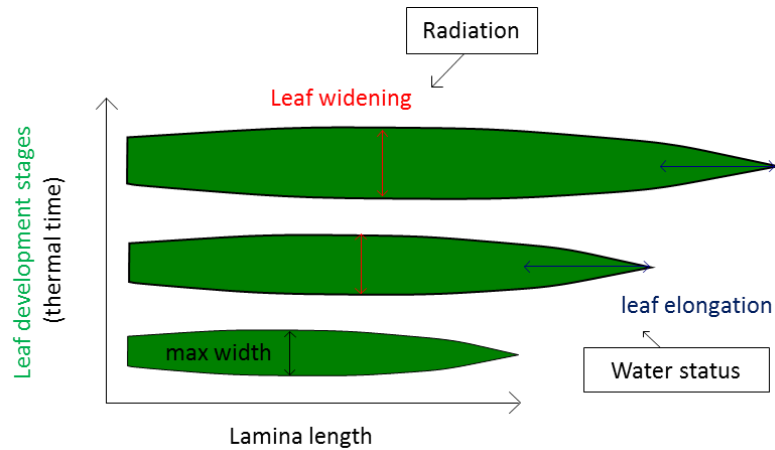

Figure 2.1 : Dissection of leaf growth into processes : Leaf development as a function of thermal time ; leaf expansion, composed of leaf elongation, affected by soil water deficit and evaporative demand and leaf widening, affected by intercepted radiation.
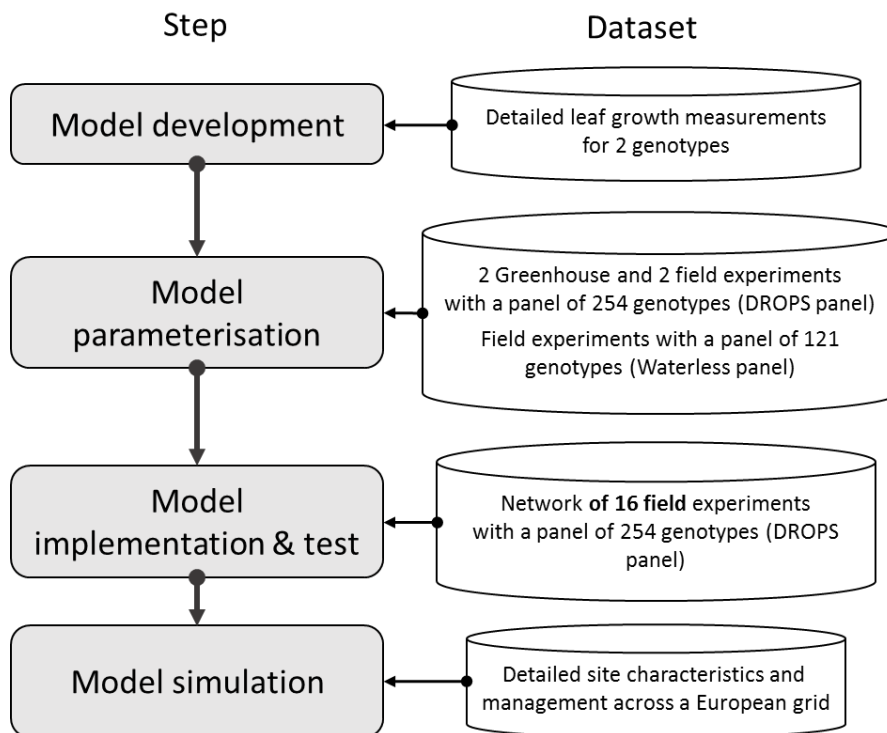
Figure 2.2 : Modelling strategy in 4 steps and involved datasets

Material and Methods

Effect of plant cycle duration (leaf number) on the profiles of final leaf length and width *(Data collected in previous studies, selected and analysed in this thesis)*

121 maize accessions (named "panel Waterless" below) representative of the main components of the maize genetic diversity were analysed in five field experiments in France (Fig. 2.2 and Table 2.1 – Dataset A), namely two in a Mediterranean site, Mauguio (43°36'37''N; 3°58'39''E; 23 m above sea level, asl) in 2006 and 2007, and three experiments in oceanic sites, Sainte Pexine (46°33'43''N; 1°08'17''W; 45 m asl), Le Magneraud (46°24'16''N; 00°04'45''E; 26 m asl) and Nerac (40°10'12''N; 00°18'36''E; 40 m asl). In each experiement, the experimental design was an alpha lattice with two replicates. Plots were 6 m long, with 0.8 m between rows and a plant density of 8 plants m^{-2}. Light, air temperature, relative humidity (RH) and wind speed were measured hourly in each experiment at 2 m height over a reference grass canopy. Light was measured with photosynthetic photon flux density sensors; air temperature and RH were measured in ventilated shelters. Soil water potential was measured every day at 30, 60 and 90 cm depths (two replicates). The length and width of every second leaf and leaf number were measured in 10 plants per plot. Final leaf area was estimated as the product of length and width by a common factor of 0.75, constant for all leaves (Fournier et al., 2005).

Genotypes were classified considering their final leaf number (N_{final}), linked to thermal time at flowering (Parent et al., 2017). Profiles of leaf dimensions (final leaf length, final maximum width, and final leaf area) for each class of N_{final} were calculated by using a smoothing function (function *loess* in R; span = 0.75) considering all genotypes of a class of N_{final} and the five experiments.

Time course of leaf development and growth in two hybrids *(Data collected in previous studies, selected and analysed in this thesis)*

Analysis of leaf development was performed on a dataset with measurements of leaf length and width for two genotypes with different leaf number every second day. The experiment was performed in the field in Mauguio (France) in 1998 (Table 2.1, Dataset B) and involved hybrids Déa (16 leaves) and Volga (19 leaves). Measurements were performed on all leaves, either mature or still enclosed in the whorl, by separating and unfolding leaves after whole plant dissection. This resulted in ten successive data point per leaf in average, with ten replicates for each hybrid.

This dataset was first summarised as the mean of 10 plants for leaf length and width of each leaf rank, genotype and date. The first four leaf ranks were not considered in view of their limited contribution to leaf area. The time courses of leaf elongation and widening were calculated as a function of thermal time with the smoothing function *loess* (in R; span = 0.5). The timings of beginning and end of leaf elongation were estimated as the 5% and 95% of final dimensions for each leaf rank. A similar analysis was used for leaf width.

Final leaf number in 254 maize hybrids *(measurements collected by myself in the field and phenotyping platform)*

Final leaf number (N_{final}) was measured in a field experiments carried out in 2016 in Saint Martin de Hinx (France) for 4 plants per genotype in a panel of 254 maize hybrids grown under well-watered conditions at a density of 10 plants m^{-2} (Table 2.1, "Panel DROPS", Dataset G). This panel covers the genetic diversity of dent maize and is fully described in Millet et al., 2016. Leaf number

corresponding to each genotype was calculated as the mean of the 4 replicates. Details on environmental conditions are summarised in SI Table 2.1.

Usage	Dataset	Module	Experiment	Location(s)	Year(s)	Genotype(s)	Variables	Frequency
Model Development	A	Leaf area growth	Field	Mauguio, France	1998	2 genotypes	leaf length and width	End of season
Model Parameterisation	B	Leaf area growth	Field	Network Europe	from 2006 to 2007	Waterless panel (121 elite maize genotypes)	leaf length and width	Every two days
							phenology	Every two days
Model parameterisation	F	Leaf area growth	Greenhouse	Montpellier, France	2016	DROPS panel (254 hybrids)	phenology	End of season
							Potential leaf growth	Dynamic
							Leaf growth sensitivity	Dynamic
	G	Leaf area growth	Field	Saint-Martin de Hinx	2016	DROPS panel (254 hybrids)	maximum leaf number	End of season
	H	Leaf area growth	Greenhouse	Montpellier, France	2015	reference hybrid B73	Leaf growth sensitivity	Dynamic
	I	Leaf area growth	Greenhouse	Montpellier, France	2013	Panel DPE	Leaf growth sensitivity	Dynamic
Model test	C	Leaf area growth	Field	DROPS network	from 2011 to 2013	reference hybrid B73	leaf length and width	End of season
	D	Yield determination	Field	DROPS network	from 2011 to 2013	DROPS panel (254 hybrids)	grain number	End of season
							grain yield	End of season
	E	Leaf area growth	Field	Mauguio, France	2016	16 hybrids from the DROPS panel	leaf length and width	End of season

Table 2.1 : Summary of datasets used for each steps of model development, model test and model parameterisation

Parameters for leaf development and whole plant leaf expansion in 254 maize hybrids
(Data collected and analysed in previous studies and re-analysed during this thesis)

An experiment was carried out in the phenotyping platform *PhenoArch* (Montpellier, France, Cabrera-Bosquet *et al.*, 2016; https://www6.montpellier.inra.fr/lepse/M3P) in 2016 (Table 2.1, "Panel DROPS", dataset G and details in SI. Table 2.1). Briefly, the *PhenoArch* platform is equipped with automated weighting and watering stations, imaging stations and environmental sensors. For each plant, 13 RGB images (2056×2454 pixels) were taken every night (one from top and 12 side images with a 30° horizontal rotation). Temperature and vapour pressure deficit (VPD) were recorded every 15 min in 8 sites of the greenhouse. The daily mean temperature in the greenhouse was 18±2 °C (night) and 25±3°C (day). Plants were grown in 9L PVC pots filled with a substrate composed of a mixture of clay and organic compost (30/70 volume). Three seeds per pot were sown at 0.025m depth, and thinned to one plant per pot at three-leaf stage. Soil water content was maintained at retention capacity in each pot by daily watering (soil water potential of -0.05MPa) in well-watered conditions. In the water deficit treatment, watering was withdrawn from the appearance of leaf 8 until soil water potential reached the target soil water potential -0.4 MPa. Soil water potential was then maintained by daily irrigation. A second dry-down period was applied to

plants until soil water potential reached -0.6 MPa The number of repetitions was 2 and 2 in well-watered and water deficient plants, respectively.

The numbers of leaves with appeared tip or ligule were scored every second day for all plants in the experiment. Leaf area was estimated by image analysis every second day. The increase in leaf area (m² °Cd^{-1}) in well-watered conditions was considered as the maximum genotypic leaf expansion rate at the considered phenological stage (m² °Cd^{-1}). The sensitivity of leaf expansion to soil water deficit (m² °Cd^{-1} MPa^{-1}) was calculated as the difference in leaf expansion rate between well-watered and soil water deficit conditions from the appearance of leaf 8 to that of leaf 14, divided by the difference in soil water potential and normalised by leaf expansion rate in well-watered conditions.

Leaf expansion rate with a definition of minutes in a subset of 16 hybrids (*I have carried out this experiment and have analysed resulting data during the thesis*)

An experiment was performed in the phenotyping platform *Phenodyn* (Montpellier, France - https://www6.montpellier.inra.fr/lepse/M3P - Table 2.1, dataset E ; SI. Table 2.1) for measuring leaf elongation rate and its sensitivity to soil water deficit at individual leaf level with a definition of 15 min. We aimed at comparing the sensitivity to soil water deficit of leaf elongation rate of individual leaves with that of whole-plant leaf expansion rate in the *PhenoArch* platform. A subset of 16 genotypes was selected from the 254 hybrids ("Panel DROPS") for maximising the genetic variability of leaf expansion rate.

Three plants of each hybrid were grown under either well-watered conditions or water deficit within the phenotyping platform *PhenoDyn*. The soil was a mixture of clay and organic compost, in pots with a height of 40 cm and a diameter of 15cm (Table 2.1, dataset E; SI. Table 2.1). The photoperiod was 14 hours day and 10 hours night with additional light from 7:00 to 20:00 when light decreased below 450 W m^{-2}. Air temperature was kept between 15°C at night and 28°C during the day with an intermediate value of 22°C from 21:00 to 0:00 (SI. Table S3). Air humidity, air temperature (HMP35A Vaisala Oy, Helsinki, Finland) and leaf temperature (thermocouples) were measured every 15 min. Leaf elongation rate (LER) was measured every 15 min with rotating displacement transducers (RDTs 60-1045 Full Smart Position Sensor; Spectrol Electronics, Ltd, Wiltshire, England) as in Sadok *et al*. (2007). LER of leaf 6 was measured from leaf 6 appearance for 5 days (during stable maximum leaf elongation rate). It was expressed per unit thermal time at each 15 minute time step. Plants under well-watered conditions were maintained at a soil water potential higher than -0.05 MPa via automatic irrigation. In the water deficit treatment, watering was stopped at appearance of leaf 5 and soil was left to naturally dry until reaching -1.5 MPa. Tip and ligule appearances were scored every day, and their rates were calculated for each genotype with a linear regression with thermal time. The genotypic maximum LER of leaf 6 was estimated for each genotype as the mean LER of well-watered plants during the night (from 20:00 to 6:00). The sensitivity of leaf elongation rate to soil water potential was estimated for each hybrid by fitting a linear regression between the mean LER from 20:00 to 6:00 and the mean soil water potential sensed by plants for the same period of time.

Estimating parameters of the APSIM model based on field measurement in 254 maize hybrids (*Data collected and analysed in previous studies, re-analysed during this thesis*)

The maximum number of grain per ear and the maximum individual grain weight were estimated for the 254 maize hybrids (Panel DROPS) from two field experiments from the total of 23 field

experiments of the DROPS and AMAZING projects (Table 2.3). The experiments were carried out in the DROPS project (Millet et al., 2016; Lacube et al., 2017) in 2011 to 2013 (19 field experiments) or Amaizing projects in 2014/2016 (4 field experiments). A well-watered and a water deficit treatment were applied. Final leaf sizes (lamina length and leaf maximum width) of all non-senescent leaves for the reference hybrid B73_H were measured in both water deficit and well-watered conditions, in all DROPS experiments in 2011 to 2013 (19 experiments - Table 2.1, Dataset D). This was extended to 16 hybrids in one field experiment (Mauguio 2016) (including 8 genotypes for the 8 genetic families structuring the panel and 8 genotypes selected for their contrasting behaviours under water deficit) (Table 2.1, Dataset E). The final grain yield (kg) and individual grain weight (gr) were measured at harvest time (Table 2.1, Dataset C).

In APSIM maize, grain number is related to plant growth rate (PGR: mean daily accumulated biomass) around flowering, with a plateau at high plant growth rates. In addition, Millet et al. (2016) showed that grain number decreases with night temperature in the network. To estimate the parameter 'maximum grain number per plant' in all genotypes, we have therefore selected the site from the total of 14 field experiments with the lowest mean night temperatures during the flowering period of the reference hybrid B73_H (SI Fig. 2.1). Parameter values for the sensitivity of grain number to night temperature in 254 hybrids were those of Millet et al., 2016 calculated from 11 field experiments of DROPS in 2012 and 2013. Grain weight depends on the amount of biomass allocated to the grain during grain filling, which in well-watered conditions is only limited by plant intercepted radiation. For estimating maximum weight per grain (parameter values in 254 genotypes), we have therefore selected the site with maximum intercepted radiation of the reference hybrid B73 during grain filling (Fig. 2.2 b; Table 2.1, Dataset D). All other parameters of APSIM were considered as common to all studied hybrids, with values stated in Harrison et al., 2014.

Model test on a dataset of 254 maize hybrids in 16 European environments *(Data collected and analysed in previous studies, reanalysed during this thesis)*

A test of the model was performed based on experimental data collected for the 254 maize hybrids grown in the field experiments of DROPS (20 experiments) and AMAZING (3 experiments). Simulations were performed by using data related to management practices, namely sowing and harvest date, sowing density, sowing depth, fertiliser application and irrigation reported by experimenters. Hourly local meteorological data were converted to APSIM daily weather files ('.met'). Three tests were performed:
- Final leaf length and width were simulated for one hybrid (reference hybrid B73) in 20 field experiments and compared with those measured in the same fields.
- The same was performed for 16 hybrids in one field experiment (Mauguio, 2016).
- Simulated grain number and grain yield were compared with measured values for 254 hybrids in 14 experiments.

Table 2,3 : Summary of all field experiments of the combined DROPS and Amaizing network. Meteorological data is summarized as the mean, minimum , maximum or sum of daily values between sowing and harvest, for each experiment.

Location	Country	Year	ID	Latitude (°N)	Longitude (°E)	Altitude (m)	Sowing date (day)	Density (plants.m^{-2})	T_{max} (°C)	T_{min} (°C)	T_{mean} (°C)	VPD_{max} (kPa)	VPD_{min} (kPa)	VPD_{mean} (kPa)	RAD_{sum} (MJ/m²)
Bernburg	France	2014	Ber14	51.8	11.73	85	16/05/2014	8.22	34.6	1.4	16.3	23.0	7.0	13.6	2346
Blois	France	2014	Blo14	47.74	1.22	82	6/05/2014	9.60	34.0	1.4	16.5	24.0	7.0	13.8	2683
Cadriano	Italy	2012	Cad12	44.93	11.88	5	17/05/2012	6.25	38.2	-2.8	20.7	30.0	5.0	17.0	2302
Campagnola	Italy	2011	Cam11	45.17	9.53	49	10/05/2011	6.43	37.7	8.6	22.5	42.0	11.0	19.8	3111
Campagnola	Italy	2012	Cam12	45.17	9.53	49	23/05/2012	6.43	37.6	9.5	22.6	25.0	12.0	18.8	3040
Campagnola	Italy	2013	Cam13	45.17	9.53	49	14/06/2013	5.71	36.2	5.7	21.6	28.0	9.0	18.2	2509
Caracal	Romania	2012	Car12	44.12	24.35	101	21/05/2012	6.73	40.8	7.1	23.9	29.0	10.0	18.5	2679
Gaillac	France	2012	Gai12	43.89	1.99	150	14/05/2012	8.44	40.8	2.8	20.0	27.0	7.0	15.5	3067
Gaillac	France	2013	Gai13	43.89	1.99	150	13/05/2013	8.75	36.2	2.0	19.1	28.0	7.0	15.9	2951
Karcag	Hungary	2011	Karc11	47.18	20.54	81	13/05/2011	6.67	35.5	1.8	20.0	24.0	7.0	15.7	2920
Karcag	Hungary	2012	Karc12	47.18	20.54	81	21/05/2012	5.68	37.7	1.3	20.3	24.0	7.0	16.0	2795
Karcag	Hungary	2013	Karc13	47.18	20.54	81	23/05/2013	7.07	37.4	-2.8	18.2	25.0	5.0	14.4	2474
Karlsruhe	Germany	2011	Karl11	49.07	8.28	115	4/05/2011	8.22	33.8	1.7	17.6	22.0	7.0	14.1	2902
Karlsruhe	Germany	2012	Karl12	49.07	8.28	115	11/05/2012	8.22	35.1	2.1	17.2	23.0	7.0	14.2	2693
Karlsruhe	Germany	2013	Karl13	49.07	8.28	100	20/05/2013	8.22	36.3	2.3	16.6	25.0	7.0	14.3	2947
Martonvasar	Hungary	2013	Mar-13	47.32	18.78	110	14/05/2013	5.87	38.1	-4.8	17.6	27.0	4.0	13.9	3122
Mauguio	France	2011	Mau11	43.61	3.98	13	14/05/2013	7.50	33.6	4.2	20.2	25.0	8.0	17.2	4010
Mauguio	France	2016	Mau16	43.61	3.98	13	16/05/2011	7.22	35.3	-1.9	15.5	25.0	5.0	13.4	5577
Murony	Hungary	2013	Mur13	46.78	21.05	85	22/05/2013	6.67	38.3	-2.6	19.3	27.0	5.0	15.5	2659
Nerac	France	2011	Ner11	44.17	0.31	40	13/05/2011	6.90	39.0	5.5	20.6	23.0	9.0	15.4	2886
Nerac	France	2012	Ner12	44.17	0.31	40	28/05/2012	7.44	39.0	3.6	20.6	25.0	8.0	16.4	2675
Nerac	France	2013	Ner13	44.17	0.31	40	15/05/2013	7.35	38.5	1.0	19.5	25.0	7.0	14.6	2842
Satolas	France	2014	Sat14	45.75	5.07	236	15/05/2014	9.50	35.4	5.2	18.5	25.0	9.0	14.9	2894

Results

Modelling leaf development from records of leaf tip and ligule appearances

Modelling the expansion of individual leaves requires the timing of beginning and end of linear elongation and widening. Because these variables cannot be collected at high throughput, we have simulated them based on the easily-scored dates of appearance of leaf tip and ligule. Fig. 2.3 presents the increase with time of leaf length and width from leaf 5 to final leaf number for two genotypes with contrasted cycle durations, estimated via final leaf number (dataset B). The length and width stayed close to zero in all leaves for 42°Cd after initiation, then it increased rapidly until reaching final dimensions.
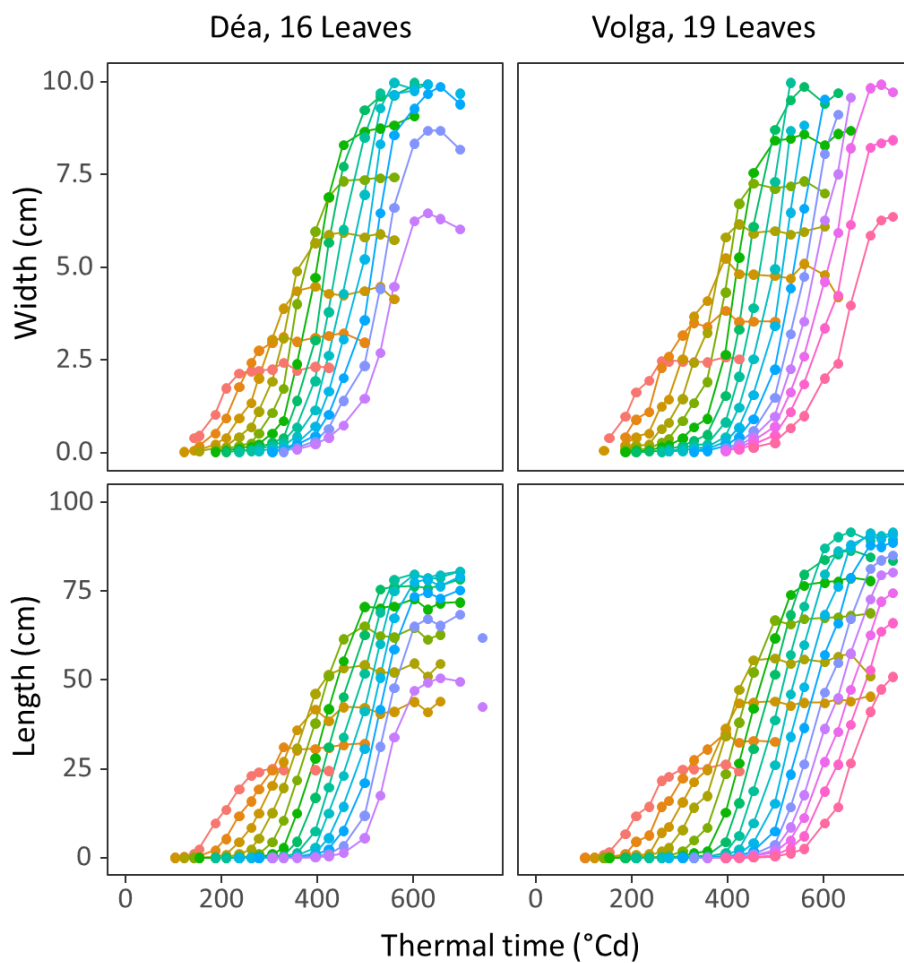
Figure 2.3 : Leaf width and length as a function of thermal time for 2 genotypes with contrasting cycle durations (estimated by leaf number : Déa : 16 leaves, Volga : 19 leaves). Colors, leaf ranks from 5 to 19. Data points, mean values for 10 plants per date and rank.

Increase of leaf elongation rate as a function of thermal time was linear for 3-6 d, as shown by time courses with temporal definitions of minutes (Welcker et al., 2011). We have therefore considered the time courses in Fig. 2.3 with a linear approximation, with the x-intercept of linear regressions considered as the beginning of linear elongation. In both genotypes, beginning of linear elongation was synchronous with the appearance of leaf tip for the first 6 leaves (Fig. 2.4 A,B). For higher leaf ranks, leaves started to elongate linearly before appearance, when they were hidden by the whorl of

older leaves. Leaf tips appeared sequentially with a common appearance rate (a_{tip}) if expressed per unit of thermal time.

$$N_{tip,tt} = a_{tip} * tt + b_{tip}$$ (Eq. 2.1)

with N_{tip} the number of appeared leaves, a_{tip} the rate of leaf tip appearance , b_{tip} intercept of regressions and tt the thermal time after plant emergence.
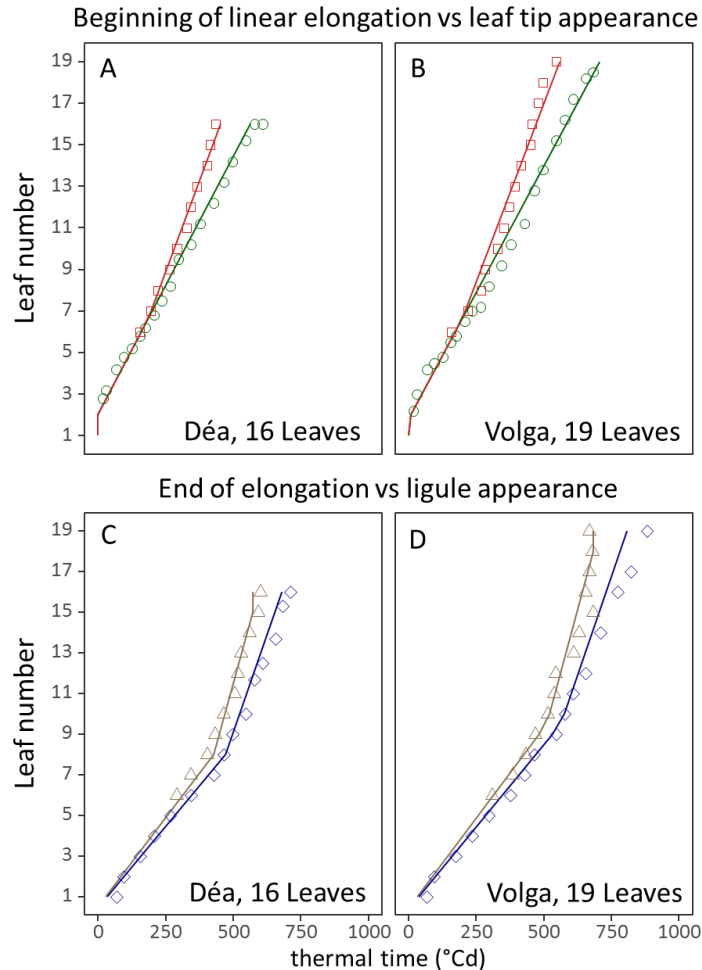
Figure 2.4 : Measurements (points) and simulations (lines) of leaf development stages for two genotypes with contrasting cycle durations, Déa, 16 leaves (A and C) and Volga, 19 leaves (B and D). Red squares, beginning of linear elongation ; green circles, leaf tip appearance ; grey triangles, end of elongation ; blue diamonds, leaf ligulation.

We have modelled the number of leaves having started linear elongation (N_{bl}) as a function of the number of appeared tips via two successive linear function (Fig. 2.4, R^2 = 0.97). The first equation 2.2 applies to the first 6 leaves in which the beginning of linear elongation occurs simultaneously with leaf tip appearance. For leaf 7 onwards, (N_{lim}, leaf 6 in both genotypes), the beginning of linear elongation (a_{bl}) differed from leaf tip appearance but was still correlated to it with a parameter (k_{bl}) valid for the two hybrids and considered common to all hybrids.

$$N_{bl,tt} = max(N_{tip} ; a_{bl} * tt + b_{bl})$$ (Eq. 2.2)

$$a_{bl} = k_{bl} * a_{tip}$$ (Eq. 2.3)

Hence, the intercept of the linear regression between thermal time and the number of leaves having started linear elongation (b_{bl}) can be calculated from the time course of leaf appearance, with two genotypic parameters (b_{tip} and a_{tip}) easily calculated from phenotypic data.

$$b_{bl} = [(N_{lim} - b_{tip}) * (k_{bl} - 1)] + b_{tip} \qquad \text{(Eq. 2.4)}$$

In the same way, we have calculated the time of the end of linear elongation from measurements of ligule appearance. The end of linear elongation and the time of ligule appearance diverged from the first leaves onwards, and were related via two linear relationships with a break point at leaves 7 to 9 depending on final leaf number (Fig. 2.4 C,D). We have therefore simulated the increase with thermal time of the number of leaves with appeared ligule ($N_{ll,tt}$) with two linear function (slopes a_{ll1} and a_{ll2}), with the breakpoint depending on the final leaf number of the considered genotype ($\alpha_{Tr} * N_{final}$). The ratio of the two slopes was common to both genotypes. We have considered the first slope (a_{ll1}) as a genotypic parameter, and the second slope (a_{ll2}) as linked to the first one with a proportional factor independent of the genotype (k_{ll}). Both intercepts are calculated from a genotypic parameter (tt_{ll1}) representing the thermal time of ligulation of the first leaf since appearance (at emergence). This results in the following equations:

for $Leaf\ rank \leq k_{ll}\ N_{final}$

$$N_{ll,tt} = a_{ll1}tt + b_{ll1} \qquad \text{(Eq. 2.5)}$$

$$b_{ll1} = 1 - (a_{bll1} * tt_{ll1}) \qquad \text{(Eq. 2.6)}$$

for $Leaf\ rank > k_{ll}\ N_{final}$

$$N_{ll,tt} = a_{ll2}tt + b_{ll2} \qquad \text{(Eq. 2.7)}$$

$$a_{ll2} = k_{ll}a_{ll1} \qquad \text{(Eq. 2.8)}$$

$$b_{ll2} = \frac{[(k_{ll}\ N_{final} - b_{ll1}) * (a_{ll1} - a_{ll2})]}{a_{ll1}} + b_{ll1} \qquad \text{(Eq. 2.9)}$$

In order to link the appearance of ligules and the end of leaf elongation, we have considered the time difference (Lag) between these two stages for each leaf (respectively $tt_{ll,n}$ and $tt_{el,n}$). For a given leaf, Lag increased linearly with leaf number from a base value (Lag$_0$) and was similar in the two hybrids. The last two leaves stopped elongation simultaneously. This results in the following equations:

If $Leaf\ rank\ (n) \leq N_{final} - 2$

$$tt_{el,n} = tt_{ll,n} - Lag \qquad \text{(Eq. 2.10)}$$

Lag =Lag$_0$ x n, with Lag$_0$ being common to the two genotypes

If $Leaf\ rank\ (n) \leq N_{final} - 2$

$$tt_{el,n} = tt_{el,n-1} \qquad \text{(Eq. 2.11)}$$

The timing of leaf widening (from beginning of widening at $tt_{bw,n}$ to end of widening at $tt_{ew,n}$) for all leaves (n) was derived from the timing of leaf elongation. We have previously shown that leaf widening ends before leaf elongation for a considered leaf (Chapter 1, Lacube et al., 2017) and that this duration can be considered as stable regardless of genotypes. We therefore used the calculated

period of leaf elongation to calculate that of leaf widening, starting with leaf elongation and ending before it ($lag_w = 39$ °Cd; Lacube et al., 2017), resulting in the following equation.

$$tt_{bw,n} = tt_{bl,n} \qquad\qquad\qquad\qquad\qquad\qquad\qquad\qquad \text{(Eq. 2.12)}$$

$$tt_{ew,n} = tt_{el,n} - lag_w \qquad\qquad\qquad\qquad\qquad\qquad \text{(Eq. 2.13)}$$

The resulting formalism uses only 5 genotypic parameters that can be easily calculated from phenological measurements, namely final leaf number, the parameters of the regressions between thermal time and leaf tip appearance (slope and intercept), and those between thermal time and ligule appearance (slope and intercept). This formalism was used for the panel of 254 hybrids of the DROPS panel (dataset G). The final leaf number (N_{final}) was measured for each genotype in a field experiments (Saint Martin de Hinx, France) and parameters for the timings of tip and ligule appearance were collected in the phenotyping platform PhenoArch (dataset F), thereby allowing the calculation of the timings of beginning and end of linear elongation for all leaves and all genotypes. An example is provided in (Fig. 2.5 A) for the reference hybrid, together with the two hybrids that allowed building the model (Fig. 2. 5 BC).
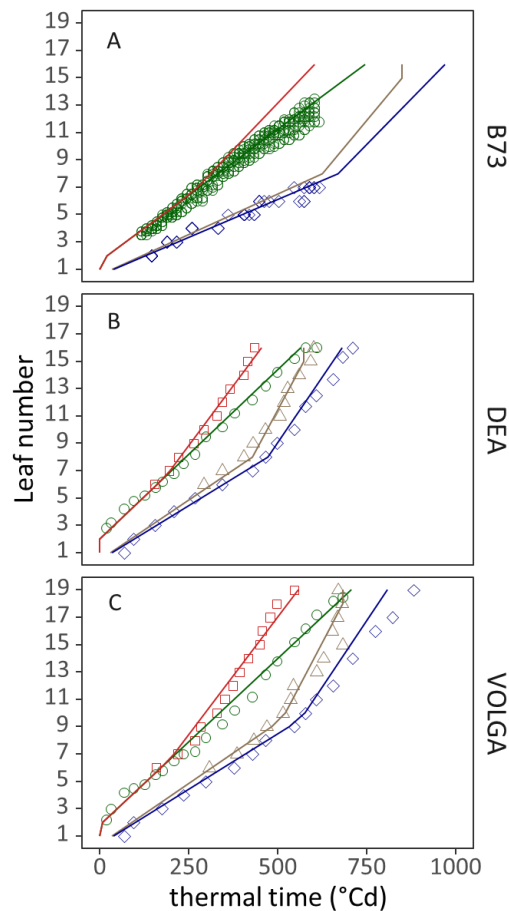
Figure 2.5 : Measurements (points) and simulation (lines) of leaf development stages for three genotypes. B73 (A); Déa (B) and Volga (C) Red squares, beginning of linear elongation; green circles, leaf tip appearance; grey triangles, end of elongation; blue diamonds, leaf ligulation.
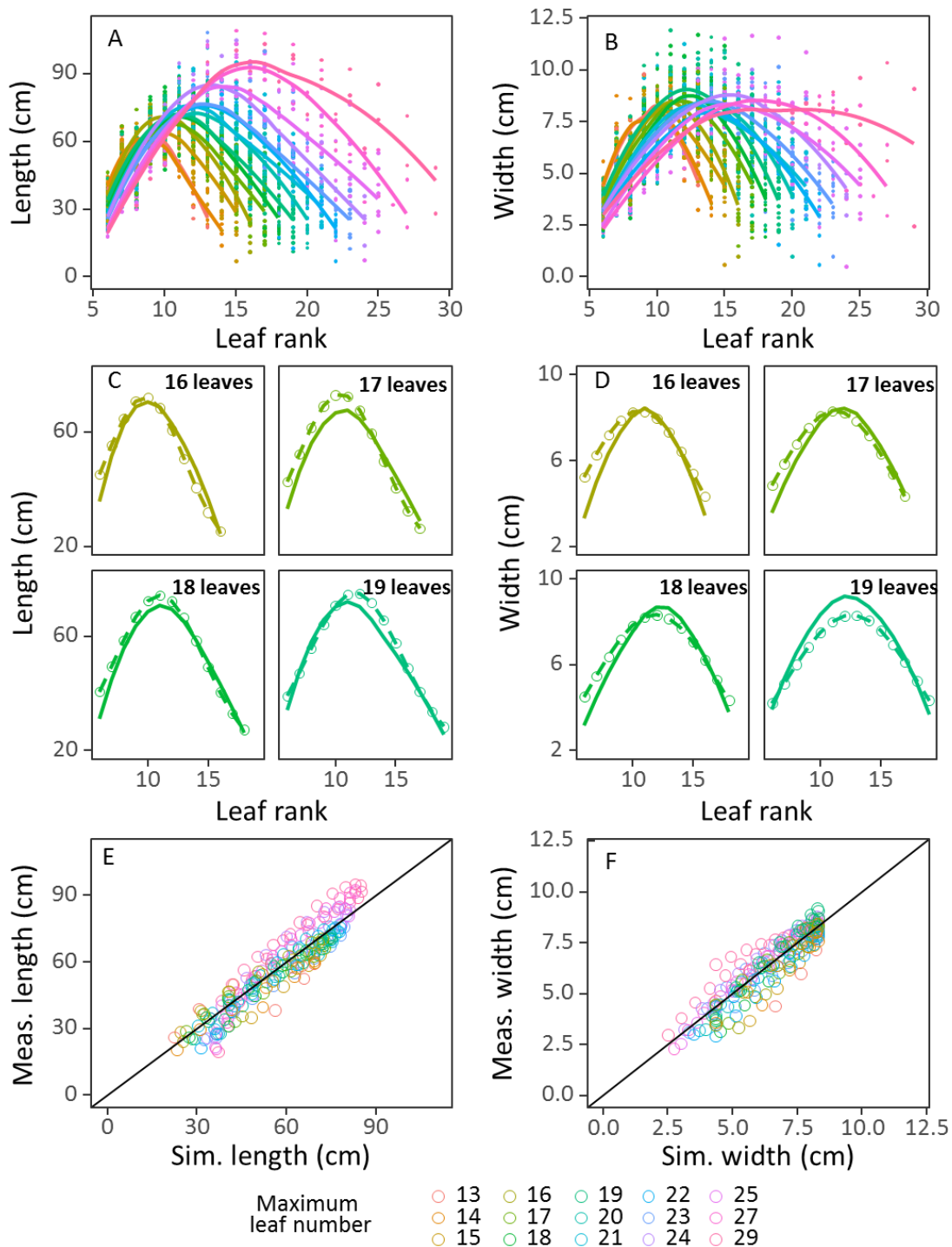
Figure 2.6 : Final leaf length (A) and width (B) as a function of leaf rank for genotypes presenting contrasting cycle durations, estimated by leaf number from 14 to 29. Symbols, measurements; lines, smoothed relations for classes of genotypes with different final leaf number. (C and D) Simulated and calculated relationships between leaf rank and eaf length (C) and width (D), for four classes of genotypes with different leaf numbers Solid line : Model, dashed line : measurements. (E and F) Scatterplot of simulated and measured values of leaf length (E) and width (F) for all studied genotypes. Colors in A, B, E and F, classes of genotypes with common leaf number.

Simulation of the profile of leaf elongation rate along the stem

The maximum leaf elongation rate for a given leaf position on the stem was modelled based on final leaf length measured in 5 well-watered field experiments with low evaporative demand, for 121 genotypes differing in final leaf number (Panel Waterless, dataset I; Fig. 2.6A). Hybrids were sorted into classes with common final leaf number (step: 2 leaf ranks), showing a pattern with a maximum leaf length at a position on the stem that depended on final leaf number (Fig. 2.6A). The same applied to leaf width (Fig. 2.6B).

For modelling purpose, we have considered the ratio of the maximum elongation rate of the considered leaf n (α_n) to that of leaf 6. We have linked this parameter to leaf rank with a two-parameter Beta function (parameters β and σ, representing the rank of the leaf with the highest growth rate and the curvature of the curve) and considered these two parameters as depending on final leaf number. This resulted in the following equation:

$$\alpha_n = 2 * \Sigma^2 * \frac{e^{\frac{-(n-B)^2}{2*\Sigma^2}}}{e^{-(n-B)^2}} \qquad\qquad \text{(Eq. 2.14)}$$

with $B = \beta * N_{final}$ and $\Sigma = \sigma * N_{final}$

Parameters of equation 2.14 were calculated based on the measured profiles of final leaf length for each class of hybrids in Fig 2.6A). This model adequately described the profiles of leaf length each class (Fig. 2.6C).

The time course of leaf elongation rate was modelled at an hourly time-step by considering the effects of temperature, evaporative demand and soil water potential, as presented in chapter 1. The effect of temperature was taken into account via the calculation of thermal time in APSIM-maize, with canopy temperature ($tht_{h,canopy}$) calculated at an hourly time step. The elongation rate of leaf 6 was calculated as:

$$LER_{6,day} = \sum_{h=1}^{h=24} LER_{6,h} \qquad\qquad \text{(Eq. 2.15)}$$

$$LER_{6,h} = (a + b * VPD_h + c * PSI_h)\,(tht_{h,canopy}) \qquad\qquad \text{(Eq. 2.16)}$$

with a, maximum elongation rate of leaf 6 (mm °Cday^{-1}) ; b, effect of vapour pressure deficit on leaf 6 elongation (mm °Cday^{-1}kPa^{-1}); c, the effect of soil water deficit on leaf 6 elongation (mm °Cday^{-1}MPa^{-1}) ; VPD, leaf-to-air vapour pressure difference (kPa) ; PSI, soil water potential (MPa). The elongation rate of any growing leaf was then calculated from that of leaf 6 by using α_n as calculated in Eq. 2.14:

$$LER_{n,\,day} = LER_{6,\,day} * \alpha_n \qquad\qquad \text{(Eq. 2.17)}$$

Hence, this formalism uses three genotypic parameters, namely the plant leaf number, the maximum leaf elongation rate of leaf 6 and its sensitivity to soil water potential. The sensitivity to evaporative demand, has a high genetic correlation with that to soil water potential, and was therefore considered as a non-independent parameters (Fig. 2.7). The other parameters of Eq. 14-17 were considered as common to all genotypes of maize, and were optimized for obtaining the best possible predictions in the whole range of studied genotypes.

Parameters a and c were estimated at the whole-plant level for the 254 hybrids of the DROPS panel in the phenotyping platform PhenoArch (dataset F), with a time definition of one day in an experiment with contrasting soil water status. Indeed, measurement based on single-leaf measurements at a definition of minutes is not feasible for such a high number of plants. We have

checked that this approximation was correct by comparing values measured on whole plants every day with those measured in individual leaves every 15 min. Values were highly correlated ($R^2 = 0.58$) so we have considered for the model the values of a and c measured in the PhenoArch platform. The sensitivity to evaporative demand (b) was calculated based on that of soil water status as in Welcker et al, (2011) (Fig. 2.7).
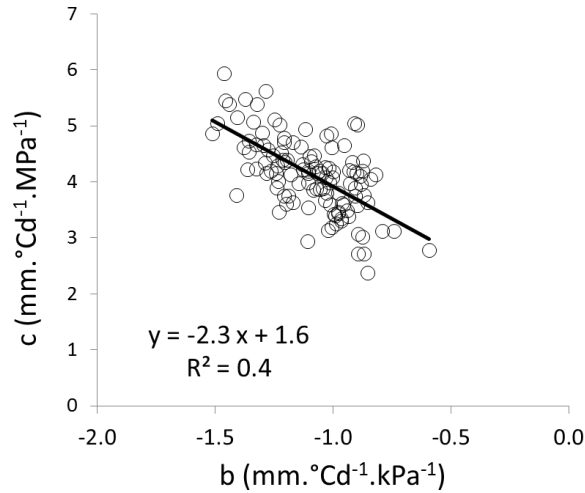

Figure 2.7 : Relationship between the parameters representing the sensitivity of leaf growth to vapour pressure deficit (b) and the sensitivity of leaf growth to soil water potential (c). Each point represents a genotype from a panel of 243 for which both sensitivities were calculated from the linear regression of 15 minutes leaf 6 elongation rate data and respectively vapour pressure deficit (for parameter b) and soil water potential (for parameter c), in a set of 16 experiments in the greenhouse and growth chamber, in well-watered and water deficit conditions.

Simulation of the profile of leaf widening along the stem

Leaf widening was simulated with (i) a reference genotypic value of width for any given leaf position on the stem and an intercepted light of 1.5 W m^{-2} plant^{-1} for the period of leaf widening ($W_{base,n}$), (ii) a genotypic sensitivity to intercepted radiation (RAD_{int}) as calculated in Chapter 1, and (iii) the profile of leaf width as a function of leaf position on the stem. Both the reference genotypic value and the genotypic sensitivity were parametrised from a linear regression using measured width corrected for the effect of leaf number and estimated plant intercepted radiation in a set of platform (PhenoArch) and field experiments (DROPS network in 2012 and 2013). This was tested for the panel of 254 hybrids described in Chapter 1 for leaves 6 to 8. Leaf width increases with the amount of radiation intercepted by the plant in the period of widening:

$$W_n = W_{base,n} + \left(d * \left(\frac{\left(\sum_{emergence}^{beg.\ elong.} RAD_i \right)}{tt_{emergence}^{beg.\ elong.}} - 1.5 \right) \right)$$

(Eq. 2.18)

The profile of leaf width in plants with any leaf number was modelled based on five field experiments with 121 genotypes (Waterless panel, dataset A, Fig. 2.6B). A clear pattern appeared, with similar widths for the different classes of genotypes (to the difference of leaf length in Fig 2.6A) but different positions on the stem of the leaf with maximum width, depending on the leaf number of the considered genotype. The function describing the profile of leaf width as a function of leaf rank $W_{base,n}$ involved four classes of leaf rank.

- Leaf ranks with common leaf width:

A common value of width (W_{min}) was observed for the first leaves until a leaf rank depending on final leaf number (ratio: L_{rank}):

$n \leq L_{rank} * N_{final}$

$$W_{base,n} = W_{min} \qquad (Eq.\ 2.19)$$

with $W_{min} = 1.5\ cm$ and $L_{rank} = 0.2$ regarless of genotype

- Leaf ranks with increasing leaf width:

A second class involved leaf ranks for which leaf width increases between two leaf ranks,

$n \leq L_{rank} * N_{final}$ and $n \leq Rank_{max} * N_{final} - (Plateau * N_{final})\ /3$

$$W_{base,n} = W_{min} + (UpSlope * (n - L_{rank} * N_{final})) \qquad (Eq.\ 2.20)$$

with

$$UpSlope = \frac{(W_{max} - W_{min})}{\left((Rank_{max}*N_{final}) - (Plateau*N_{final})\ /3 - (L_{rank}*N_{final})\right)}$$

$Rank_{max} = 0.66\ N_{final}$ for all genotypes

$Plateau = 0.29\ N_{final}$ for all genotypes

- Leaf ranks with a plateau width (third class of leaf ranks):

$n \leq Rank_{max} * N_{final} + (Plateau * N_{final})\ /3 - 1$

$$W_{base,n} = W_{max} \qquad (Eq.\ 2.21)$$

- Leaf ranks with decreasing width (fourth class of leaf ranks)

The slope of decrease with leaf rank was calculated in proportion of the previous upward slope

$n > Rank_{max} * N_{final} + (Plateau * N_{final})\ /3 - 1$

$$W_{base,n} = W_{base,\ (n-1)} - (UpSlope * SLopeScale * (n - LimSup)) \qquad (Eq.\ 2.22)$$

with

$LimSup = (Rank_{max} * N_{final}) + (Plateau * N_{final})\ /3 - 1$

$SlopeScale = 0.25$ in all genotypes, ratio between the increase in width in the second class of leaf ranks s and the decrease in width for the last leaves.

Overall this formalism of leaf widening uses two genotypic parameters, namely the final leaf number and the sensitivity to intercepted radiation. Other parameters were considered as non-genotypic and were optimised to best describe a range of genotype with a genotypic maximum leaf number between 10 and 30 leaves (Fig. 2.6B).

This formalism was able to reproduce the profiles of leaf width observed for the several classes of genotypes with contrasting final leaf number (Fig. 2.6D dataset A; R² = 0.78 for 16 leaves and R² = 0.84 for 19 leaves), with a regression of R² = 0.85 between observed and simulated data for all leaves of all classes of genotypes with common leaf numbers (Fig. 2.6F). For the 254 genotypes of the DROPS panel, we have used the final leaf number characterised above and the sensitivities of leaf width to intercepted radiation calculated in Chapter 1 (Lacube et al., 2017).

Simulation of the impact of leaf elongation rate on grain number

Grain number was simulated based on the current algorithm used in APSIM, which relates grain number to plant growth rate (PGR, g.m^{-2}d^{-1}) around flowering time, as modified by Chenu et al. (2008) in which the parameters of this relation depend on parameters affecting the genetic control of leaf elongation rate. The rationale for this modification is that the sensitivity of grain abortion is genetically linked to that of leaf elongation rate, via the control of silk elongation rate. Briefly, leaf

elongation rate and silk elongation rate show similar patterns in response to evaporative demand and soil water deficit and the sensitivities of both processes are closely linked in a collection of genotypes (Turc et al 2016). In turn, silk elongation rate is the main determinant of ovary abortion (Oury et al, 2016ab). This results in genetic correlations between the parameters of leaf elongation rate and those of grain number (Welcker et al., 2006; Chapuis et al., 2012).

In APSIM, grain number is calculated by taking into account the daily time course of PGR from 150 °C.d before silking to 260 °C.d after it. Grain number (GN) is calculated as a logarithmic function of the genotypic maximum grain number (GN_{max}), with a minimum PGR (PGR_{base}) at which grain number starts to increase, and a parameter of shape (GNk), the PGR at which 50% of GN_{max} is reached. Here, GN_{max} was estimated based on the four experiments with highest grain numbers, the shape parameter was kept common to all hybrids and PGR_{base} was affected in such a way that the most sensitive hybrids for grain number in water deficit were those that had the highest sensitivity of leaf growth to water deficit, as in Turc et al., 2016. For that, PGR_{base} linearly depended on the sensitivity of leaf growth to soil water deficit (c).

$$GN = GN_{max} * \left(1 - e^{-GN_k*(PGR - PGR_{base})}\right) \qquad \text{(Eq. 2.23)}$$

With $PGR_{base} = a + b * PSI_{effect}$ (Eq. 2.24)

An additional effect of air temperature on grain number was detected in the study of Millet et al. (2016). This was taken into account via a negative relation between grain number and mean night temperature ($\overline{T_{night}} - °C$) with the sensitivity ($r_{Tnight}$) evaluated in Millet et al. (2016).

$$GNfinal = GN - \left(\left(\overline{T_{night}} - 15\right) * r_{Tnight}\right) \qquad \text{(Eq. 2.25)}$$

Test of the model.

The resulting module includes nine genotypic parameters (Table 2.2) which have been parameterised for the 254 genotypes: maximum number of leaf (N_{final}), slopes and intercepts of the relationship of leaf appearance and ligulation with thermal time (a_{tip}, b_{tip}, a_{ll1}, b_{ll1}) maximum leaf elongation rate (a), sensitivities of leaf elongation to evaporative demand (b) and to soil water deficit (c), leaf widening sensitivity to plant intercepted radiation and sensitivity of grain number to night temperature (r_{Tnight}).

- The model was first tested on final leaf length and width of the reference hybrid B73_H measured in 19 fields. Simulations resulted in final dimensions close to those observed experimentally in well-watered conditions (R^2 for length: 0.96 and R^2 for width: 0.96, Fig. 2.8 A,B) and under water deficit (R^2 for length: 0.90 and R^2 for width: 0.89, Fig. 2.8 C,D). The model was therefore able to simulate the effect of environmental conditions on final leaf dimensions.
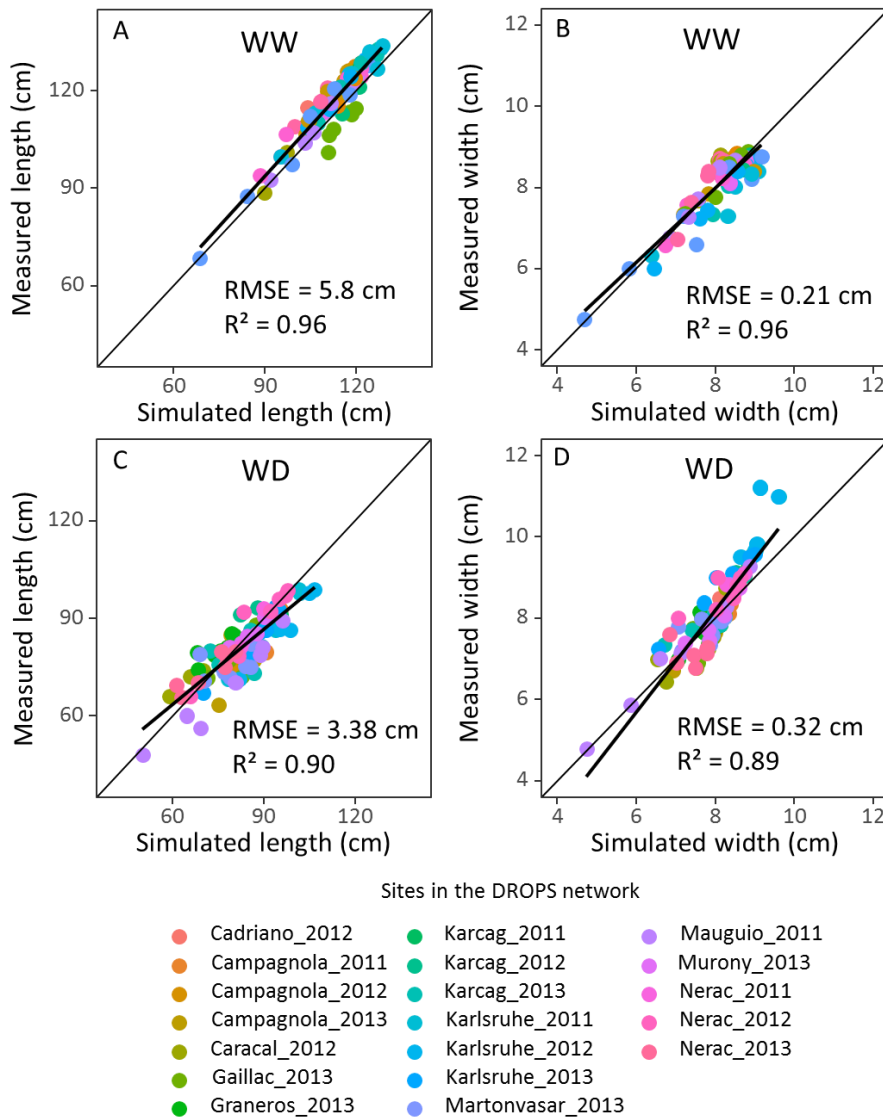

Figure 2.8: Measured and simulated final leaf length (A and C) and final leaf width (B and D) of the hybrid B73_H in well-watered (A and B) and water deficit (C and D) in a network of field experiments. Colours, experiments.

Table 2.2: Summary of all fixed and genotype dependent parameters in the model

Formalism	Variable	Parameter	Description	Unit	Status
		Nfinal	Maximum number of leaves	leaf	Genotype dependent
Leaf development phases	$N_{tip,tt}$: number of appeared leaves at thermal time "tt"	a_{tip}	Slope of the relationship between number of appeared leaves and thermal time	leaf °Cday^{-1}	Genotype dependent
		b_{tip}	Number of leaves appeared at emergence (at thermal time 0 °Cday)	leaf	Genotype dependent
	$N_{bl,tt}$: number of leaves that have started their linear expansion at thermal time "tt"	a_{bl}	Slope of the relationship between number of leaves at linear expansion and thermal time	leaf °Cday^{-1}	Fixed
		b_{bl}	Intercept of the number of leaves at linear expansion with thermal time	leaf	Fixed
		k_{bl}	Ratio between a_{tip} and a_{bl}	(-)	Fixed
		N_{lim}	Number of leaves at which the slope of N_{tip} and N_{bl} differs with thermal time	leaf	Fixed
	$N_{ll,tt}$: number of ligulated leaves at thermal time "tt"	a_{ll1}	First slope of the relationship between number of ligulated leaves and thermal time	leaf °Cday^{-1}	Genotype dependent
		b_{ll1}	Intercept of the number of ligulated leaves with thermal time	leaf	Genotype dependent
		a_{ll2}	Second slope of the relationship between number of ligulated leaves and thermal time	leaf °Cday^{-1}	Fixed
		b_{ll2}	Intercept of the number of ligulated leaves with thermal time	leaf	Fixed
		k_{ll}	Relative leaf number at which the number of ligulated leaves with thermal time changes slope from all1 to all2	(-)	Fixed
	$tt_{el,n}$: thermal time of end of linear expansion of leaf n	Lag_0	Base value of the lag in thermal time between leaf ligulation and end of linear expansion	°Cday	Fixed
	$tt_{bw,n}$: thermal time of end of widening of leaf n	Lag_w	Thermal time difference, for all leaves, between end of leaf elongation and end of leaf widening	°Cday	Fixed
Leaf elongation	α_n : ratio of maximum leaf elongation rate of leaf n to that of leaf 6	β	Rank of the leaf with the highest growth rate of the expression of α_n with leaf number	(-)	Fixed
		σ	Curvature of the expression of α_n with leaf number	(-)	Fixed
	$LER_{6,h}$: leaf elongation rate of leaf 6 at hour h	a	maximum leaf elongation rate of leaf 6	mm °Cday^{-1}	Genotype dependent
		b	sensitivity of leaf elongation LER_6 to evaporative demand	mm °Cday^{-1}kPa^{-1}	Genotype dependent
		c	sensitivity of leaf elongation LER_6 to soil water deficit	mm °Cday^{-1}MPa^{-1}	Genotype dependent
Leaf widening	W_n : maximum width of leaf n	d	sensitivity of leaf width to intercepted radiation	cm MJ °Cday^{-1} m^{-2}	Genotype dependent
	$W_{base,n}$: base leaf width of leaf n	W_{min}	Value of the minimum base leaf width	cm	Fixed
		L_{rank}	Relative rank of the last leaf with minimum base leaf width	(-)	Fixed
		W_{max}	Value of the maximum base leaf width	cm	Fixed
		$Rank_{max}$	Relative rank of the leaf with maximum base leaf width	(-)	Fixed
Grain number	GN_{final} : calculated final grain number	r_{Tnight}	sensitivity of grain number to mean night temperature (base temperature of 15°C)	grain °C^{-1}	Genotype dependent

- The model was then tested by simulating leaf expansion in a set of 16 genotypes in one experiment (Fig. 2.9). The results showed that the model was able to simulate the effect of the genetic variability on final leaf dimensions (R^2 for length = 0.87 and R^2 for width = 0.92).
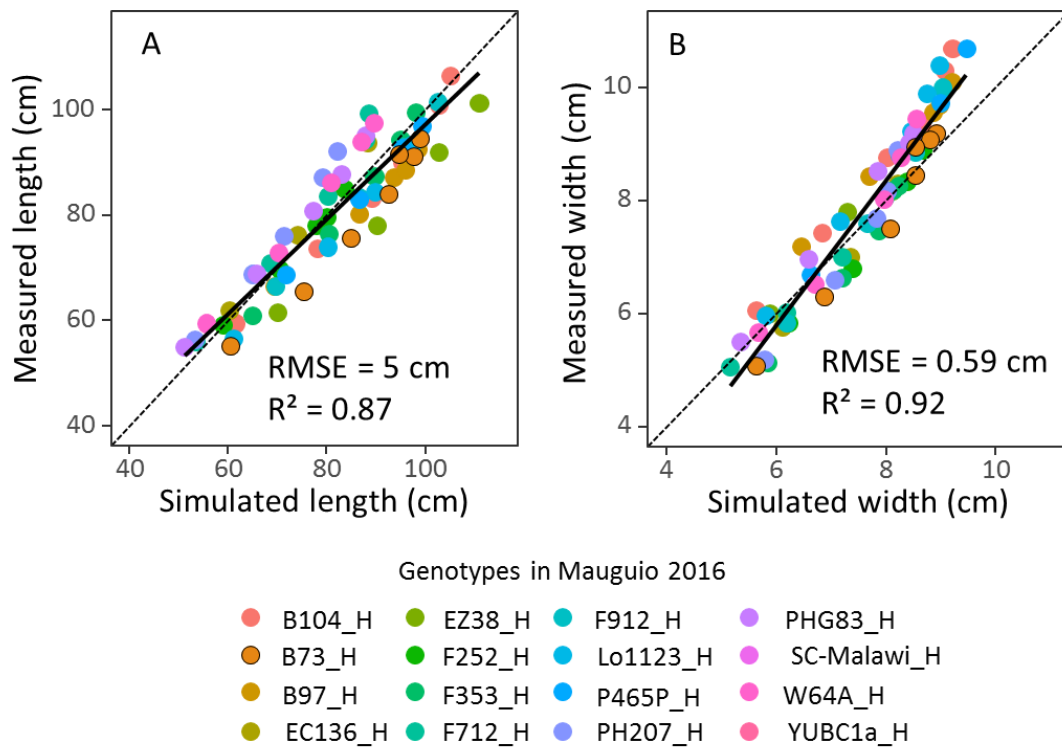
Figure. 2.9: Observed and measured values of final leaf length (A) and width (B) for a set of 16 hybrids in one field experiment (Mauguio 2016). Colors, different hybrids. Points highlighted in black show the reference hybrid B73_H. Solid black line, linear model.

- Finally, the model was tested by comparing predicted and observed yield and grain number for the 254 in the 14 field experiments of 2012 and 2013, Fig. 2.10A,B). The model explained from 12 to 57% of the measured variability of grain number (Fig. 2.10C), and from 8 to 35% of grain yield (Fig. 2.10C), depending on the experiment.

Site	R^2_{GN}	R^2_{GY}
Cadriano_2012	0.12	0.15
Campagnola_2013	0.15	0.17
Caracal_2012	0.16	0.12
Gaillac_2012	0.29	0.33
Gaillac_2013	0.26	0.29
Graneros_2013	0.16	0.17
Karlsruhe_2012	0.4	0.35
Karlsruhe_2013	0.23	0.26
Martonvasar_2013	0.57	0.22
Murony_2013	0.28	0.29
Nerac_2012	0.27	0.31
Bernburg_2014	0.27	0.19
Blois_2014	0.24	0.08
Satolas_2014	0.17	0.22

Sites in the DROPS and AMAZING network

- Bernburg_2014
- Blois_2014
- Satolas_2014
- Cadriano_2012
- Campagnola_2013
- Caracal_2012
- Gaillac_2012
- Gaillac_2013
- Graneros_2013
- Karlsruhe_2012
- Karlsruhe_2013
- Martonvasar_2013
- Murony_2013
- Nerac_2012

Figure 2.10 : (A and B) Simulated (y-axis) and observed (x-axis) grain number (A) and grain yield (B) for the DROPS panel of 254 hybrids simulated over the network of 13 environments. One point represent the mean measured yield or grain number per hybrid in each experiment. Colors show the different combinations of sites and years. (C) Table of calculated R squares (calculated with the function 'lm', R software) for each site, between simulated and measured grain number (GN) and grain yield (GY)

Discussion

This study had the ambitious purpose of developing a model adapted to the large genotypic variability found in a panel of 254 genotypes. This has required the use of nine large datasets obtained in different conditions, namely experiments in two phenotyping platforms, low-throughput field experiments with few genotypes and detailed measurements of leaf length and width, and high throughput experiments with measurements of yield and yield components of all hybrids and leaf dimensions of one hybrid. This strategy is therefore labor-intensive and needs to concentrate on a few panels of genotypes. It also requires that different datasets are available and easily accessible, which was not the case here. Some datasets used in Chapters 1 and 2 were stored on old floppy disks, so an appreciable part of the work has consisted of first reading, and then making sense of these datasets in the absence of appropriate metadata. This experience stresses the need for FAIR access of datasets (findable, accessible, interoperable and reusable). The absence of these standards has caused a considerable extra work in this study.

In spite of the large datasets used here, we were still short of data for several processes. This explains why the model was established on two hybrids only, thereby obliging one to take decisions for modelling based on limited experimental evidence. We accept that several equations could have been written with a different form. However, the module presented here is probably one of those best backed on experimental data. We shall shortly have access to more datasets allowing to either accept these decisions or to change them.

The limited number of genotypic parameters was a necessary condition for designing a model in which parameters are directly measured, or estimated via measurements of traits presenting a short "phenotypic distance" with parameters. Limiting the parameter number was based on different arguments.

- It was in some cases based on the experimental result of the absence of genetic variability of the considered parameter. This is the case for the response of growth and development processes to temperature which has been shown to be common to genotypes with diverse origins, in particular either tropical or temperate (Parent and Tardieu, 2012).

- In other cases, it was based on an experimentally-established genetic correlation, as in the case of the genetic correlation between the sensitivities to water deficit of leaf growth and abortion rate (Turc et al, 2016, Chapuis et al, 2016) or of the sensitivities of leaf elongation rate to soil water deficit and evaporative demand (Welcker et al, 2011).

- In many cases, it was a deliberate exercise aiming at obtaining independent parameters based on model design and/or intuition, for example in the relation of the genotypic leaf number and the parameters controlling the profiles of leaf width or length.

- Finally, we have to acknowledge that in some case this choice was linked to the absence of available data, so the parsimony principle led us to consider that parameters did not differ between genotypes.

In spite of the limits mentioned above, the model was successfully tested on its ability to represent the variations in leaf dimensions between environments for one genotype, the variations in leaf dimensions between genotypes in one environment, and the variations in yield in a network of field experiments. We are therefore confident on the fact that the model can be used for simulating the consequences of plant development and of leaf traits on yield, as presented in chapters 3-5.

It is probably useful to re-affirm here that the purpose of this model was not to improve yield predictions for a standard genotype, but to provide elements for designing genotypic ideotypes for different regions and environmental scenarios, including those in future climates (Chapter 4). It is unlikely that the improved generality of our model mechanically translates to more accurate yield predictions for one genotype. An avenue for progress would be to predict the model parameters used here as a function of genetic markers, based on QTL allelic effects and/or genomic predictions. This avenue is currently followed, on the same datasets, by Emilie Millet in Wageningen and by Santiago Alvarez Prado in LEPSE.

References

Boyer JS (1970) Leaf Enlargement and Metabolic Rates in Corn, Soybean, and Sunflower at Various Leaf Water Potentials. Plant Physiology **46:** 233-235

Cabrera-Bosquet L, Fournier C, Brichet N, Welcker C, Suard B, Tardieu F (2016) High-throughput estimation of incident light, light interception and radiation-use efficiency of thousands of plants in a phenotyping platform. New Phytologist **212:** 269-281

Casadebaig P, Zheng B, Chapman S, Huth N, Faivre R, Chenu K (2016) Assessment of the Potential Impacts of Wheat Plant Traits across Environments by Combining Crop Modeling and Global Sensitivity Analysis. PLOS ONE **11:** e0146385

Chapuis R, Delluc C, Debeuf R, Tardieu F, Welcker C (2012) Resiliences to water deficit in a phenotyping platform and in the field: How related are they in maize? European Journal of Agronomy **42:** 59-67

Chenu K, Chapman SC, Hammer GL, McLean G, Salah HB, Tardieu F (2008) Short-term responses of leaf growth rate to water deficit scale up to whole-plant and crop levels: an integrated modelling approach in maize. Plant Cell Environ **31:** 378-391

Chenu K, Chapman SC, Tardieu F, McLean G, Welcker C, Hammer GL (2009) Simulating the yield impacts of organ-level quantitative trait loci associated with drought response in maize: a "gene-to-phenotype" modeling approach. Genetics **183:** 1507-1523

Fournier C, Durand JL, Ljutovac S, Schaufele R, Gastal F, Andrieu B (2005) A functional-structural model of elongation of the grass leaf and its relationships with the phyllochron. New Phytol **166:** 881-894

Gouache D, Bogard M, Pegard M, Thepot S, Garcia C, Hourcade D, Paux E, Oury F-X, Rousset M, Deswarte J-C, Le Bris X (2017) Bridging the gap between ideotype and genotype: Challenges and prospects for modelling as exemplified by the case of adapting wheat (Triticum aestivum L.) phenology to climate change in France. Field Crops Research **202:** 108-121

Guérif M, Duke CL (2000) Adjustment procedures of a crop model to the site specific characteristics of soil and crop using remote sensing data assimilation. Agriculture, Ecosystems & Environment **81:** 57-69

Hammer GL, Kropff MJ, Sinclair TR, Porter JR (2002) Future contributions of crop modelling—from heuristics and supporting decision making to understanding genetic regulation and aiding crop improvement. European Journal of Agronomy **18:** 15-31

Hammer GL, van Oosterom E, McLean G, Chapman SC, Broad I, Harland P, Muchow RC (2010) Adapting APSIM to model the physiology and genetics of complex adaptive traits in field crops. Journal of Experimental Botany **61:** 2185-2202

Harrison MT, Tardieu F, Dong Z, Messina CD, Hammer GL (2014) Characterizing drought stress and trait influence on maize yield under current and future conditions. Glob Chang Biol **20:** 867-878

Hoogenboom G, White JW, Messina CD (2004) From genome to crop: integration through simulation modeling. Field Crops Research **90:** 145-163

Lacube S, Fournier C, Palaffre C, Millet EJ, Tardieu F, Parent B (2017) Distinct controls of leaf widening and elongation by light and evaporative demand in maize. Plant, Cell & Environment**:** n/a-n/a

Martre P, Quilot-Turion B, Luquet D, Memmah M-MO-S, Chenu K, Debaeke P (2015) Chapter 14 - Model-assisted phenotyping and ideotype design A2 - Sadras, Victor O. *In* DF Calderini, ed, Crop Physiology (Second Edition). Academic Press, San Diego, pp 349-373

Millet EJ, Welcker C, Kruijer W, Negro S, Coupel-Ledru A, Nicolas SD, Laborde J, Bauland C, Praud S, Ranc N, Presterl T, Tuberosa R, Bedo Z, Draye X, Usadel B, Charcosset A, Van Eeuwijk F, Tardieu F (2016) Genome-Wide Analysis of Yield in Europe: Allelic Effects Vary with Drought and Heat Scenarios. Plant Physiology **172:** 749-764

Oury V, Caldeira CF, Prodhomme D, Pichon J-P, Gibon Y, Tardieu F, Turc O (2016) Is change in ovary carbon status a cause or a consequence of maize ovary abortion in water deficit during flowering? Plant Physiology

Oury V, Tardieu F, Turc O (2015) Ovary apical abortion under water deficit is caused by changes in sequential development of ovaries and in silk growth rate in maize. Plant Physiology

Parent B, Shahinnia F, Maphosa L, Berger B, Rabie H, Chalmers K, Kovalchuk A, Langridge P, Fleury D (2015) Combining field performance with controlled environment plant imaging to identify the genetic control of growth and transpiration underlying yield response to water-deficit stress in wheat. J Exp Bot **66:** 5481-5492

Parent B, Tardieu F (2012) Temperature responses of developmental processes have not been affected by breeding in different ecological areas for 17 crop species. New Phytologist **194:** 760-774

Parent B, Tardieu F (2014) Can current crop models be used in the phenotyping era for predicting the genetic variability of yield of plants subjected to drought or high temperature? J Exp Bot **65:** 6179-6189

Rosenzweig C, Jones JW, Hatfield JL, Ruane AC, Boote KJ, Thorburn P, Antle JM, Nelson GC, Porter C, Janssen S, Asseng S, Basso B, Ewert F, Wallach D, Baigorria G, Winter JM (2013) The Agricultural Model Intercomparison and Improvement Project (AgMIP): Protocols and pilot studies. Agricultural and Forest Meteorology **170:** 166-182

Rötter RP, Tao F, Höhn JG, Palosuo T (2015) Use of crop simulation modelling to aid ideotype design of future cereal cultivars. Journal of Experimental Botany **66:** 3463-3476

Saab IN, Sharp RE (1989) Non-hydraulic signals from maize roots in drying soil: inhibition of leaf elongation but not stomatal conductance. Planta **179:** 466-474

Sadok W, Naudin P, Boussuge B, Muller B, Welcker C, Tardieu F (2007) Leaf growth rate per unit thermal time follows QTL-dependent daily patterns in hundreds of maize lines under naturally fluctuating conditions. Plant Cell Environ **30:** 135-146

Tardieu F (2012) Any trait or trait-related allele can confer drought tolerance: just design the right drought scenario. Journal of Experimental Botany **63:** 25-31

Tardieu F, Cabrera-Bosquet L, Pridmore T, Bennett M (2017) Plant Phenomics, From Sensors to Knowledge. Current Biology **27:** R770-R783

Tardieu F, Parent B, Caldeira CF, Welcker C (2014) Genetic and physiological controls of growth under water deficit. Plant Physiol **164:** 1628-1635

Turc O, Bouteillé M, Fuad-Hassan A, Welcker C, Tardieu F (2016) The growth of vegetative and reproductive structures (leaves and silks) respond similarly to hydraulic cues in maize. New Phytologist **212:** 377-388

Welcker C, Boussuge B, Bencivenni C, Ribaut JM, Tardieu F (2006) Are source and sink strengths genetically linked in maize plants subjected to water deficit? A QTL study of the responses of leaf growth and of Anthesis-Silking Interval to water deficit. Journal of Experimental Botany **58:** 339-349

Welcker C, Sadok W, Dignat G, Renault M, Salvi S, Charcosset A, Tardieu F (2011) A Common Genetic Determinism for Sensitivities to Soil Water Deficit and Evaporative Demand: Meta-Analysis of Quantitative Trait Loci and Introgression Lines of Maize. Plant Physiology **157:** 718-729

Chapter 3: Simulation framework to study the impact of genetic variability of leaf expansion processes on maize yield over European environmental scenarios.

This chapter presents the necessary elements for running simulations at a European scale, as presented in chapters 4 and 5 of this thesis. It summarizes the developments I undertook for multi-site multi-year simulation. As such, it can be viewed as a 'material and method' for these simulations. It will be the publication that will follow chapter 5.

Simulation framework to study the impact of genetic variability of leaf expansion processes on maize yield over European environmental scenarios.

Sebastien Lacube[1], Margot Leclere[2], Llorenç Cabrera-Bosquet[1], Boris Parent[1] and François Tardieu[1]

[1] INRA, UMR759 LEPSE, F-34060 Montpellier, France

[2] UMR Agronomie, INRA, AgroParisTech, Université Paris-Saclay, 78850 Thiverval-Grignon, France.

Abstract

The different processes of leaf development, elongation and widening studied in chapter 1 and 2 of this thesis have been implemented in the crop model APSIM-maize in Chapter 2. This results in a modified version of APSIM-maize, able to integrate and simulate the effects on yield of the genotypic variability of leaf growth, including growth and developmental parameters such as final leaf number, leaf appearance rate, ligule appearance rate, leaf growth rate and sensitivities. Further adaptations were implemented in the model to study the impact of the genetic variability of leaf expansion processes on maize yield over European environmental scenarios. We first present the network of European sites used in simulations, together with environmental and management information associated with each site. We then present the fine tuning of phenology in APSIM for European genotypes with varying cycle duration. Finally, the workflow for multi-site multi-year simulation is presented, together with the methods that were developed for the analysis of model outputs.

Introduction

Further development were needed in addition to the the modules presented in chapter 1 and 2 for simulating yields of a range of hybrids in contrasted European environments as presented in chapter 4 and 5 :

- First, simulation of yields over a set of environments around Europe requires establishing a network of European sites that represents the diversity of environmental conditions in which maize is grown in Europe. This involves designing this network, collecting environmental data associated with each site based on European information systems, but also collecting and/or simulating management practices such as irrigation, sowing dates, harvesting dates, and fertilisation rates.

- Secondly, taking into account the genotypic diversity of cycle duration requires some fine tuning of the APSIM-maize model, which were not presented in chapter 2 which deals with the establishment of leaf area. In particular, a fine tuning of the simulation of plant phenological stages was necessary to take into account the non-photoperiodic control of flowering time in European maize genotypes, and to adjust the respective duration of each phase of development in genotypes with varying whole-cycle duration.

- Finally, the process of multi-site multi-year simulation requires procedures allowing one to carry out large number of simulations in an automatized way.

This chapter first presents the network of European sites, with environmental and management information associated with each site. It then presents the fine tuning of the phenology in APSIM-maize for European genotypes with varying cycle duration. The workflow for simulations is then presented, together with the methods that were developed for multi-site multi-year simulations and for the analysis of model outputs.

A network of European sites with the necessary information to run the model

Presentation of the network

We have used the network of sites designed by Harrison et al. (2014), which consisted of 55 European sites in 11 countries in which maize is currently grown. The number of sites selected in each country was proportional to the maize area in this country. Four sites have been added to this network for improving the regularity of the spatial distribution of sites. This results in a network of 59 sites presented in Fig. 3.1 and Table 3.1.

Figure 3.1 : Locations of the 59 sites used in model simulation in Europe. *Points*: sites location; *Grey zones*: mountains; *black lines*: limits between countries.

Meteorological data used here are 36 years of daily weather (1975-2010) from (i) the AGRI4CAST database of the Joint Research Network (https://ec.europa.eu/jrc/en) for the 55 sites of Harrisson al. (2014) and (ii) the INRA CLIMATIK database for the four added sites. The 36 years were considered with a mean atmospheric CO_2 concentration of 380 ppm. Daily meteorological data were converted into input files of APSIM ('.met' files) which contains site-specific information (name, latitude, longitude and altitude) and a table of daily environmental data, namely year, day of year, minimum temperature ('minT') and maximum temperature ('maxT'), rainfall ('rain' in mm), incident radiation ('radn' in $MJ\ m^{-2}$), and wind speed ('wind' in $m\ s^{-1}$).

Climate scenarios in 2050 were simulated at each site by using the stochastic weather generator LARS-WG (Semenov and Stratonovitch, 2010) and were based on climate projections from the Coupled Model Intercomparison Project Phase 5 (CMIP5) ensemble with two Representative Concentration Pathways (RCPs), namely 4.5 and 8.5 (487 and 541 ppm CO_2 in 2050) and four global circulation models (GCMs) in order to account for the uncertainty in the CMIP5 ensemble (namely GFDL-CM3, HadGEM2-ES, MIROC5, MPI-ESM-MR). Hundred years were generated for each combination of Site, RCP, and GCM.

Table 3.1 : Characteristics of the 59 sites used in model simulation. Columns : site name, latitude and longitude in degrees, mean sowing date, plant density (m^{-2}), amount of nitrogen applied at sowing (as NO$_3$N fertiliser in kg ha^{-1}) and value of the optimum genotype cycle duration, expressed as maximum leaf number.

Site	Longitude (°)	Latitude (°)	Sowing date	Density (plant.m²)	Nitrogen (NO3N gk.ha^{-1})	Optimum genotype (N$_{final}$)
Austria_Leibnitz	15.55	46.78	14/03	7.63	420	16
Bulgaria_General_Toshevo	28.03	43.72	01/04	6	700	21
Bulgaria_Glavinitsa	26.83	43.90	10/04	6	420	22
France_Achenheim	7.62	48.57	20/04	7.75	350	16
France_Avignon	4.80	43.94	20/03	7.51	70	22
France_Chemille	-0.72	47.20	10/04	7.66	560	17
France_Clermont_Ferrand	3.08	45.77	30/04	7.51	70	18
France_Estrees_Mons	3.00	49.88	20/04	7.72	560	16
France_Marmande	0.15	44.50	01/04	7.51	490	21
France_Montelier	5.03	44.95	01/04	7.51	70	21
France_Orthez	-0.77	43.48	01/04	7.42	490	21
France_Ouges	5.07	47.26	10/04	7.72	420	19
France_Palaminy	1.07	43.20	01/04	7.42	630	21
France_Pamproux	-0.05	46.38	20/04	7.6	420	18
France_Patay	1.70	48.05	20/04	7.72	490	16
France_Saint_Bonnet	0.10	45.48	01/04	7.57	490	20
France_Toulouse	1.43	43.60	20/03	7.45	630	23
France_Vitre	-1.22	48.12	10/04	7.72	630	16
Germany_Augsburg	10.90	48.37	30/04	10	490	15
Germany_Hanover	9.73	52.37	30/04	10	350	15
Germany_Werl	7.93	51.57	30/04	10	560	15
Greece_Evropos	22.57	40.92	20/03	7.3	420	26
Hungary_Foldeak	20.48	46.32	20/04	6	490	21
Hungary_Kondoros	20.80	46.77	30/04	6	630	19
Hungary_Kormend	16.60	47.02	20/04	6	490	18
Hungary_Lajoskomarom	18.33	46.85	10/04	6	630	20
Hungary_Nyirbator	22.13	47.83	20/04	6	420	19
Hungary_Ormenyes	20.58	47.18	10/04	6	700	21
Hungary_Papa	17.47	47.32	20/04	6	490	18
Hungary_Szederkeny	18.47	46.00	20/04	6	490	20
Italy_Asola	10.42	45.22	20/03	7.54	350	22
Italy_Bologna	11.35	44.50	20/03	7.51	350	24
Italy_Campoformido	13.17	46.02	01/04	7.6	350	22
Italy_Orgiano	11.47	45.35	20/03	7.54	280	24
Italy_Paese	12.15	45.67	20/03	7.57	350	24
Italy_Pantigliate	9.35	45.43	20/03	7.54	350	22
Italy_Santena	7.77	44.95	01/04	7.51	350	21
Poland_Tuszyn	16.65	50.80	30/04	7.87	560	15
Poland_Wrzesnia	17.57	52.32	30/04	7.97	350	15
Romania_Alexandria	25.35	43.98	10/04	6	420	22
Romania_Arad	21.32	46.17	20/04	6	490	21
Romania_Barca	23.63	43.97	01/04	6	490	22
Romania_Barlad	27.67	46.23	10/04	6	490	21
Romania_Botosani	26.67	47.75	20/04	6	630	18
Romania_Bulbacata	25.80	44.28	10/04	6	420	21
Romania_Chirnogeni	28.23	43.90	10/04	6	560	22
Romania_Daia_Romana	23.67	46.02	20/04	6	560	18
Romania_Dochia	26.57	46.92	20/04	6	490	16
Romania_Dor_Marunt	26.92	44.43	10/04	6	420	22
Romania_Gataia	21.43	45.43	20/04	6	420	21
Romania_Lovrin	20.77	45.97	20/04	6	420	21
Romania_Medgidia	28.27	44.25	01/04	6	630	22
Romania_Parscoveni	24.23	44.28	10/04	6	490	22
Romania_Puchenii_Mari	26.08	44.82	10/04	6	420	21
Romania_Salard	22.03	47.22	20/04	6	490	19
Romania_Viziru	27.70	45.00	10/04	6	350	21
Spain_Barbues	-0.42	41.98	20/03	7.3	210	22
Spain_Gomecello	-5.53	41.05	20/04	7.3	140	17
Spain_Villamanan	-5.58	42.32	30/04	7.36	280	16

Soil depths in every site ranged from 0.6 to 1.5 m, a reasonable range in European conditions. Soil parameters used by APSIM include, for each horizon (i) the depth and bulk density of the considered horizon, (ii) the lower limit of soil water content defined as the driest water content at which water extraction occurs (LL15), (iii) the upper limit or field capacity (DUL), (iv) the saturated water content limit above which the soil cannot retain water (SAT), (v) the rate at which water can be extracted in a given layer (KS) and (vi) the parameters describing the maximum water extraction in the considered layer for the considered species. In this study, the parameters describing water extraction in each layer were considered as non-genotypic. All parameters were either calculated from available data from the JRC network for each site, or derived from expert knowledge. The initial soil water content at the beginning of the 36-year simulations was set at field capacity for the whole soil profile in all sites. In further years, the final soil water content simulated at the end of each year was used as initial soil water content on the next year.

Sowing dates were calculated for each site by estimating the first day, calculated from the 35 years of climate data, for which the frequency of frost in the next 15 days is lower than 5% (Table 3.1). Harvesting dates were defined to occur during a time window after plant maturity that depended on soil water content. We have considered that harvest could not occur if soil water content exceeded 90% of field capacity in the upper soil layer, thereby simulating the impossibility for harvesting machines to enter into the considered field because of an insufficient load bearing capacity. No harvest possibility before 1st November resulted in a total yield loss due to high risk of ear fall or diseases, combined with the necessity for farmers to sow the next winter crop at that time.

We have optimised the nitrogen fertilization based on a first round of simulations aimed at testing a grid of values of nitrogen application levels (from 200 to 1200 NO_3N applied at sowing) and estimate optimum nitrogen application in each site (Table 3.1).

Three watering scenarios were used in further chapters. In the well-watered scenario daily irrigation was applied when the available soil water dropped below 90% of the maximum. No runoff was considered, with an efficiency of irrigation of 1. The rainfed scenario considered no irrigation. The irrigated scenario simulated irrigation if cumulated rainfall was less than 30 mm in the last seven days, with a minimum time of seven days before a new irrigation could be applied.

Environmental conditions sensed by virtual plants during simulated crop cycles

A first round of simulation was run with APSIM-maize with the reference hybrid to visualize environmental conditions sensed by plants during key phenological stages of plant managed with the rules presented above, in order to better characterize the network of sites. Minimum temperatures at simulated flowering time, averaged over 35 years, ranged from 12 to 19°C and maximum temperatures from 23 to 31°C (Fig. 3.2 C and D). On the same period, plant intercepted radiation ranged from 150 to 300 MJ Fig. 3.2, B. The degree of water deficit during flowering time in rain fed fields was simulated via the supply/demand ratio simulated in APSIM. The latter ranged from 1 in conditions in which plants do not suffer any drought to 0.3 in very severe water deficits. Fig. 3.2, A presents the mean S/D ratio over the 35 years of simulation. Water deficit was frequent in southern sites, but appreciable water deficits were also observed in more northern sites. High year to year variabilities were observed in all cases. It is noteworthy that the very severe droughts simulated in Spain and Italy are not realistic for maize, which is irrigated in most cases in these regions.
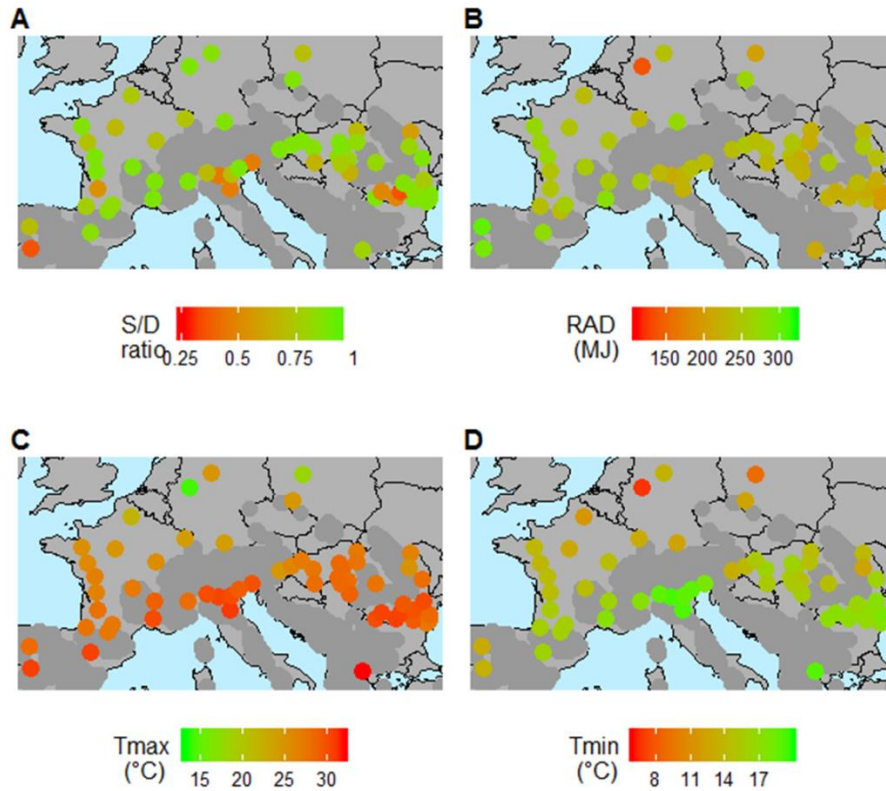
Figure 3.2: Environmental conditions in the network of European sites. (A) Distribution of soil depth, (B) distribution of water deficit estimated by supply /demand ratio, from 0.3 (severe stress, red) to 1 (well-watered, blue) (C,D)Distribution of maximum and minimum temperatures at flowering time, averaged in each site over 35 years. Circles, sites with maize simulations.
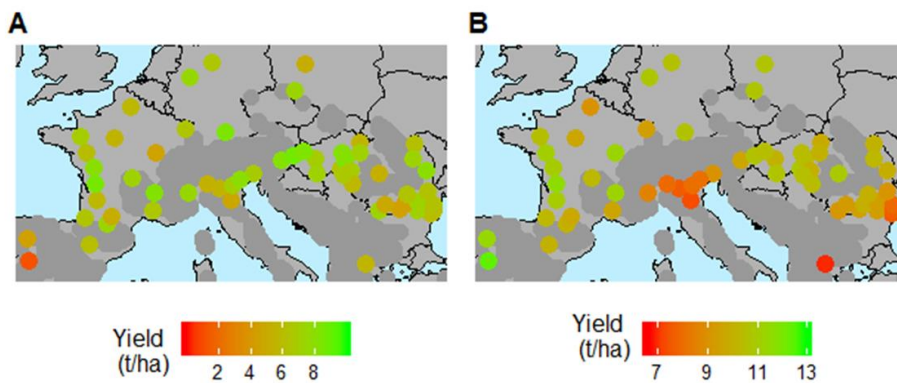

Figure 3.3: Simulated yields for maize. (A) Rain fed conditions (B) Irrigated conditions.

Maize yields simulated with APSIM ranged from 0.9 to 9.5 t Ha^{-1} in rain fed conditions, and from 7.5 to 12 t ha^{-1} in well-watered conditions (Fig. 3.3). This exactly corresponds to the range of yields that have been observed in the DROPS networks of experiments, thereby suggesting that the calibration of the model is correct. Highest yields were simulated in the deep soils of Eastern Europe, while sites at higher latitudes had intermediate yields. Yields were in a narrower range in well-watered conditions, the sites with highest performance slightly differed in rain fed and irrigated conditions, with highest yields in the Po valley.

Adapting the model for taking into account the genetic variability of phenology over Europe

Fine tuning the duration of APSIM phenological stages in genotypes with varying final leaf number

Maize phenology is characterised in APSIM by the thermal time that elapses between key phenological stages, namely sowing, plant emergence, end of juvenile phase (period after which plant development is affected by photoperiod, *endjuv*), floral initiation (end of sensitivity to photoperiod), flag leaf, flowering, beginning and end of grain filling and maturity (Fig. 3.4). The period of time from *endjuv* to floral initiation is affected by the photoperiod and is recalculated daily. A photoperiod higher than a critical value (12 hours) shortens the thermal time to floral initiation. The durations of other phases (expressed in thermal time) are model parameters.
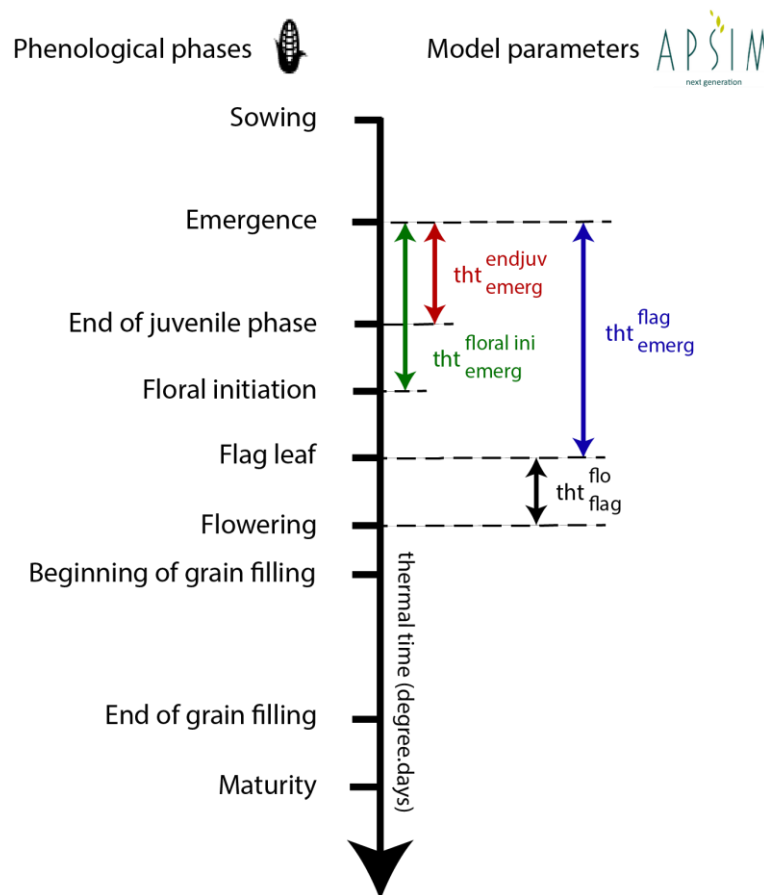

Figure 3.4: Maize phenological stages (left) with thermal time (from top to bottom) and parameters names in APSIM (right).

The model used here applies to temperate maize, in which the photoperiod has no effect on the duration of the period from emergence to floral initiation. Hence, the maximum leaf number and thermal time from emergence to floral initiation ($tht_{emerg\ to\ floral\ ini}$) are genotypic traits, independent of environmental conditions other than temperature. In the modified APSIM-maize, it depended on three parameters, namely leaf initiation rate (a_{ini}), the number of initiated leaves at emergence ($N_{ini\ at\ emerg} = 6$) and genotypic maximum leaf number (N_{final}). Leaf initiation rate was linked to leaf appearance rate (a_{tip}) by a non-genotypic factor ($k_{ini} = 2$) meaning that one leaf

appears when two leaves are initiated. This allowed calculation of the thermal time between emergence and floral initiation (Eq. 3.1).

$$tht_{emerg\ to\ floral\ ini} = LIR * (N_{final} - N_{ini\ at\ emerg})$$ (Eq. 3.1)

With: $LIR = k_{ini} * a_{tip}$

The end of the juvenile phase (*enjuv*) involves, in APSIM, switches in formalisms involved in processes other than flowering transition, in particular the first day for which a nitrogen deficiency affects leaf area, and the control of leaf area by a maximum specific leaf area. We had therefore to adjust the date of *endjuv* for genotypes with varying duration of the vegetative period. *Endjuv* was calculated as a constant (non-genotypic) fraction of the thermal time between emergence and floral initiation (Eq. 3.2; $\alpha_{endjuv} = 0.34$).

$$tht_{emerg\ to\ endjuv} = \alpha_{endjuv} * tht_{emerg\ to\ floral\ ini}$$ (Eq. 3.2)

The thermal time between emergence and flag leaf was defined as the thermal time of appearance of the last leaves (dependent of the genotypic maximum leaf number). The thermal time between emergence and flag leaf was modelled through the leaf appearance rate (Eq. 3.3).

$$tht_{emerg\ to\ flag\ leaf} = a_{tip} * (N_{final} - b_{tip})$$ (Eq. 3.3)

These formalisms therefore involved genotypic value for the final leaf number, the slope and intercept of the leaf appearance rate as a function of thermal time since sowing, as measured in three experiments in the PhenoArch platform over the whole panel, and a non-genotypic duration of the thermal time from flag leaf to flowering ($tht_{flag\ leaf\ to\ flo} = 10\ degree.days$ – non genotypic).

Adapting leaf senescence to genotypic variations of the leaf appearance rate

Senescence through ageing was simulated based on a linear equation with thermal time (Eq. 3.4). The intercept of beginning of leaf senescence (b_{sen}) was considered as non-genotypic, considering that the senescence of leaves 1-5 can begin at leaf 6 appearance ($N_{tip\ at\ sen} = 6$ leaves). The rate of leaf senescence (a_{sen}) was considered as linked to leaf tip appearance (a_{tip}) with a non-genotypic ratio (k = 0.29).

$$N_{senesced\ leaves} = a_{sen} * tht + b_{sen}$$ (Eq. 3.4)

With $a_{sen} = k * a_{tip}$ and $b_{sen} = \frac{(N_{tip\ at\ sen} - b_{tip})}{a_{tip}}$

The two non-genotypic parameters were calibrated to simulate leaf senescence in one experiment (Mauguio 2011, Table 2.1) for the reference hybrid B73 in well-watered conditions (Fig. 3.5). Whole plant leaf area and proportion of senescent leaves were estimated for three plants every seventh day throughout the growing season. Senescence was also linked to plant nitrogen status, with unchanged formalisms in relation to the standard APSIM-maize version.
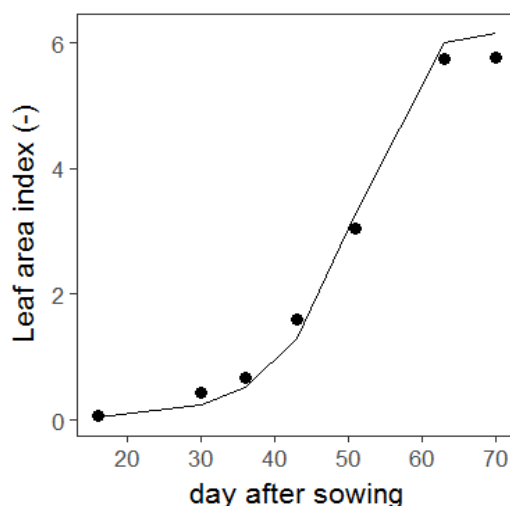
Figure 3.5: Measured (points) and simulated (line) leaf area index in one field experiment in Mauguio (2011). Circles: mean measurements of leaf area index calculated from whole plant non senescent leaf area in 3 plants per date; Line : simulated leaf area index with the modified version of APSIM-maize.

A workflow for high throughput model simulation

Because the APSIM user interface involves too much user intervention, it was not adapted for multi-site multi-year simulations requiring millions of runs. We have developed an automatic procedure in the language 'R' (version 3.3.3) to dialog with the APSIM model (Fig. 3.6). The main R script (Figure SI 3.1) uses various libraries to read raw data (meteorological, site management, field or platform measurements) and write all files used by APSIM. It then directly dialogs with APSIM for simulation, reads the outputs and stores them in an R object, which uses far less space than all simulation output files combined in a computer folder. As an example, a simulation with 55 locations, for 36 years, 254 genotypes, and 3 watering scenarios produces more than 100 000 files that can use more than 10 Gb of storage whereas an R object containing the same dataset uses less than 100 Mb.

Model simulation characteristics were written with a file system called 'eXtensible Markup Language' (XML). The XML language uses a system of tags that can be created and defined by the user. These tags can represent all the parameters of the simulation. Those parameters can be as simple as the simulation name, the initial water content of the first soil layer, or the value of a genotypic parameter. The use of this file system allows organisation of simulations as an arborescence. This arborescence is easily read from any software adapted for code development (R software or Matlab) and each tag can be searched to automatically change parameters value directly into the code, without using the APSIM interface. As a result, parameters values that are calculated for many genotypes via data analysis in R scripts can be directly used as model parameters, making multi-genotype simulation easier. The final simulation files are of type XML, saved with a new extension name '.apsim' to be recognisable by the APSIM model.
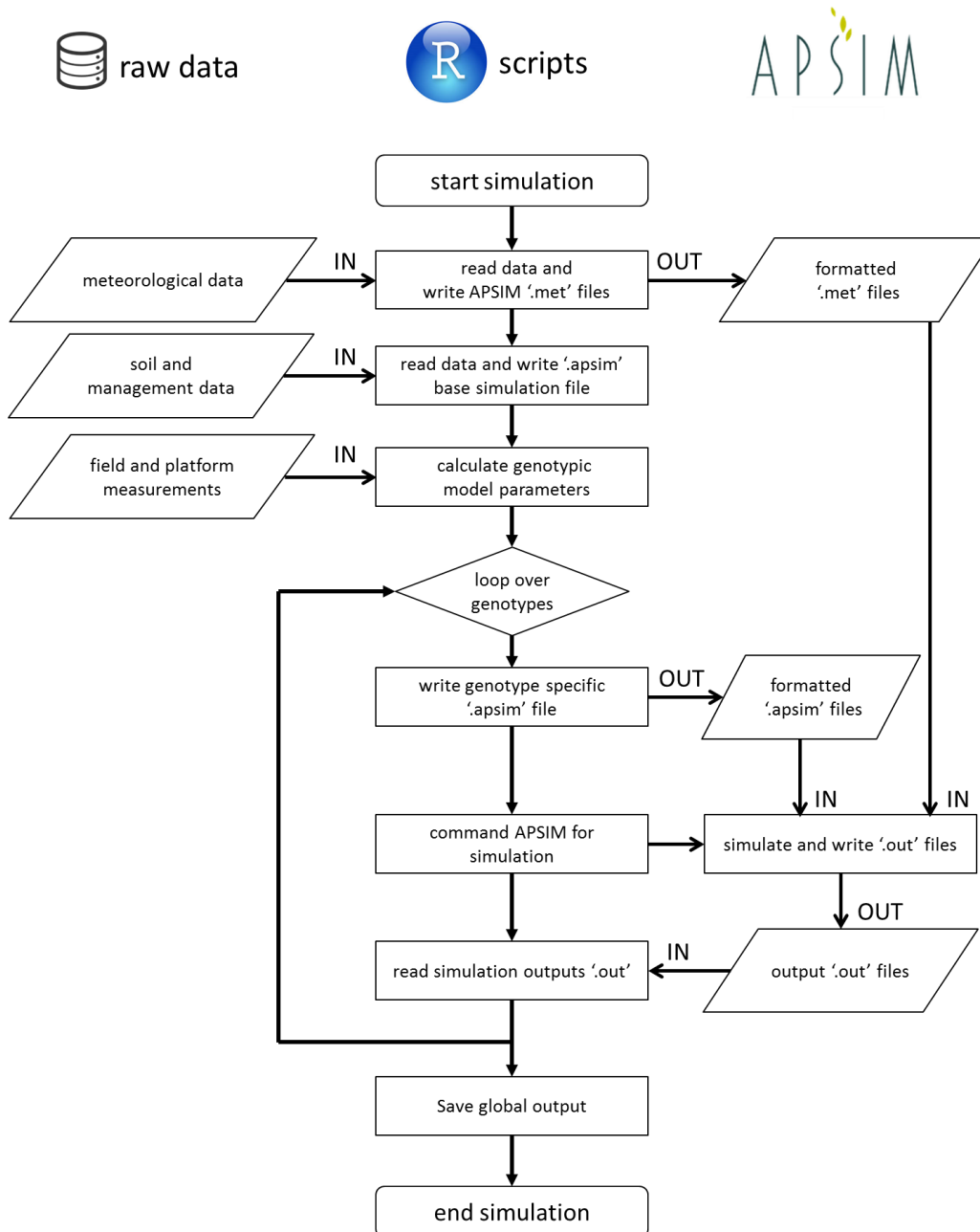
81

Figure 3.6: Schematic representation of the workflow for multi-simulation. The framework uses raw data (left), read and analysed by R scripts (centre) that produce input files for APSIM (right), and dialogs with the model for simulation.

For model simulation, APSIM can either be used with a fully functional interface, or by calling the model from the any computer interface (via Microsoft Disk Operating System or 'MS-DOS') by entering the command 'apsim.exe' and adding the name of the '.apsim' file to be used for simulation. As a result, it can be launched from any interface able to dialog with the command system on a computer. In the context of this thesis, the R software was used for multi-simulation, because it is widely used for data analysis, and because an APSIM library (package 'APSIM' version 0.9.1, Justin Fainges 2016) is available that allows reading, writing and transformations of the different files used by APSIM.

The outputs of the model can be defined by the user from any daily simulated variables in the model. Because parts of the model were adapted and transformed and new formalisms implemented, new intermediate variables were defined and used as model outputs. For each simulated site, model outputs were stored in a classic text file and automatically saved with the extension '.out'. Those files can be easily read automatically and sequentially via the R software and stored in an R object (function 'loadAPSIM', package 'APSIM', R software).

All simulations outputs were read and analysed with the R software. Functions have been developed to rapidly and efficiently analyse outputs files (with more than 100 million lines of data) to gather output data or estimate environmental variables at specific crop phenological stages.

The maps shown in chapters 4 and 5 were produced using the package 'rworldmap', and are represented using the 'GCS_WGS_1984' coordinate system. The polygons (shapefiles; '.shp') containing oceans and mountains limits were downloaded from the Natural Earth Data file repositories[5].

---

[5] http://www.naturalearthdata.com/downloads

References

Harrison MT, Tardieu F, Dong Z, Messina CD, Hammer GL (2014) Characterizing drought stress and trait influence on maize yield under current and future conditions. Glob Chang Biol **20:** 867-878

Semenov MA, Stratonovitch P (2010) Use of multi-model ensembles from global climate models for assessment of climate change impacts. Climate Research **41:** 1-14

Justin Fainges (2016). General Utility Functions for the 'Agricultural Production Systems Simulator'. R -package version 0.9.1. https://CRAN.R-project.org/package=APSIM

Chapter 4: Future European maize production may be maintained if farmers adapt crop cycle duration

---

This chapter uses the model presented in chapter 2 and the simulation framework and workflow presented in chapter 3 to simulate yields with and without adaptation of cycle duration and sowing date in current and future climatic conditions. The calculation of optimum durations is based on a pre-existing dataset and on simulations. The model integrates all developments presented in this thesis except the simulation of leaf widening and its response to intercepted radiation, and the effect of night temperature on grain number.

In addition to the simulation framework, I have performed the simulations themselves with contrasted transpiration coefficients dependant on CO_2, and the optimisation of nitrogen application. Furthermore, I developed most of the code used for treatment and analysis of model input/output.

This chapter is written as an article that has been submitted to a journal. The order of authors reflects the fact that I have not participated directly to the project design nor to the writing of the manuscript.

Future European maize production may be maintained if farmers adapt crop cycle duration

Boris Parent[1], Margot Leclere[1,*], Sebastien Lacube[1], Mikhail A. Semenov[2], Claude Welcker[1], Pierre Martre[1]and François Tardieu[1]

[1] UMR LEPSE, INRA, Montpellier SupAgro, 34060 Montpellier, France.

[2] Rothamsted Research, Harpenden, Herts AL5 2JQ, UK

[*] Current address: UMR Agronomie, INRA, AgroParisTech, Université Paris-Saclay, 78850 Thiverval-Grignon, France.

Abstract

Projections (Asseng et al., 2014; Zhang et al., 2015) and experimental datasets indicate that climate change will have deleterious consequences on yields. However, historical statistics suggest that some species still show yield progress in farmer's fields (Moore and Lobell, 2015). This discrepancy may be due to the fact that most projections involve unchanged farmer's practices, whereas farmers currently adapt cropping systems to local environmental changes (Welch et al., 2010; Zhang et al., 2016), potentially decreasing their effects (Challinor et al., 2014; Challinor et al., 2016). Here, we show that maize yields simulated over Europe could be maintained or increased between present and 2050 if farmers continue adopting rules they currently use for adjusting sowing date and crop cycle duration to local environment. Projected European maize production decreases by 1.1% without adaptation in the maize growing area, compared with 8 to 14% increase with adaptation depending on transpiration efficiency hypotheses. Rules for farmer adaptation were based on field experiments and comparisons of farmer's practices with simulations that optimize yield in each site. Between present and 2050 the combined effects of climate change and farmer adaptation reduce the gradient of maize yield between south and north of Europe. One can therefore foresee changes in maize growing areas but minor effects on European production provided that farmers continue to adapt the sowing date and duration of crop growth cycle.

Main

We have first tested experimentally if farmers have access to varieties presenting a sufficient range of cycle duration to allow identification of the optimum that maximizes yield. For that, we have analysed a panel of 121 public maize accessions with a large range of cycle duration in six experiments with different climatic scenarios and water regimes (three sites by two watering scenarios, Fig. 4.1a and Supplementary Figs S4.1-4.3). Because the main source of variation of cycle duration is the length of the vegetative phase (Li et al., 2016), we focus on the sowing-flowering period. Best-adapted accessions with vegetative duration maximizing yield were identified in each experiment (Fig. 1a and SI. Fig. S 4.3). For each accession, vegetative duration was common to all sites if expressed in time corrected for temperature (SI. Fig. 1). We have also checked the validity of scoring it by counting the final leaf number, a classical farmer's practice (SI. Fig. S 4.2). Experimentally, yield increased with vegetative duration below the optimum (Fig. 4.1a) because of an increased light interception (SI. Fig. 4.4), and decreased beyond it due to flowering and/or grain filling occurring in adverse conditions such as low light or terminal drought[14]. As expected, optimum durations differed between sites and water regimes, depending on local environmental conditions (SI. Fig. S 4.3). Hence, a well-organized genetic variation of cycle duration is available to farmers, and durations that optimize yield can be identified in each field.
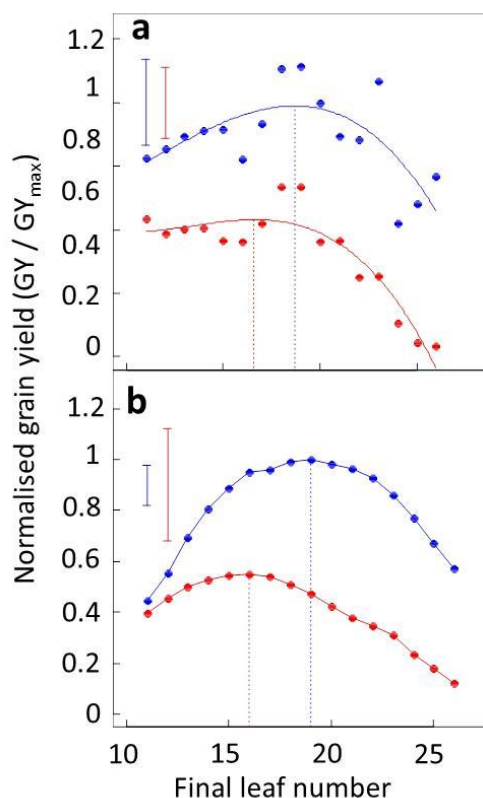

Figure 1: Observed and simulated optimum durations of the duration of the vegetative period (sowing-flowering time), expressed as plant leaf number.
a, Relationship between plant leaf number and yield in irrigated (blue dots and lines) or rainfed conditions (red dots and line) in a field experiment with 121 maize accessions (Sainte Pexine, France, 2006; two additional field experiments are presented in Supplementary Fig. 3). For better intuition, the duration of the vegetative period is expressed as final leaf number, closely related to it. Yield is normalized by its maximum values in fully-irrigated conditions. Dots are mean values for accessions presenting a common leaf number. Error bars, confidence intervals (P = 0.95). Plain lines, third order polynomial regressions. Vertical dashed lines, optimum leaf number. **b**, Relationship between plant leaf number and simulated yield at Ouges (France, SI.Table S1). Each dot, mean of 30 years. Error bars, confidence intervals (P = 0.95). Two additional sites are presented in Supplementary Fig. 6.

It can therefore be hypothesized that, by trial and error, farmers choose cycle durations and sowing dates that maximise yield in the most frequent climatic scenario corresponding to their site. To test this assumption, we have compared farmer's practices as reported in the European AgroPheno database (Agri4cast database[6], Joint Research Center) to optimum sowing dates and vegetative

---

[6] http://agri4cast.jrc.ec.europa.eu/DataPortal/Index.aspx, consulted in November 2016.

durations simulated in 59 European sites representative of the European maize growing area (Supplementary Table 1,Harrison et al., 2014), over a period of 35 years (1975-2010). Simulations were performed in each site with three watering strategies, namely full-irrigation, optimised irrigation around flowering as suggested by extension services and rainfed (no irrigation). We used the APSIM-maize (Hammer et al., 2010) model modified by taking into account the growth of individual leaves (Chenu et al., 2008).

Sowing dates were simulated in each site according to farmer's practices, and were closely related to observations in the European database[1] (SI. Fig. 4.5a). The rule was that sowing occurs at the first date of early spring for which the risk of frost for 10 days after sowing is lower than 5% over 35 years. It combines a minimum risk of frost with highest cumulated photosynthesis and potential yield. Simulated sowing dates ranged from 20th March to 30th April with later dates at northern latitudes.

Optimum vegetative duration was simulated in each site by considering the duration that maximises yield over 35 years. The median of yield was related to vegetative duration with bell shapes similar to those observed experimentally in the 59 sites (examples in Fig. 4.1b and SI Fig. 4.6a,c,e). These simulations resulted in anthesis times that were similar to farmer's ones in the European database[15] (SI. Fig. 4.5a). In irrigated conditions, optimum duration from sowing to flowering ranged from 822 to 1462°Cdays (hybrids with 15 to 26 leaves) and was closely correlated with latitude (Fig. 4.2a and SI. Fig. 4.7a). Hence, later sowing dates in northern sites such as Germany or Poland were compensated for by shorter vegetative duration (Fig. 4.2a), resulting in flowering dates that were nearly independent of latitude in our simulation outputs as well as in the AgroPheno database (SI. Fig. 4.5a). Simulated optimum duration was shorter (592 to 1056°Cdays) in rainfed conditions (Fig. 4.2b and SI. Fig. 4.7b), and the difference in flowering time between fully irrigated and rainfed conditions was linearly related to the level of water stress (SI. Fig. 7c).

Because simulations closely matched farmer's practices, we have considered hereafter a 'virtual farmer' who adopts, on average, sowing dates and cycle durations that optimize yield in each location. Mean yields simulated with this rule closely correlated with historical yields for the period 2000-2010[20] (SI. Fig. 5b). They ranged from 7.0 to 14.6 t ha^{-1} (Fig. 4.3a and SI. Fig. 4.8) in irrigated conditions and were negatively correlated to latitude (Fig. 4.3a). They were lower in rainfed conditions (mean yield of 7.4 t ha^{-1}, from 2.4 to 12.5 t ha^{-1}, Fig. 4.3e and SI. Fig. 4.8), with maximum yield in intermediate latitudes 44-47° N (Fig. 4.3e and Supplementary Fig. 4.8).
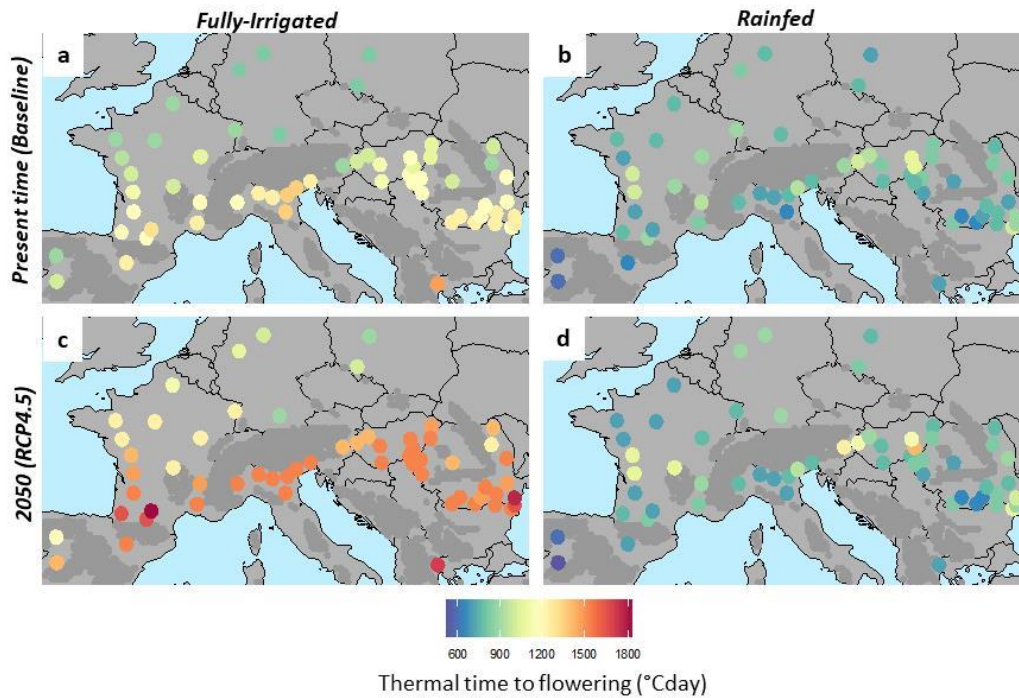
Figure 4.2: Maps of optimum cycle duration in current and future conditions, fully-irrigated and rainfed.
Colors represent the optimum thermal time between sowing and flowering in each site for maximizing yield for present time (average yield over the 35 years of the baseline period) or 2050 (average yield for 30 predicted years in 2050 x 4 GCM; RCP4.5).
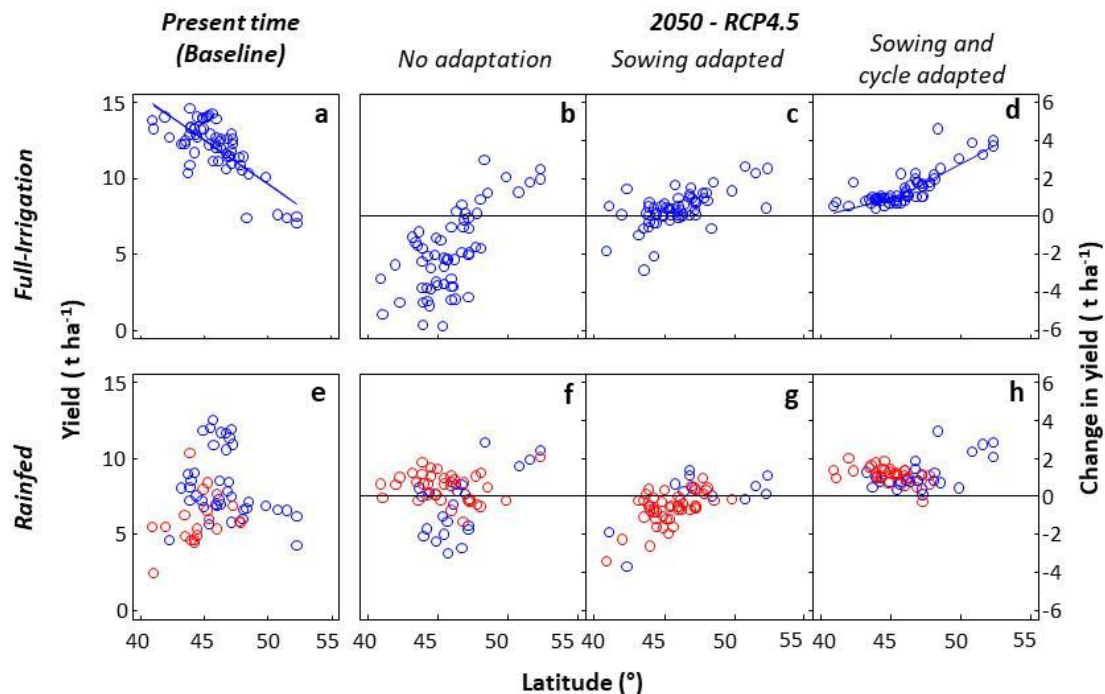

Figure 4.3: Change in yield with climate change under different options of adaptation. a, **e**, Current yield in fully-irrigated and rainfed conditions. **b-d** and **f-h,** Change in yield between the baseline period and 2050 (RCP4.5) without adaptation (**b**, **f**), with adaptation of sowing date (**c**, **g**), and of both adaptation of sowing date and duration of growth cycle (**d**, **h**). Red and blue dots denote the presence or absence of water deficit at flowering time (threshold supply/demand ratio = 0.75).

We have then simulated yields for 2050 by considering that rules presented above for sowing date and cycle duration will apply in the future, and compared them with yields simulated for 2050 with the assumption of invariant sowing dates and varieties. Daily local-scale climate scenarios for 2050 were generated by the stochastic weather generator LARS-WG (Semenov and Stratonovitch, 2010) for the representative concentration pathways (RCPs) 4.5 and 8.5 (487 and 541 ppm CO_2 in 2050, respectively). For each RCP, we used four global climate models (GCMs) representative of the CMIP5 GCM ensemble for the studied area (Manderscheid et al., 2014). Hundred years were generated for each RCP-GCM combination. Maize yield was simulated with the APSIM maize model by taking into account these conditions. The direct impact of increase in CO_2 concentration on transpiration (Allen et al., 2011; Manderscheid et al., 2014) was taken into account by increasing transpiration efficiency (TE) by +0.21% for each ppm increase in atmospheric CO_2 concentration (Allen et al., 2011). We have also considered the possibility of an unchanged TE in view of the lower long term effect (Kimball, 2016) in the field (Manderscheid et al., 2014) than that observed in open-top chambers or free-air CO2 enrichment experiments (KIM et al., 2006; Allen et al., 2011). Radiation use efficiency, a proxy for photosynthetic capacity and respiration, was kept constant in spite of the higher CO_2 concentration because maize is a C4 species (KIM et al., 2006; Allen et al., 2011). Simulations were run for each combination of year, site, RCP, GCM, irrigation strategy, crop cycle duration and CO_2 effect on TE (> 9 million simulations in total). Compared with the baseline period (1975-2010), RCP4.5 and RCP8.5 result in a projected increase in temperature averaging 2.8°C and 3.3°C , respectively at flowering time (mid-July) for the 59 European sites considered in our study (SI. Fig. 9a,b). Water deficit at flowering time was similar in 2050 compared to the baseline period (SI. Fig. 9c), if TE was considered as increasing with CO_2 concentration (KIM et al., 2006; Allen et al., 2011) because increased TE reduced water use, thereby compensating the increase of transpiration demand (SI. Fig. 4.9c,e). Conversely, water deficit increased in most sites if TE was considered constant (SI. Fig. 4.9e).

In the absence of adaptation of varieties and sowing dates, a decrease in yield was simulated in fully-irrigated conditions between the baseline period and 2050, with a negative effect in 79% of fields (RCP4.5, Fig. 4.3b), especially in southern locations that represent the major growing area for maize. This was linked to the increase in summer temperature (SI. Fig. 4.9a,b), which resulted in a decrease in crop growth cycle duration (SI. Fig. 4.10) and therefore cumulated light interception. Reductions in yield were also simulated in fields with optimal irrigation and in rainfed fields without water deficit around flowering (i.e. with supply / demand ratio for water < 0.75, Fig. 4.3f). Yield slightly increased in most rainfed fields under water deficit (averaging +0.5 t ha^{-1} for RCP4.5). Overall, upscaling these results for whole Europe resulted in a decrease of the European maize production of -1.1 % (RCP4.5, Fig. 4.4). A larger negative effect was simulated if no effect of CO_2 on TE was considered (-4.8%, Fig. 4.4), and also if restrictions in irrigation reduced the current proportion of irrigated field[26], used here for both simulations in present time and future conditions.

The simulated negative impact of climate change disappeared if one assumed that farmers will use in 2050 the rules for sowing date and cycle duration that they currently follow (Fig.4. 4). Optimal sowing dates were earlier by 10 to 39 days depending on sites in 2050 (RCP4.5) compared with the baseline period (SI. Fig. 10a). Cycle duration of adapted varieties increased by 325°Cd on average for RCP4.5 in irrigated fields, corresponding to an increase in final leaf number by 5.5 (Fig. 4.2 and SI. Figs 4.7, 4.11, 4.12). This increase was smaller in rainfed conditions (+21°Cd on average for RCP4.5) with a deviation with irrigated fields that increased linearly with water deficit (SI. Fig. 4.7), suggesting that a drought-avoidance strategy based on early varieties (Harrison et al., 2014) will still be valid in the future. If farmers follow these management rules in 2050, the projected impact of climate change becomes positive in irrigated fields or in rainfed fields without water deficit (averaging +1.4 t ha^{-1} for

RCP4.5, Fig. 4.3d,h), with an effect that increases with latitude (Fig. 4.3d) and is largely accounted for by the increase in intercepted light during the crop cycle (averaging +24% for RCP4.5, SI. Fig. 4.13). Adapting the crop cycle duration had less effect in fields with water deficit (Fig. 4.3h and SI. Fig. 4.12). Changing sowing dates without changing varieties also had a limited effect (Fig. 4.3g). Overall, simulations showed a positive impact of climate change on global European maize production by +14.5% for RCP4.5 (Fig. 4.4) if both sowing date and varieties were adapted. This effect was still of +8.4% I we consider no effect of CO_2 on TE (Fig. 4.4).
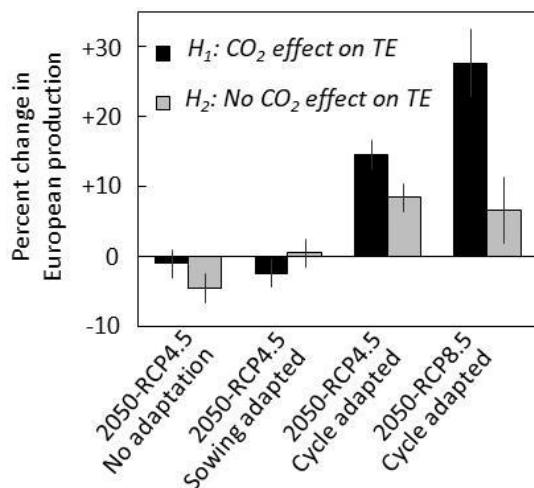
Figure 4.4: Impact of climate change on European maize production considering three adaptation options. Impact of climate change on European maize production considering that the maize area and access to water will be the same in 2050 compared with the baseline period. Black: simulation performed with a transpiration efficiency (TE) that changes with CO_2. Grey: simulation with an unchanged TE in 2050 compared with the baseline period. Error bars, standard deviation calculated over the four GCMs.

The combined effects of climate change and of adaptation were much larger in northern than in southern locations (Fig. 4.3d). The gradient of yield, of 0.58 t ha^{-1} per degree of latitude for the baseline period (Fig. 4.3a) decreased to 0.26 t ha^{-1} per degree in 2050 (RCP4.5). The current north-south difference in yield in the absence of stress was therefore largely decreased by the combined effects of climate change and adaptation to it (Fig. 4.3d). Because southern fields will have a lesser competitive advantage in both irrigated and rainfed conditions (Fig. 4.3d,h), one might expect a displacement of the maize growing area by 2050. In particular, regions such as Germany and Poland could become major maize growing areas in Europe. If such changes of maize growing area occurred in the near future, the positive impact of climate change on European maize production could be even higher than predicted here.

Are farmers likely to adopt these changes in varieties and sowing dates by 2050? We can consider this hypothesis as reasonable because (i) farmers have already adapted varieties in recent years. For example, in middle latitudes of France, varieties of the group mid-earliness dent lines were mostly grown in latitudes of 44.8 to 45.9° in 1996 while they have shifted to 46.5 to 47.5° in 2009 (Arvalis[7], 2016); adaptation of crop growth cycle duration to reduce the risk of water deficit is strongly advised and made possible by increasingly good records of meteorological and soil conditions (ii) genetic resources and alleles for adapting crop growth cycle duration have been identified (Buckler et al., 2009). Hence, the effect of climate change on maize yield could be more positive than previously reported (Urban et al., 2015; Zhang et al., 2016), and northern areas in which maize is not economically viable may become significant producers in the future. This is not sufficient in view of

[7] Choisir et Décider : Préconisation régionales 2016,
https://www.arvalisinfos.fr/file/galleryelement/pj/1c/49/26/b7/choisirmais2016_aquitaine_midipyrenees3339 212297883866791.pdf. (2016).

the increasing demand for food and industrial needs based on plants (Field et al., 2014) and further improvements of plant performance based on increased photosynthesis, adapted reproductive development or resistance to pests and diseases will be necessary. The large genetic variability for responses to these cues (Buckler et al., 2009), including the identification of alleles (Millet et al., 2016) allowing significant yield increase can raise hopes on the capacity of agriculture to increase crop production by 2050.

Acknowledgements

Author contributions

B.P. and FT wrote the paper, analysed data and compiled figures.

M.L. performed most simulations and drew maps.

S.L. built the crop model used in the study.

M.A.S. simulated climates in 2050.

C.W. assembled the genetic material, and designed and supervised experiments.

P.M. indicated relevant analyses and participated to the paper writing

Methods

Field experiments

Genetic material measurements and growth conditions

We have tested a panel of 121 maize accessions representative of main components of the maize genetic diversity (Brandenburg et al., 2017) in three experimental sites in France with two water regimes each. Sites included a Mediterranean site, Mauguio (43°36'37''N; 3°58'39''E; 23 m above sea level, asl), and and two oceanic sites, Sainte Pexine (46°33'43''N; 1°08'17''W; 45 m asl) and Le Magneraud (46°24'16''N; 00°04'45''E; 26 m asl). In each site, two water regimes were imposed, with either irrigation over the whole crop cycle or restricted irrigation during late vegetative and reproductive stages in order to get soil water deficit at flowering time. A rainout shelter was used in Le Magneraud to ensure water deficit so the number of accessions was 57 in view of the limited available space. In each site, the experimental design was an alpha lattice with two replicates in the irrigated treatments and three replicates in the rainfed treatments. Plots were 6 m long, with 0.8 m between rows and a plant density of 8 plants m^{-2}. Irrigation was withdrawn in rainfed treatments at the 8 visible leaf stage, until flowering time plus 10 days. In rainfed treatments, watering was still applied when plants showed leaf rolling in early morning for two consecutive days. Light, air temperature, relative humidity (RH) and wind speed were measured hourly in each experiment at 2 m height over a reference grass canopy. Light was measured with photosynthetic photon flux density sensors; air temperature and RH were measured in ventilated shelters. Soil water potential was measured every day at 30, 60 and 90 cm depths in irrigated (two replicates) and rainfed plots (three replicates). Mean soil water potential was -0.3 MPa on average during duration of water deficit period in Sainte Pexine and Le Magneraud, and was -0.6 MPa in Mauguio. Emergence, flowering time, yield and yield components were assessed at plot level. The length and width of every second leaf width and leaf number were measured in 10 plants per plot.

Analysis of field data

Thermal time was calculated from sowing time as in the APSIM-maize (Hammer et al., 2010) model at a 3 h time-step, with a broken linear relationship between development rate and temperature (cardinal temperature: 0, 18, 34, and 44°C). Temperature at 3 h time-step was calculated from daily minimum and maximum temperatures with the third order polynomial function of APSIM-maize (Hammer et al., 2010).

The phyllochron of each accession was calculated in each experiment by dividing the mean thermal time at flowering time by the mean final number of leaves of the studied accession. Because cycle duration and number of leaves were highly correlated and stable between experiments (Supplementary Fig. 2), the duration of the vegetative period was finally expressed as final leaf number in Fig. 1, Supplementary Figs 3, 4, 5. We then averaged data of accessions with common final leaf number (± 1).

Leaf area and light interception were calculated every day from sowing to harvest for all accessions. Profiles of final leaf length and width for each average variety with final leaf number from 11 to 25 were obtained from measured data of leaf width and length every second leaf. The time of appearance of each leaf was calculated from the phyllochron expressed in thermal time. Leaf expansion was considered linear during ten days from leaf appearance and therefore growing the tenth of final length each day from leaf appearance (Lacube et al., 2017) . In the same way, leaf width was calculated daily from the measured maximum width via a linear interpolation. No leaf

senescence was considered in the calculation of leaf area index during the vegetative stage. Light interception was then calculated by using measured incident light and the proportion of intercepted light calculated from leaf area as in APSIM-maize (Hammer et al., 2010).

Model parameterisation and evaluation

Crop parameters and varieties

We have used the APSIM-maize (Hammer et al., 2010) model modified for expansion of individual leaves (Chenu et al., 2008) and calibrated with data of the line B73 in replicated field experiments in Mauguio. The parameter representing transpiration efficiency (TE) before correction by the effect of VPD (parameter 'transp_eff_cf' in APSIM-maize) was set at 0.007 g kPa g^{-1} for the baseline period. In order to take into account the effect of CO_2 on stomatal conductance (KIM et al., 2006; Allen et al., 2011) TE was increased by 0.21% for each ppm increase in atmospheric CO2 concentration resulting in an increase of TE of 23 % and 34 % in 2050 for RCP4.5 and RCP8.5, respectively,. However, in view of debates on long term effect of CO_2 on TE (Kimball, 2016) we also considered simulations without change in TE between the baseline period and 2050. No effect of CO_2 was considered on radiation use efficiency as maize is a C4 plant. Parameters of leaf growth were those of Chenu et al. (2008).

A set of virtual hybrids with contrasted crop cycle durations was derived from the reference hybrid B73xUH007 whose yield has been measured in 29 European fields (Millet et al., 2016). In this panel, crop cycle duration mostly depended on the duration of the vegetative stage with nearly constant thermal time between flowering and maturity (Millet et al., 2016). The duration of the vegetative period was driven by the final leaf number consistent with experimental data (Supplementary Fig. 1). Therefore, we parameterised varieties with contrasted crop growth cycle duration by (i) changing leaf number from 10 to 40, with a constant leaf appearance of 0.0193 °C day $leaf^{-1}$ for all accessions (Supplementary Fig. 2) and (ii) a constant thermal time from flowering to maturity corresponding to the reference hybrid (820 °C day). The durations of phenological stages of the vegetative period (emergence to flowering) were affected proportionally to changes in thermal time from emergence to flowering. This was in particular the case for thermal time from the end of juvenile stage to floral initiation, an essential parameter in APSIM-maize.

All other parameters were those of the reference hybrid parameterised in Harrison et al. (2014). The hybrid with 16 leaves was therefore the actual UH007xB73 hybrid, whereas hybrids with leaf number ranging from 10 to 40 were virtual hybrids, similar to B73 but with contrasted leaf numbers.

Sowing and harvesting

Sowing dates were simulated in each field as the first day from January to May in which the frequency of frost was < 5% in the following 10 days (calculated over 35 years in each site; Supplementary Fig. 9). The same rule was applied for the 2050 climate scenarios. Harvest date was simulated as being after physiological maturity. The model simulated a total yield loss if physiological maturity was reached after November 1st, or if soil water content of the 0-30 cm top layer did not decrease below 90% of saturation until November 1st. The latter rule simulated the impossibility for harvesting machines to enter into the considered field because of an insufficient load bearing capacity. The date of 1st November was chosen in relation to the high risk of total yield loss due to ear fall and diseases, combined with the necessity for farmers to sow the next winter crop at that time.

Sites

We have used 59 field locations representative of the European maize growing area and of typical soil types of these regions. Fifty five sites were those described in Harrison et al. (2014), representing the ten countries with the highest maize growing areas in the 2004-2009 period [20] and the main maize growing regions within these countries (Harrison et al., 2014). Four sites were added to the latter lattice in order to improve its spatial distribution. Soil data were obtained from the JRC European Soil Commission database and from the Crop Growth Monitoring System (Harrison et al., 2014) . Because soil depth can highly vary within each region and because the aim of this study was a sensitivity analysis on other variables, we considered a soil depth of 1.5m in all sites.

Crop management

Three watering regimes were simulated in each site, namely full irrigation, rainfed and optimal irrigation. Full irrigation considered systematic watering until field capacity over the entire soil profile (1.5 m depth). The optimal irrigation regime considered 30 mm watering every seven days from the 10-leaf stage to mid-grain filling, with a water volume equalling the difference between reference evapotranspiration and rainfall over the last seven days. For comparisons with observed yield values at national scale, nitrogen fertilisation rates at each location were obtained from the CAPRI database (Leip et al., 2011; Webber et al., 2015) . Plant density was adjusted in each country based on the JRC database[1] and local variations inside each country were adjusted via local expertise collected from 29 field experiments in Europe in the frame of the DROPS project (Millet et al., 2016). These rules were considered as invariant in 2050 compared with present. For both baseline period and future climate scenarios, nitrogen supply at sowing was calculated as 70% of nitrogen needed to reach the maximum yield of the optimum genotype with optimum sowing date. Therefore, we assumed that the management intensity would not change in 2050.

Meteorological data

Meteorological data used for the baseline period are 35 years of daily weather (1975-2010) obtained from (i) the AGRI4CAST database of the JRC for the 55 sites of Harrison et al. (2014) and (ii) the INRA CLIMATIK database for the 4 added sites. These years were considered as a climate baseline with an atmospheric CO_2 concentration of 380 ppm.

The climate scenarios in 2050 were simulated at each site by using the stochastic weather generator LARS-WG (Semenov and Stratonovitch, 2010) and were based on climate projections from the Coupled Model Intercomparison Project Phase 5 (CMIP5) ensemble with two Representative Concentration Pathways (RCPs), namely 4.5 and 8.5 (487 and 541 ppm CO_2 in 2050, respectively) and four Global circulation Models (GCMs) in order to account for the uncertainty in the CMIP5 ensemble (namely GFDL-CM3, HadGEM2-ES, MIROC5, MPI-ESM-MR). Hundred years of weather data were generated for each combination of site, RCP, and GCM

Simulations and upscaling

Thirty years were selected for crop simulations, selected for presenting the same mean and variance as the 100 years generated using LARS-WG. A total of 9'292'500 simulations were run with APSIM-maize parameterised as described above (for the baseline period: 2 managements x 3 irrigations scenarios x 30 accessions x 59 sites x 35 years; for climate scenarios: 2 scenarios x 4 GCMs x 3 irrigations scenarios x 30 accessions x 59 sites x 30 years x 2 options for TE). To upscale results from site to country level, simulated data under full-irrigation and rainfed scenarios were weighted for each site by the proportion of irrigated field in the area (FAOSTAT, 2016). Results were then averaged

at country level. To upscale to European level, results at country levels were multiplied by the area of maize cultivation in each country based on year 2010. Recent studies have shown that temperature impact on crop yield at regional to global scales are similar for point-based simulations (as in our studied) and grid-based simulations (Liu et al., 2016; Zhao et al., 2017).

References

Allen LH, Kakani VG, Vu JC, Boote KJ (2011) Elevated CO 2 increases water use efficiency by sustaining photosynthesis of water-limited maize and sorghum. Journal of plant physiology **168:** 1909-1918

Asseng S, Ewert F, Martre P, Rötter RP, Lobell DB, Cammarano D, Kimball BA, Ottman MJ, Wall GW, White JW, Reynolds MP, Alderman PD, Prasad PVV, Aggarwal PK, Anothai J, Basso B, Biernath C, Challinor AJ, De Sanctis G, Doltra J, Fereres E, Garcia-Vila M, Gayler S, Hoogenboom G, Hunt LA, Izaurralde RC, Jabloun M, Jones CD, Kersebaum KC, Koehler AK, Müller C, Naresh Kumar S, Nendel C, O'Leary G, Olesen JE, Palosuo T, Priesack E, Eyshi Rezaei E, Ruane AC, Semenov MA, Shcherbak I, Stöckle C, Stratonovitch P, Streck T, Supit I, Tao F, Thorburn PJ, Waha K, Wang E, Wallach D, Wolf J, Zhao Z, Zhu Y (2014) Rising temperatures reduce global wheat production. Nature Climate Change **5:** 143-147

Brandenburg J-T, Mary-Huard T, Rigaill G, Hearne SJ, Corti H, Joets J, Vitte C, Charcosset A, Nicolas SD, Tenaillon MI (2017) Independent introductions and admixtures have contributed to adaptation of European maize and its American counterparts. PLoS genetics **13:** e1006666

Buckler ES, Holland JB, Bradbury PJ, Acharya CB, Brown PJ, Browne C, Ersoz E, Flint-Garcia S, Garcia A, Glaubitz JC (2009) The genetic architecture of maize flowering time. Science **325:** 714-718

Challinor AJ, Koehler A-K, Ramirez-Villegas J, Whitfield S, Das B (2016) Current warming will reduce yields unless maize breeding and seed systems adapt immediately. Nature Climate Change **6:** 954-958

Challinor AJ, Watson J, Lobell D, Howden S, Smith D, Chhetri N (2014) A meta-analysis of crop yield under climate change and adaptation. Nature Climate Change **4:** 287-291

Chenu K, Chapman SC, Hammer GL, McLean G, Salah HB, Tardieu F (2008) Short-term responses of leaf growth rate to water deficit scale up to whole-plant and crop levels: an integrated modelling approach in maize. Plant Cell Environ **31:** 378-391

Field CB, Barros VR, Mach K, Mastrandrea M (2014) Climate change 2014: impacts, adaptation, and vulnerability, Vol 1. Cambridge University Press Cambridge and New York

Hammer GL, van Oosterom E, McLean G, Chapman SC, Broad I, Harland P, Muchow RC (2010) Adapting APSIM to model the physiology and genetics of complex adaptive traits in field crops. Journal of Experimental Botany **61:** 2185-2202

Harrison MT, Tardieu F, Dong Z, Messina CD, Hammer GL (2014) Characterizing drought stress and trait influence on maize yield under current and future conditions. Glob Chang Biol **20:** 867-878

KIM SH, Sicher RC, Bae H, Gitz DC, Baker JT, Timlin DJ, Reddy VR (2006) Canopy photosynthesis, evapotranspiration, leaf nitrogen, and transcription profiles of maize in response to CO2 enrichment. Global Change Biology **12:** 588-600

Kimball BA (2016) Crop responses to elevated CO 2 and interactions with H 2 O, N, and temperature. Current opinion in plant biology **31:** 36-43

Lacube S, Fournier C, Palaffre C, Millet EJ, Tardieu F, Parent B (2017) Distinct controls of leaf widening and elongation by light and evaporative demand in maize. Plant, Cell & Environment**:** n/a-n/a

Leip A, Britz W, Weiss F, de Vries W (2011) Farm, land, and soil nitrogen budgets for agriculture in Europe calculated with CAPRI. Environmental pollution **159:** 3243-3253

Li D, Wang X, Zhang X, Chen Q, Xu G, Xu D, Wang C, Liang Y, Wu L, Huang C (2016) The genetic architecture of leaf number and its genetic relationship to flowering time in maize. New Phytologist **210:** 256-268

Liu B, Asseng S, Müller C, Ewert F, Elliott J, Lobell DB, Martre P, Ruane AC, Wallach D, Jones JW (2016) Similar estimates of temperature impacts on global wheat yield by three independent methods. Nature Climate Change **6:** 1130-1136

Manderscheid R, Erbs M, Weigel H-J (2014) Interactive effects of free-air CO 2 enrichment and drought stress on maize growth. European Journal of Agronomy **52:** 11-21

Millet EJ, Welcker C, Kruijer W, Negro S, Coupel-Ledru A, Nicolas SD, Laborde J, Bauland C, Praud S, Ranc N, Presterl T, Tuberosa R, Bedo Z, Draye X, Usadel B, Charcosset A, Van Eeuwijk F, Tardieu F (2016) Genome-Wide Analysis of Yield in Europe: Allelic Effects Vary with Drought and Heat Scenarios. Plant Physiology **172:** 749-764

Moore FC, Lobell DB (2015) The fingerprint of climate trends on European crop yields. Proceedings of the National Academy of sciences **112:** 2670-2675

Semenov MA, Stratonovitch P (2010) Use of multi-model ensembles from global climate models for assessment of climate change impacts. Climate Research **41:** 1-14

Urban DW, Sheffield J, Lobell DB (2015) The impacts of future climate and carbon dioxide changes on the average and variability of US maize yields under two emission scenarios. Environmental Research Letters **10:** 045003

Webber H, Zhao G, Wolf J, Britz W, de Vries W, Gaiser T, Hoffmann H, Ewert F (2015) Climate change impacts on European crop yields: do we need to consider nitrogen limitation? European Journal of Agronomy **71:** 123-134

Welch JR, Vincent JR, Auffhammer M, Moya PF, Dobermann A, Dawe D (2010) Rice yields in tropical/subtropical Asia exhibit large but opposing sensitivities to minimum and maximum temperatures. Proceedings of the National Academy of Sciences **107:** 14562-14567

Zhang S, Tao F, Zhang Z (2016) Changes in extreme temperatures and their impacts on rice yields in southern China from 1981 to 2009. Field Crops Research **189:** 43-50

Zhang Y, Zhao Y, Chen S, Guo J, Wang E (2015) Prediction of maize yield response to climate change with climate and crop model uncertainties. Journal of Applied Meteorology and Climatology **54:** 785-794

Zhao C, Liu B, Piao S, Wang X, Lobell DB, Huang Y, Huang M, Yao Y, Bassu S, Ciais P (2017) Temperature increase reduces global yields of major crops in four independent estimates. Proceedings of the National Academy of Sciences**:** 201701762

Supporting information
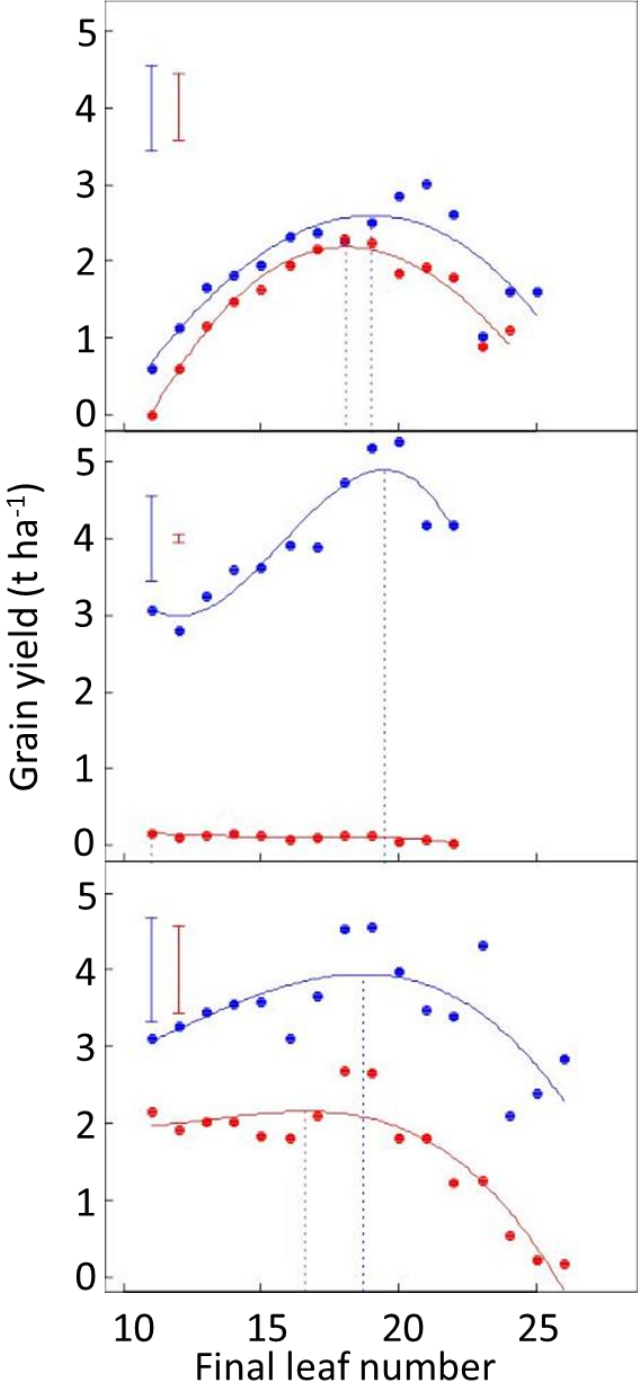
Supplementary figure 4.1:
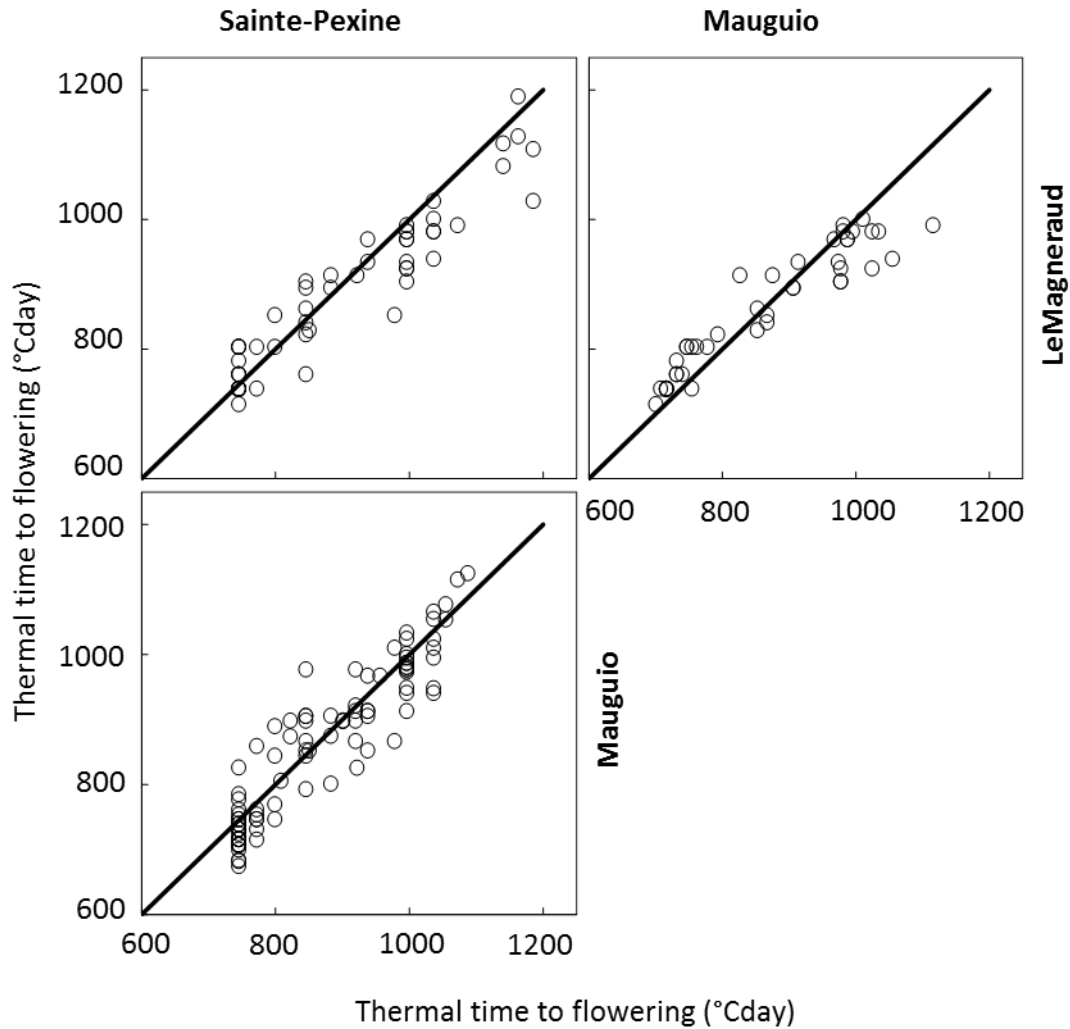
Supplementary Figure 4.1 | Correlation between measured values of flowering time in three field experiments with full irrigation. Dots are experimental values for 121 maize varieties (57 in Le Magneraud) measured in the three experiments (LeMagneraud, France; Mauguio, France; Sainte Pexine, France). Flowering time is expressed as thermal time from sowing to anthesis. Lines are the 1:1.

Supplementary figure 4.2:
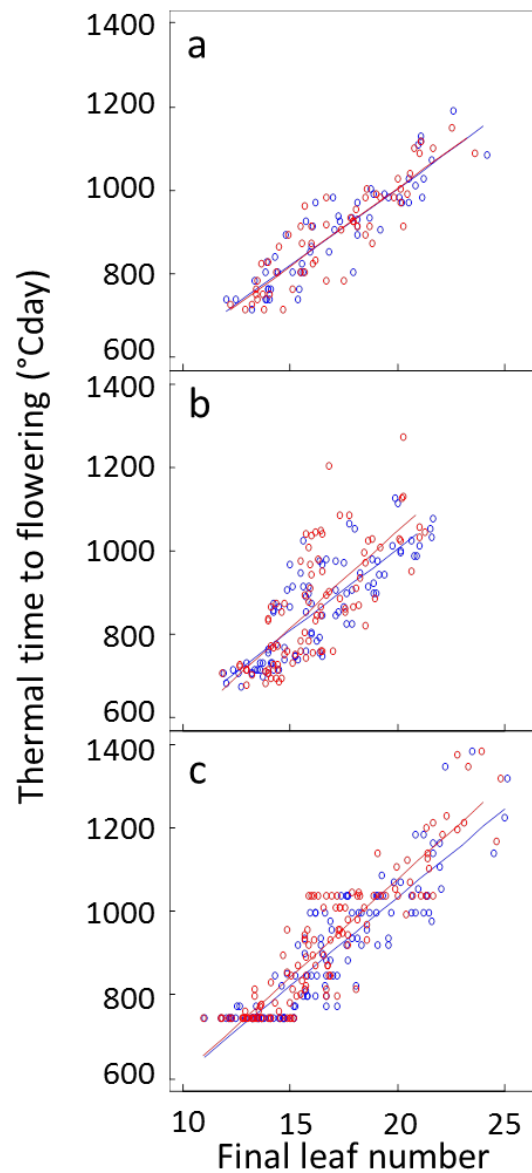
Supplementary Figure 4.2 | Relationship between final leaf number and thermal time to flowering in three field experiments. a-c, Thermal time between sowing and flowering plotted against final leaf number for 121 maize varieties (57 in Le Magneraud) in three field experiments in irrigated (blue dots) or rainfed conditions (red dots). Dots are experimental values averaged for each accession, with ten plants per accession. **a**, LeMagneraud, France. **b**, Mauguio, France. **c,** Sainte Pexine, France.

Supplementary figure 4.3:

Supplementary Figure 4.3 | Observed optimum durations of the vegetative period (sowing-flowering time), expressed as plant leaf number in three sites and two watering regimes.
Relationship between plant leaf number and yield in irrigated (blue dots and lines) or rainfed conditions (red) in three experiments with 121 maize accessions (**a**, Le Magneraud, France, 57 accessions; **b**, Mauguio, France; **c**, Sainte Pexine, France). For better intuition, the duration of the vegetative phase is expressed as plant leaf number, closely related to it. Dots are mean values for maize accessions presenting a common plant leaf number. Optimum values maximizing yield can be identified in all situations except in Mauguio in rainfed conditions, where yield was low in all accessions. Error bars are confidence intervals (P = 0.95). Plain lines, third order polynomial regressions. Vertical dashed lines, optimum cycle durations.
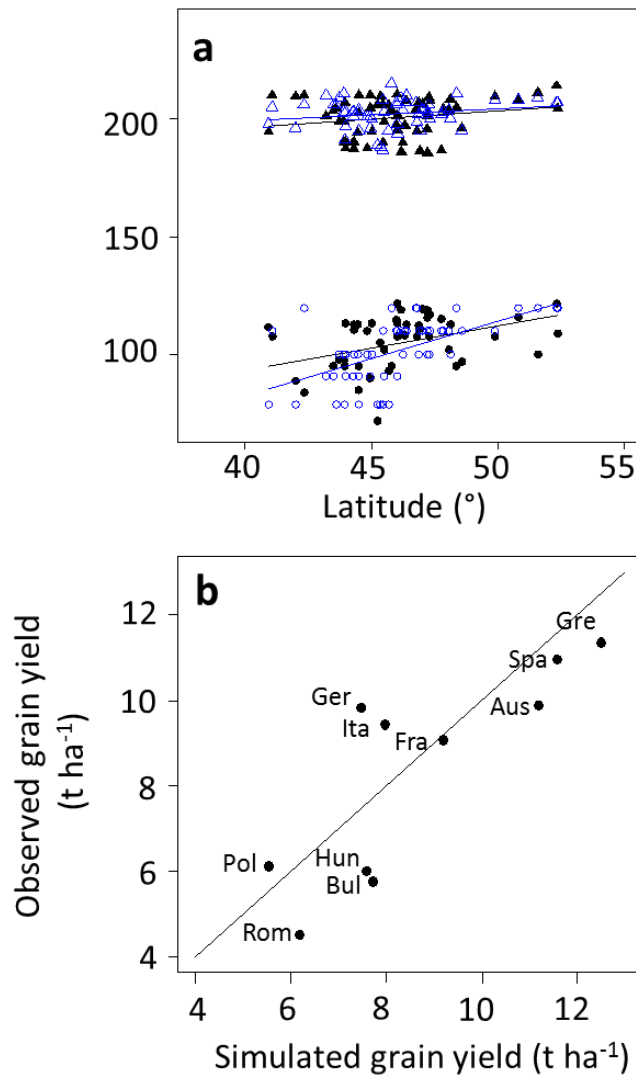
Supplementary figure 4.4:
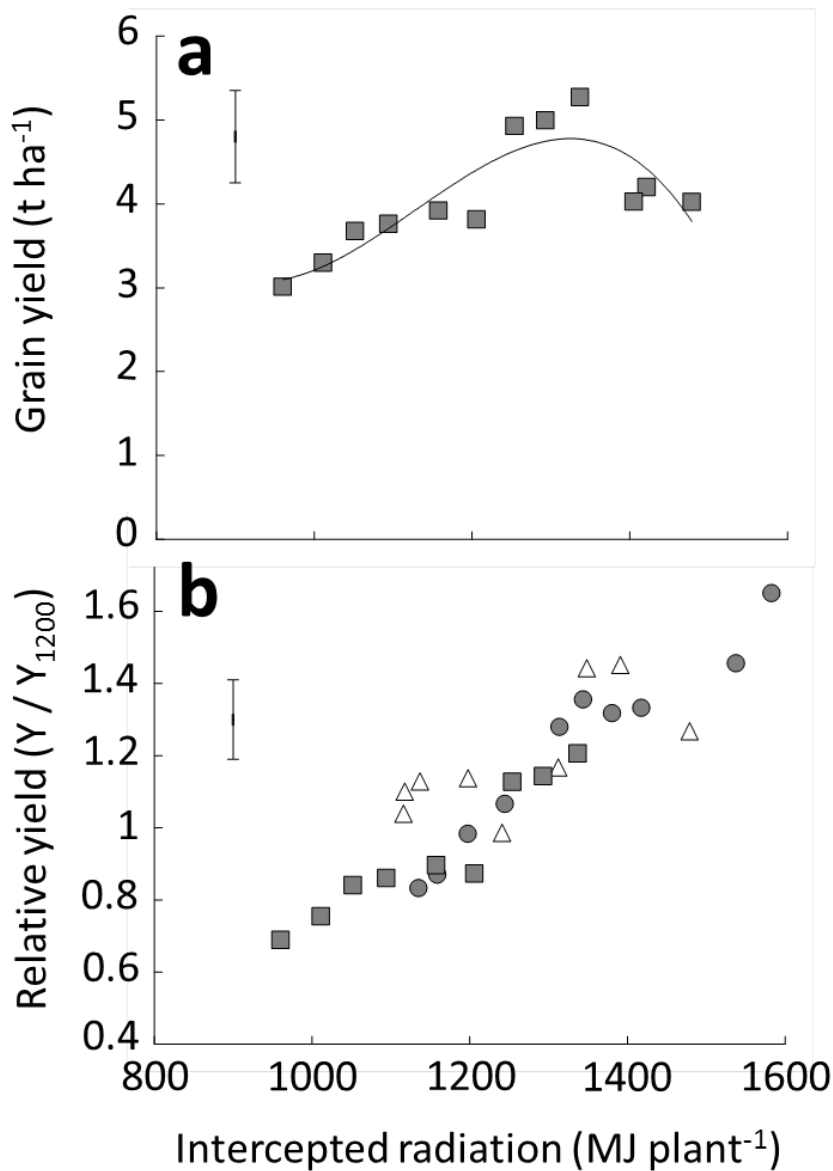
Supplementary Figure 4.4 | Relationship between yield and intercepted radiation in three experiments.
a, Relationship between yield and intercepted radiation from emergence to 10 days after flowering for maize varieties with common plant leaf number in the irrigated treatment in Mauguio, France, 2007. Line is the 3rd order polynomial regression. **b,** Relationship between yield and intercepted radiation in the irrigated treatment of the three experiments (squares: Mauguio, France, 2007; circles: LeMagneraud, France, 2007; triangles: Sainte Pexine, France, 2006). Only values for varieties with final leaf number below the optimum identified in Fig. S3 are presented. For an easier comparison between experiments, yield has been normalized by its value at 1200 MJ plant^{-1} predicted by the polynomial regression in each field experiment.

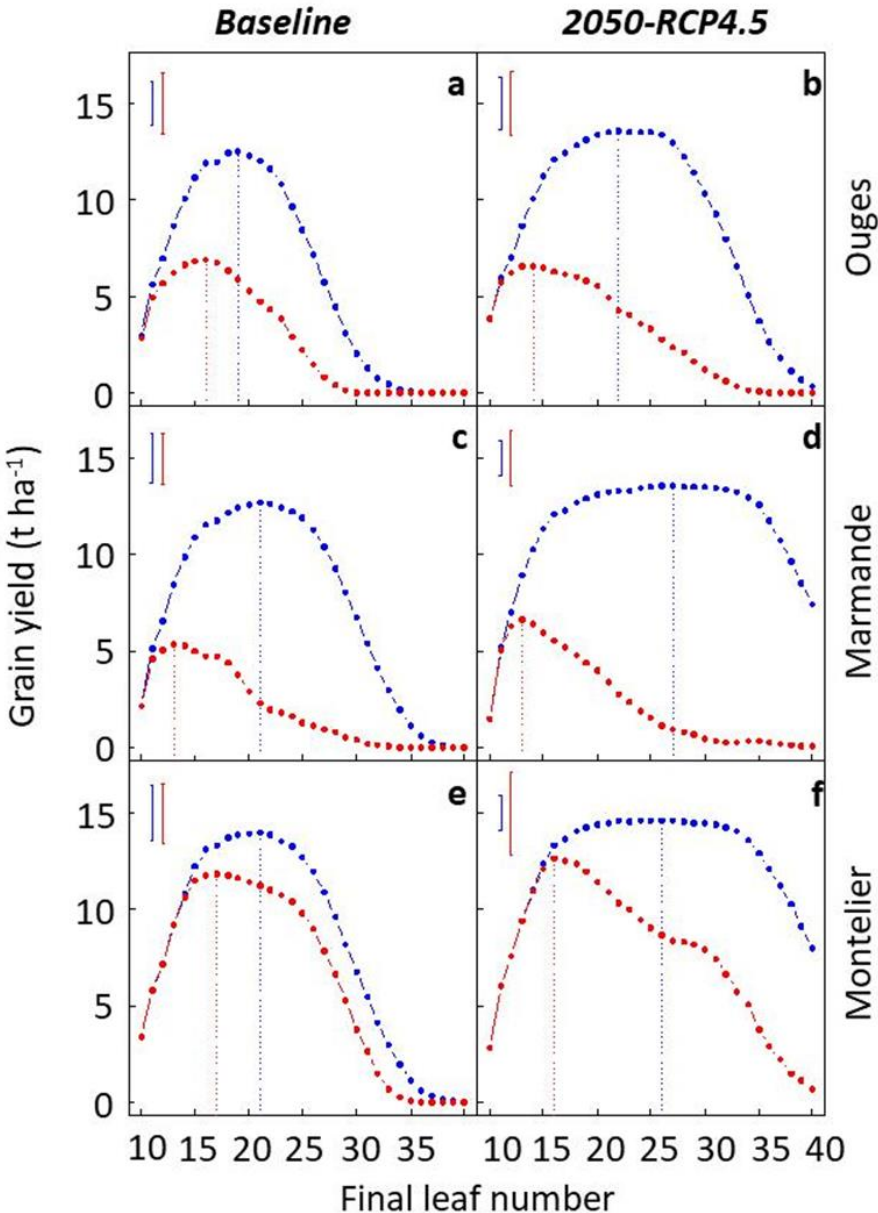**Supplementary figure 4.5:**

Supplementary Figure 4.5 | Relationship between simulated and observed data .
a, Relationship between latitude and sowing or flowering dates, either simulated (blue dots) or observed (black dots, data from *AgroPhenoDB* of the Joint Research Centre). Each dot is the mean of 10 years (2000-2010) in one location, either for observed or simulated data in fully-irrigated conditions. Circles, sowing date; triangles, flowering date. Lines, linear regressions.
**b,** Observed and simulated yield in ten European countries. Observed values are mean values for the 2000-2010 period at the country level (Eurostat database). Simulated values for the 2000-2010 period were up-scaled by applying the ratio of irrigated/rainfed fields for each country (FAOstat DB).

Supplementary figure 4.6:

Supplementary Figure 4.6 : Grain yield simulated for virtual varieties differing in cycle duration in three sites in current and future conditions (2050, RCP4.5). Relationship between cycle duration and yield simulated for the sites at "Ouges" (**a**,**b**), "Marmande" (**c**,**d**) and "Montelier" (**e**,**f**) in fully-irrigated (blue dots and lines) or rainfed conditions (red dots and lines). For better intuition, cycle duration is expressed as final leaf number. Dots are averaged values for 35 years. Error bars, confidence intervals (P = 0.95). Vertical dashed lines indicate the optimum cycle duration.
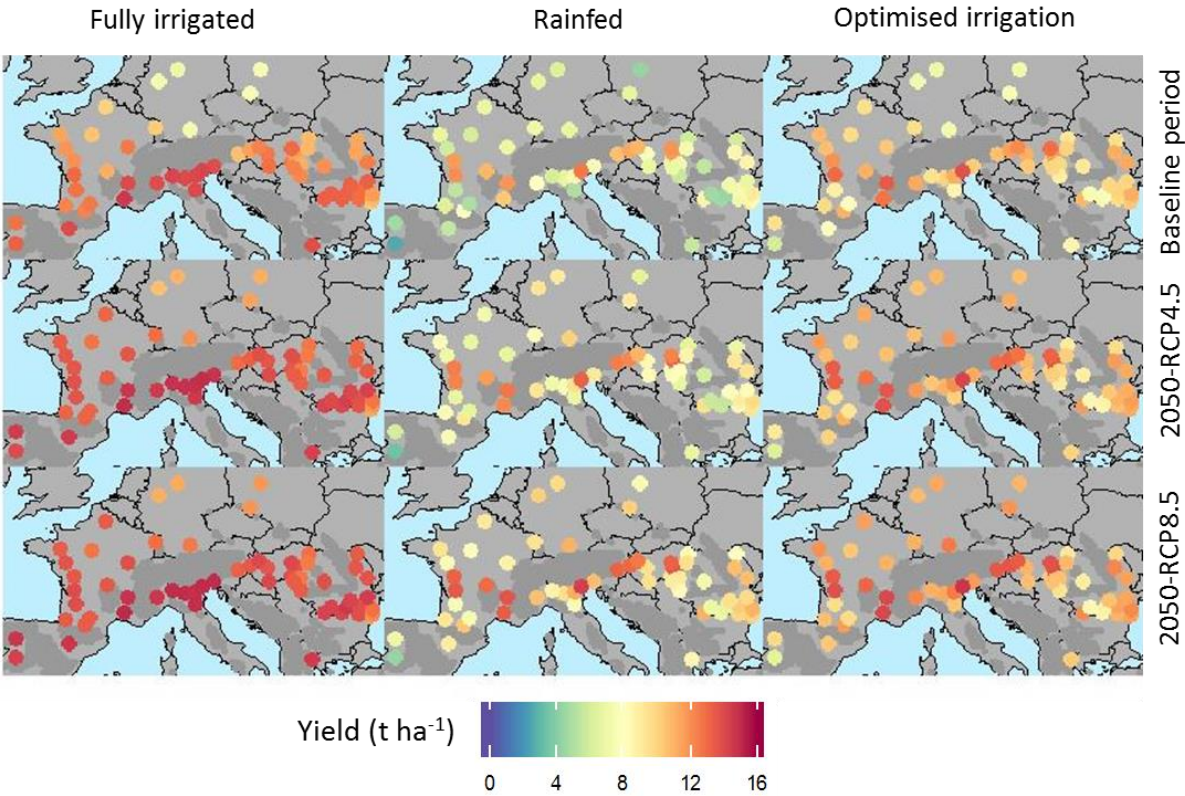
Supplementary figure 4.7:
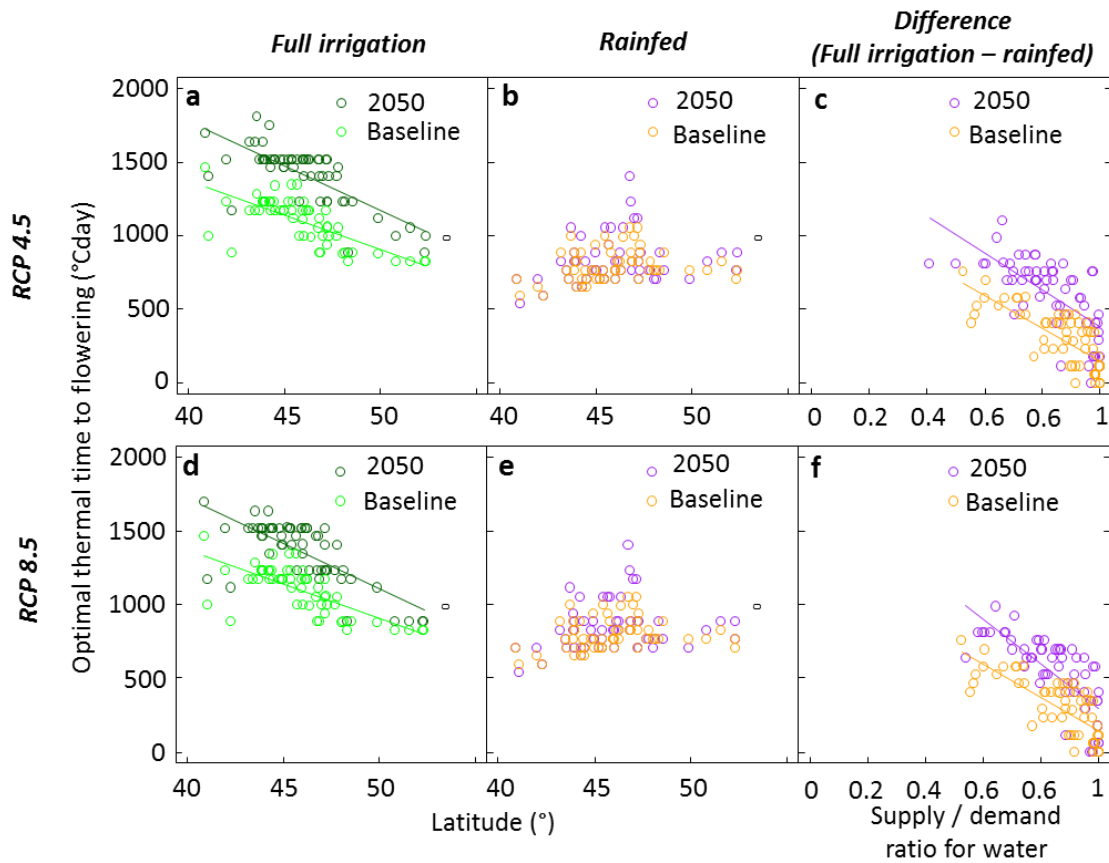
Supplementary Figure 4.7 : Crop growth cycle duration that optimizes yield in current and future climates, as a function of latitude and supply / demand ratio for water.

a, b, d, e, Optimum time to flowering (°Cdays) as a function of latitude for the baseline period and 2050 with RCP4.5 (**a**, **b**) and RCP8.5 (**d**, **e**), fully-irrigated (**a**, **d**) or rainfed (**b**, **e**).

c, f, Difference between values in rainfed conditions (either for baseline period or 2050, RCP4.5, **c** and RCP8.5, **f**) and the corresponding value in fully-irrigated conditions, plotted against the mean supply/demand ratio for water around flowering (1 : well-watered, 0 : very severe stress).

106

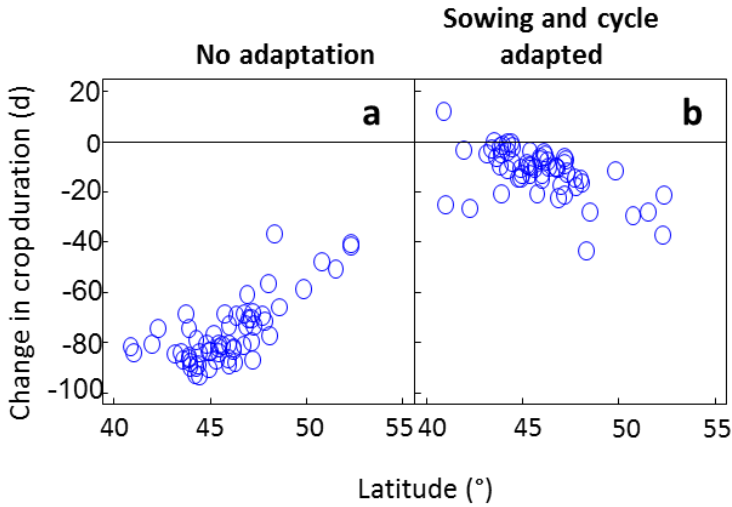**Supplementary figure 4.8:**

Supplementary Figure 4.8 : Maps of Simulated yield over for the baseline period and in 2050 (RCP4.5 and RCP8.5) in the three studied irrigation strategies. Data are averaged for 30 years in the 59 sites. Data for 2050 are mean of 4 GCMs.

Supplementary figure 4.9:
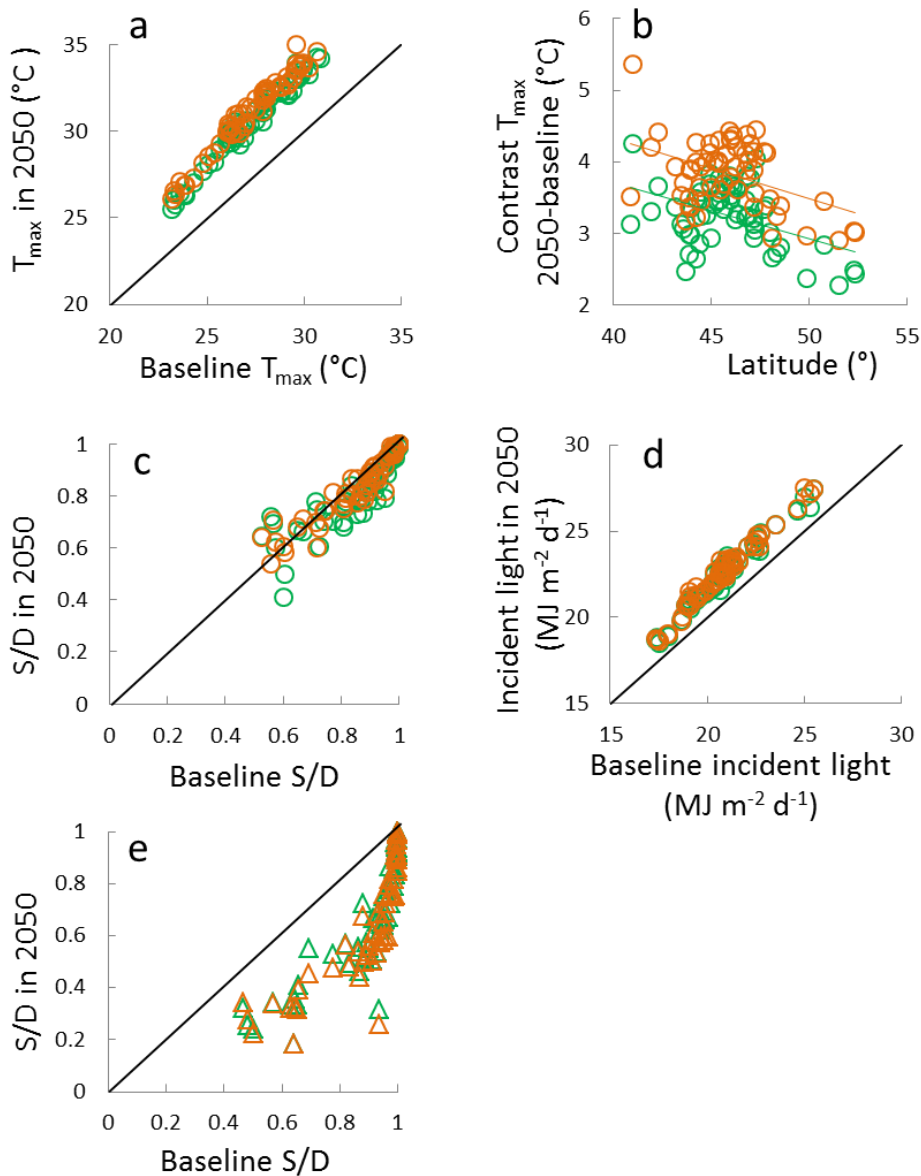
Supplementary Figure 4.9 : Change in temperature, ratio of supply/demand for water and incident light between current and future conditions around maize flowing time. a, Average daily maximum temperature (T_{max}) for the baseline period and 2050 conditions. **b,** Contrast in T_{max} plotted against latitude. **c,** Supply/demand (S/D) ratio for water for the baseline period and 2050 conditions for simulations considering an increase in transpiration efficiency linked to increased CO_2 concentration. **d,** incident light for the baseline period and 2050 conditions. **e,** S/D ratio for water for the baseline period and 2050 conditions for simulations that did not consider an increased transpiration efficiency. Green, RCP 4.5, median of four GCMs. Orange, RCP8.5, median of four GCMs. All data are monthly mean for July.
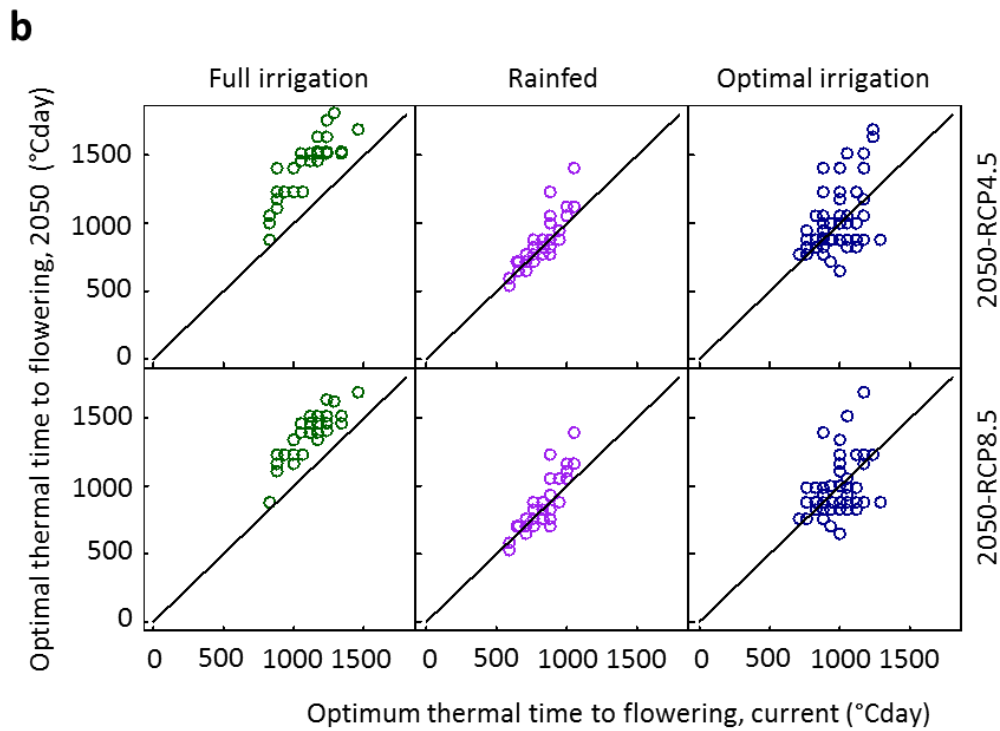
Supplementary figure 4.10:

Supplementary Figure 4.10 : Contrast in total crop duration from sowing to harvest between the baseline period and 2050 (RCP4.5).
a, No adaptation of sowing and cycle duration by farmer. **b,** an adaptation of sowing date.
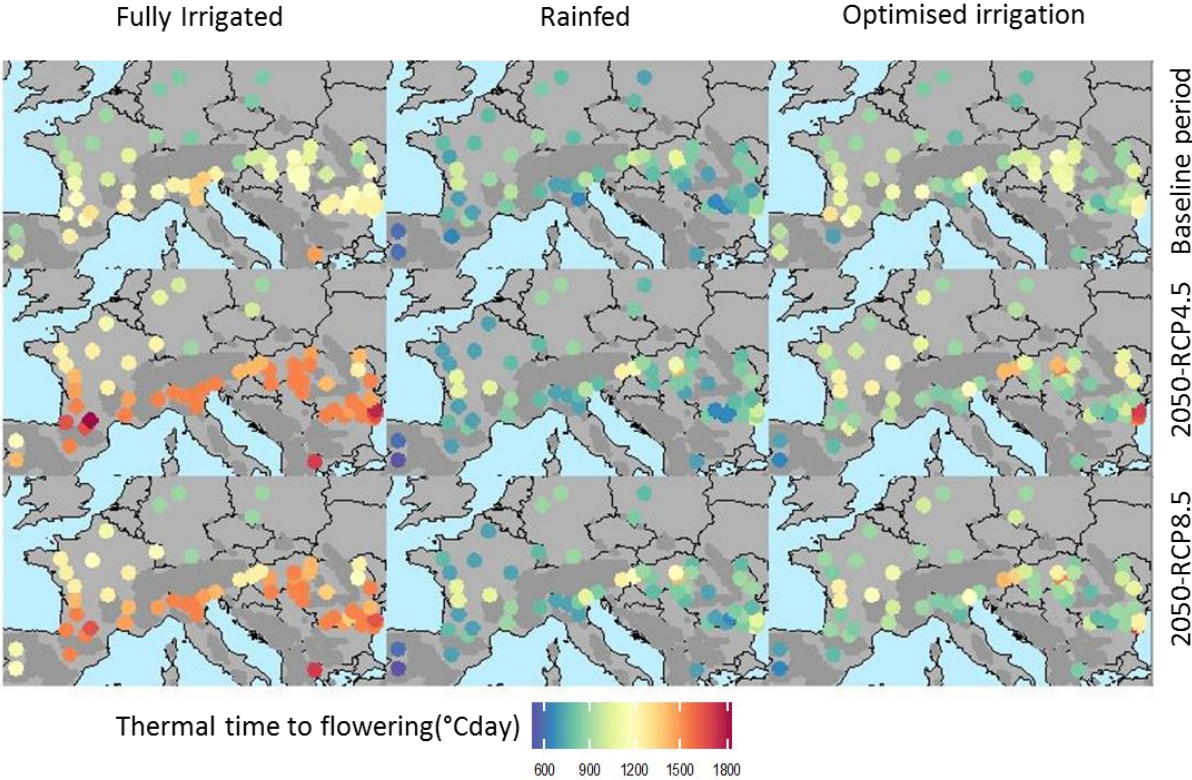
Supplementary figure 4.11:

| a	Sowing date current	Sowing date 2050 (RCP4.5)	Sowing date 2050 (RCP8.5)	Change (day) baseline-RCP4.5	Change (day) baseline-RCP8.5
Mean	10th April	21th March	19th March	-20	-22
Median	10th April	25th March	20th March	-19	-22
min	20th March	17th Febr.	7th Febr.	-39	-41
max	30th April	20th April	17th April	-10	-9

Supplementary Figure 4.11 : Optimal sowing date and relationship between current and future optimal time to flowering. a, Table of optimal sowing date in current and future conditions. **b,** Relationship between optimal time to flowering in the baseline period and in for RCP4.5 and RCP8.5 in the 59 European sites under fully-irrigated, rainfed or optimised irrigation conditions. Lines are the 1:1 relationships.

Supplementary figure 4.12:

Supplementary Figure 4.12 : Maps of optimum crop growth cycle duration for the baseline period and in 2050 (RCP4.5 and RCP8.5) in the three studied irrigation strategies. Data for 2050 are mean of 4 GCMs.

Supplementary figure 4.13:
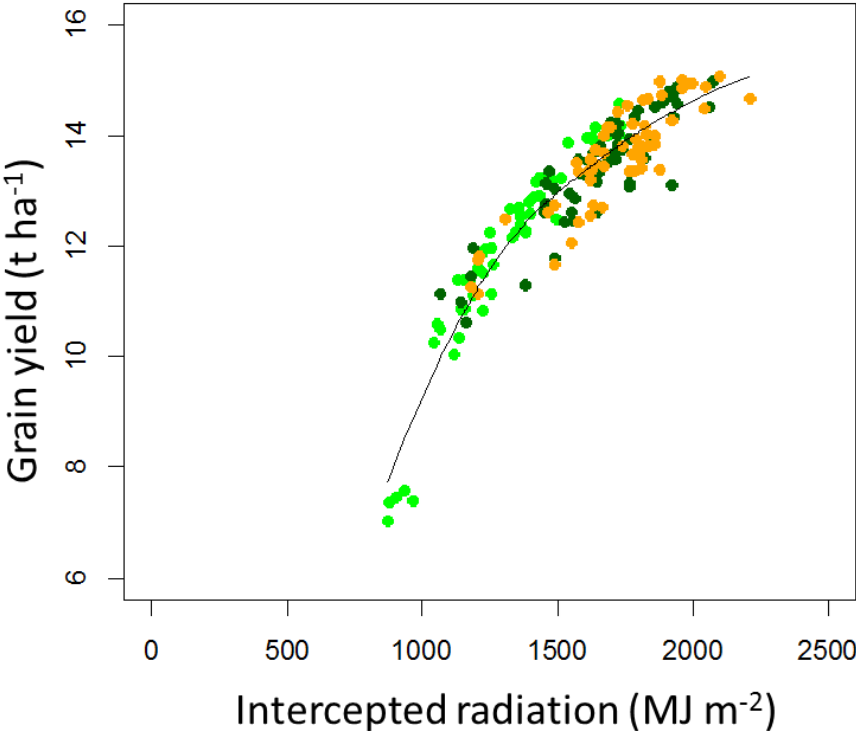
Supplementary Figure 4.13 : Relationship between simulated intercepted radiation and grain yield in fully-irrigated conditions for the baseline period and in 2050. Each dot is a the average value for one site for the baseline period (green) or in 2050 for RCP4.5 (dark green) or RCP8.5 (orange).

Supplementary table 4.1: Summary of maize growing sites used in simulations.

Site	Longitude (°)	Latitude (°)	Site	Longitude (°)	Latitude (°)
Austria_Leibnitz	15.55	46.78	Italy_Asola	10.42	45.22
Bulgaria_General_Toshevo	28.03	43.72	Italy_Bologna	11.35	44.50
Bulgaria_Glavinitsa	26.83	43.90	Italy_Campoformido	13.17	46.02
France_Achenheim	7.62	48.57	Italy_Orgiano	11.47	45.35
France_Avignon	4.80	43.94	Italy_Paese	12.15	45.67
France_Chemille	-0.72	47.20	Italy_Pantigliate	9.35	45.43
France_Clermont_Ferrand	3.08	45.77	Italy_Santena	7.77	44.95
France_Estrees_Mons	3.00	49.88	Poland_Tuszyn	16.65	50.80
France_Marmande	0.15	44.50	Poland_Wrzesnia	17.57	52.32
France_Montelier	5.03	44.95	Romania_Alexandria	25.35	43.98
France_Orthez	-0.77	43.48	Romania_Arad	21.32	46.17
France_Ouges	5.07	47.26	Romania_Barca	23.63	43.97
France_Palaminy	1.07	43.20	Romania_Barlad	27.67	46.23
France_Pamproux	-0.05	46.38	Romania_Botosani	26.67	47.75
France_Patay	1.70	48.05	Romania_Bulbacata	25.80	44.28
France_Saint_Bonnet	0.10	45.48	Romania_Chirnogeni	28.23	43.90
France_Toulouse	1.43	43.60	Romania_Daia_Romana	23.67	46.02
France_Vitre	-1.22	48.12	Romania_Dochia	26.57	46.92
Germany_Augsburg	10.90	48.37	Romania_Dor_Marunt	26.92	44.43
Germany_Hanover	9.73	52.37	Romania_Gataia	21.43	45.43
Germany_Werl	7.93	51.57	Romania_Lovrin	20.77	45.97
Greece_Evropos	22.57	40.92	Romania_Medgidia	28.27	44.25
Hungary_Foldeak	20.48	46.32	Romania_Parscoveni	24.23	44.28
Hungary_Kondoros	20.80	46.77	Romania_Puchenii_Mari	26.08	44.82
Hungary_Kormend	16.60	47.02	Romania_Salard	22.03	47.22
Hungary_Lajoskomarom	18.33	46.85	Romania_Viziru	27.70	45.00
Hungary_Nyirbator	22.13	47.83	Spain_Barbues	-0.42	41.98
Hungary_Ormenyes	20.58	47.18	Spain_Gomecello	-5.53	41.05
Hungary_Papa	17.47	47.32	Spain_Villamanan	-5.58	42.32
Hungary_Szederkeny	18.47	46.00			

Chapter 5: Identifying maize ideotypes from observed or unconstrained phenotypic spaces of model parameters in contrasting environmental scenarios.

In this chapter, I use the model developed in chapters 1 and 2, the simulation framework developed in chapter 3 and parameters of phenology for best-adapted genotype in each site as identified in chapter 4, to simulate the impact of the genetic variability of leaf growth parameters on plant production and identify best ideotypes in European conditions.

Identifying maize ideotypes from observed or unconstrained phenotypic spaces of model parameters in contrasting environmental scenarios.

Sebastien Lacube, Boris Parent and François Tardieu

INRA, UMR759 LEPSE, F-34060 Montpellier, France

Abstract

The ideotyping approach uses crop models to define which combination of parameter/trait values could maximize crop production in target environmental scenario. Defining an ideotype which could be attainable by breeding is possible only if (i) crop models have adapted formalisms capturing the genetic diversity and simulating genotype by environment interactions as observed for yield in rainfed environments and (ii) if the set of possibilities considering all traits/parameters together is well-defined. We used two approaches to determine maize ideotypes of leaf expansion and sensitivity to evaporative demand, soil water deficit and light which maximise yield in 59 European sites, 36 years and 3 irrigation scenarios. The first approach considered an unconstrained phenotypic space of 216 virtual maize hybrids defined by a grid of parameter values. The second approach considered an observed phenotypic space determined by phenotyping 254 maize hybrids maximising the genetic diversity. This phenotypic space was constrained by observed relationship between parameters values, limiting the field of possibilities for breeding. Analysis of results in four clusters of environments depending on pattern of water stresses resulted in contrasted ideotypes in both approaches, with sensitive hybrids being better for southern region under rainfed conditions while less-sensitive genotypes better in northern Europe or in irrigated fields. However, the best combination of parameters determined in the unconstrained phenotypic space was not available in the observed genetic diversity. Overall, this study indicates to breeder the environmental scenarios in which such or such leaf growth strategy would be beneficial and highlight the importance of considering observed constraints between parameters in ideotype studies

Introduction

In the context of climate change, yield improvement will largely depend on the capacity of breeding new varieties that perform better in stressing environments (Casadebaig et al., 2008). Indeed, crops will probably experience higher frequencies of abiotic stresses (Bindi and Olesen, 2011) such as warmer temperatures and limited rainfall in summer (Asseng et al., 2014; Harrison et al., 2014; Reynolds et al., 2016). Breeding of such varieties is a long process, but the use of crop models may allow identifying traits of interest for yield improvement in specific target environment (Perego et al., 2014; Martre et al., 2015; Rötter et al., 2015; Tao et al., 2017). This is possible only if crop models have the capacity of capturing and simulating genotype by environment interactions (Parent and Tardieu, 2014; Chenu et al., 2017). Recent advances in crop modelling allow adaptation of formalisms to integrate the observed diversity of parameter values (Hammer et al., 2010; Martre et al., 2015). If the model design is convenient, it can be used to analyse the sensitivity of a given trait to environment variables, thereby guiding breeders to identify traits of interest in each targeted environmental scenario (Jeuffroy et al., 2014; Marcaida et al., 2014; Gouache et al., 2017).

In this context, testing trait values for parameter linked to leaf growth appears crucial. Indeed, leaf expansion is one of the first processes affect by water stress and evaporative demand with a large genetic variability observed in crops such as maize (Welcker et al., 2011), rice (Parent et al., 2009) or wheat (Parent et al., 2015). Limiting leaf expansion allows plant to reduce transpiration and save water for late stages of crop cycle but decreases carbon acquisition. This trade-off results in contrasted yield benefit or loss depending on environmental scenarios (Tardieu, 2012) and the necessity of defining which strategy is positive in such or such environment. A possibility is to explore it via crop modelling, the '*ideotyping*' approach (Casadebaig et al., 2011; Chapman et al., 2012; Asseng et al., 2014; Challinor et al., 2014; Rötter et al., 2015). This approach aims at defining the best combination of parameters to maximize crop production in each environmental scenario (Jeuffroy et al., 2014; Perego et al., 2014).

A difficulty of such an approach is the definition of the set of possibilities considering all traits/parameters together. Indeed, in the observed genetic diversity, all combinations of trait values are not available, and sometimes will never be, due to physiological or physical constraints resulting in genetic correlations between traits. This defines the phenotypic space of parameters, which is of great importance if the aim is defining an ideotype which could be attainable for breeders (Yin et al., 2003). For example, the leaf economic spectrum (Wright et al., 2005) defines physiological constraints linking leaf nitrogen, specific leaf area and net photosynthesis in plant kingdom. Development of phenotyping facilities now allows to measure several traits in hundreds of genotype (Tardieu et al., 2017), to highlight potential trade-offs between traits, and allows the bounding of the possible parameters combinations (Townsend et al., 2017).

This study aims at defining the best ideotypes from the genetic diversity of parameters linked to leaf growth and its sensitivity to evaporative demand, soil water deficit and radiation, in multiple environmental scenarios over European maize growing regions. We have used two strategies to deal with the constraints on phenotypic space. The first strategy considers a grid of parameter values without *a priori* information on the constraints or correlation between parameters (named "unconstrained phenotypic space" hereafter). The second strategy considers measured parameter values in a panel of 254 hybrids maximising the genetic diversity of maize ("observed phenotypic space"). However, this second strategy still involves virtual hybrids with (i) cycle duration adapted to

each site as identified in Chapter 4 and (ii) all parameters other than those involved in leaf growth and in cycle duration considered as common to all tested hybrids.

Simulations were performed for three irrigation scenarios, namely rainfed, optimised irrigation and fully irrigated, in 36 years and 59 sites summarising the European maize growing region. Results were summarised by clustering environments into 4 classes depending on frequencies and types of water stresses encountered by the crop in each site defined by Harrison et al. (2014). The study on the unconstrained phenotypic spaces resulted in contrasted ideotypes, with sensitive hybrids being better for southern region under rainfed conditions and non-plastic hybrids being better for northern region or in irrigated fields. The second approach based on observed phenotypic space gave similar tendencies but showed that the best combination of parameters was not available in the observed phenotypic space. These differences between the two approaches highlight the importance of considering observed constraints between parameters in ideotype studies and gives keys to breeders for plant improvement in different target environments.

Complements of material and method

Model parameters

Two strategies were adopted in this study, by considering either an unconstrained space of three parameters linked to leaf growth or the observed phenotypic space of these parameters. For both strategies, parameters related to phenology as well as sowing dates were fixed for each site as those maximising yield in each site (Chapter 4). All other parameters used in the crop model are those of the reference hybrid, for which simulations were tested over a network of site (DROPS network) around Europe for end of season leaf width and length and grain number and grain yield (B73, Chapter 2).

Measured parameters of the three traits of interest for the 254 hybrids were estimated from platform and field measurements. Briefly, maximum leaf elongation rate ('a') and the sensitivity of leaf elongation rate to water deficit and evaporative demand ('c_0') were estimated by analysing the dynamics of leaf expansion in platform experiments under optimal conditions and soil water deficit (Chapter 1 and 2). 'c_0' is the x-intercept of the relationship between leaf elongation rate and soil water potential, i.e. the water potential value that stops leaf elongation. It was better adapted to this study than the slope of relationships, which are highly correlated to the maximum elongation rate a. The response of leaf widening ('s_{RAD}') to intercepted radiation was estimated from leaf width measurements in field and platform experiments (Chapter 2).

The grid of parameters values used in the unconstrained phenotypic space was constructed by using the 6 sextiles of the parameter distributions, and considering all combinations between parameter values to obtain a set of 216 (6^3) sets of parameter values .

Drought scenarios

We have used the four drought scenarios identified in Harrisson et al., 2014 (Fig. 5.1 A and B), calculated by clustering the time courses of supply/demand ratios over 36 years of simulations for the reference hybrid in 55 sites. This analysis was extended here with the same algorithm as Harrisson et al., 2014 on the four new sites added in Chapter 4. The algorithm used was the function 'kmeans' (R software) for clustering mean values of supply demand ratio in classes of 50 °Cd during the studied period.

The four drought scenarios (Fig. 5.1, B) presented different frequencies of occurrence between sites (Fig. 5.1, A). One cluster ('no stress': supply demand close to 1 during the whole cycle) shows relatively low to no stress during the whole crop cycle, and is mostly dominant in the northern sites. The most severe scenario ('Early terminal': water deficit during and after flowering) is dominant in southern sites, and intermediate scenarios ('Late terminal': water deficit after flowering; 'Recovery': water deficit at flowering with soil rehydration during grain filling) were dominant in intermediate latitudes.

Simulations and analyses

Simulations were performed for all sets of years (36) x sites (59) x irrigation scenarios (3) x parameter values in both strategies (observed and unconstrained phenotypic spaces, respectively 254 and 216 genotypes), leading to 3 001 212 simulation runs.

In a first step, results were analysed in each site, considering the average yield for each genotype (set of parameters) in each site and irrigation scenario. In this case, the 'best ideotype' is the genotype with highest mean yield in that environment (site x irrigation). In a second step, we used the clusters of environments to analyse simulations. Results of any set of year x site x irrigation were grouped in one of the four cluster. In this case, an ideotype was therefore the set of parameter maximising yield for the considered scenario, regardless of the year, site or scenario of irrigation.
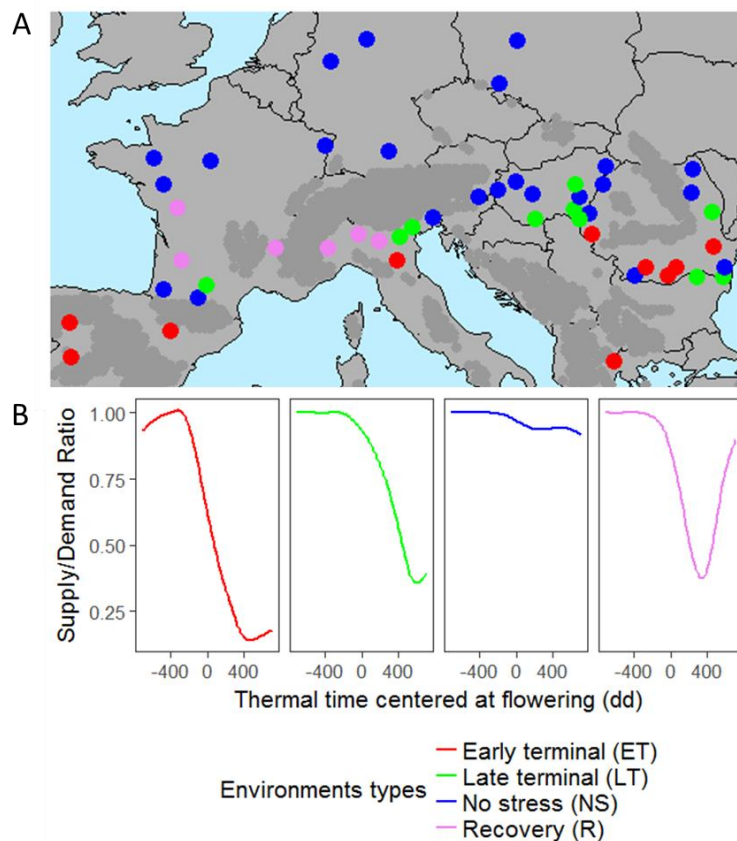

Figure 5.1: Dominant drought scenarios in each of the 59 European sites.
(A) (Blue: no stress; Red: water deficit before and after flowering time; Green: late water deficit after flowering, Purple: flowering-time water deficit with soil rehydration during grain filling).
B) Drought scenarios are defined by clustering the time courses of the supply / demand ratio calculated by APSIM. Clustering was performed based on simulations of the reference hybrid B73_H.

Results

Ideotypes for leaf growth largely depended on scenarios of water deficit within an unconstrained phenotypic space.

The observed genetic variability was high for the three studied parameters, which all displayed normal distributions in spite of a tendency to a skewed distribution for c_0 (Fig.5.2). From these observed value, an unconstrained phenotypic space of three dimensions was built, based on the sextiles values of the distribution of each parameter (Fig.5.3, red points). This leads to 216 sets of parameter values covering this theoretical phenotypic space. For each combination of site x year and irrigation, the set of parameter values maximising final yield was identified every year (Fig.5.4). A set of parameter values maximising mean yield over the 36 year was then identified. A large G x E interaction was observed at European scale with the best set of parameter largely differing between sites and irrigation strategies (Fig.5.5).
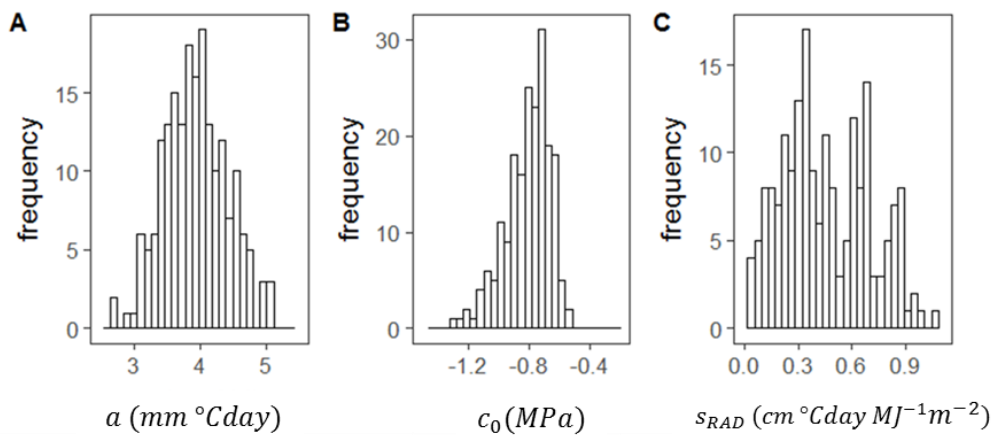

Figure 5.2: Distribution of values for the three studied parameters in 255 maize hybrids. (A) Distribution of maximum leaf elongation rate, parameter 'a'. (B) Distribution of the soil water potential that stops leaf elongation, parameter 'c_0'. (C) Distribution of the response of leaf widening to intercepted light 's_{RAD}'.
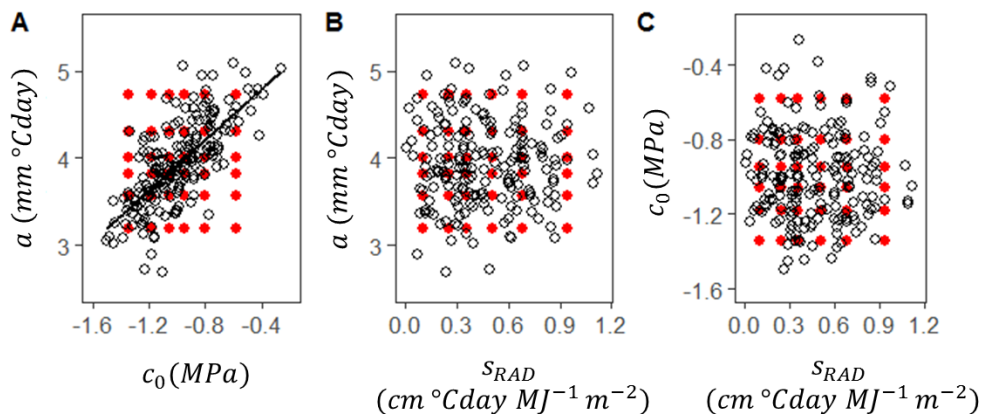

Figure 5.3: Scatterplot of the relationships between measured values of the three studied parameters (A,B,C). Black points: measured value in the studied panel of 255 hybrids defining the observed phenotypic space. Line: linear regression. Red points: grid of parameter values used to define genotypes in the unconstrained phenotypic space.
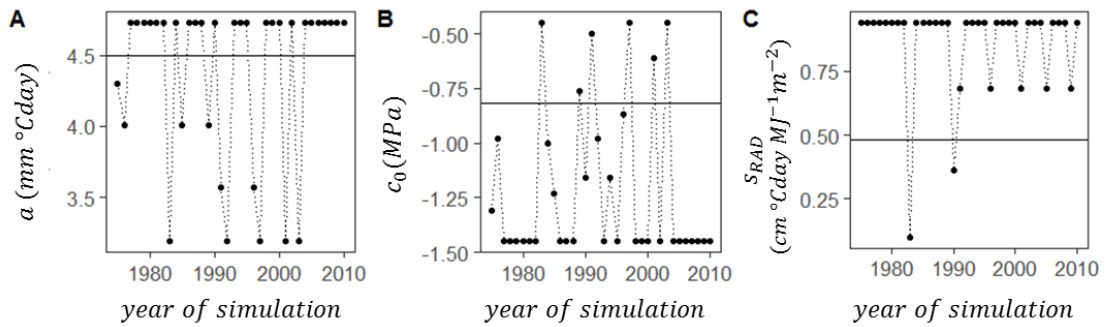
Figure 5.4: Best parameter values over 36 years for one site (Austria Leibnitz) for each studied parameter. Points and dotted line: best parameter value per year. Horizontal solid line: parameter value resulting in the highest mean yield over the 36 years of simulation in rainfed conditions.
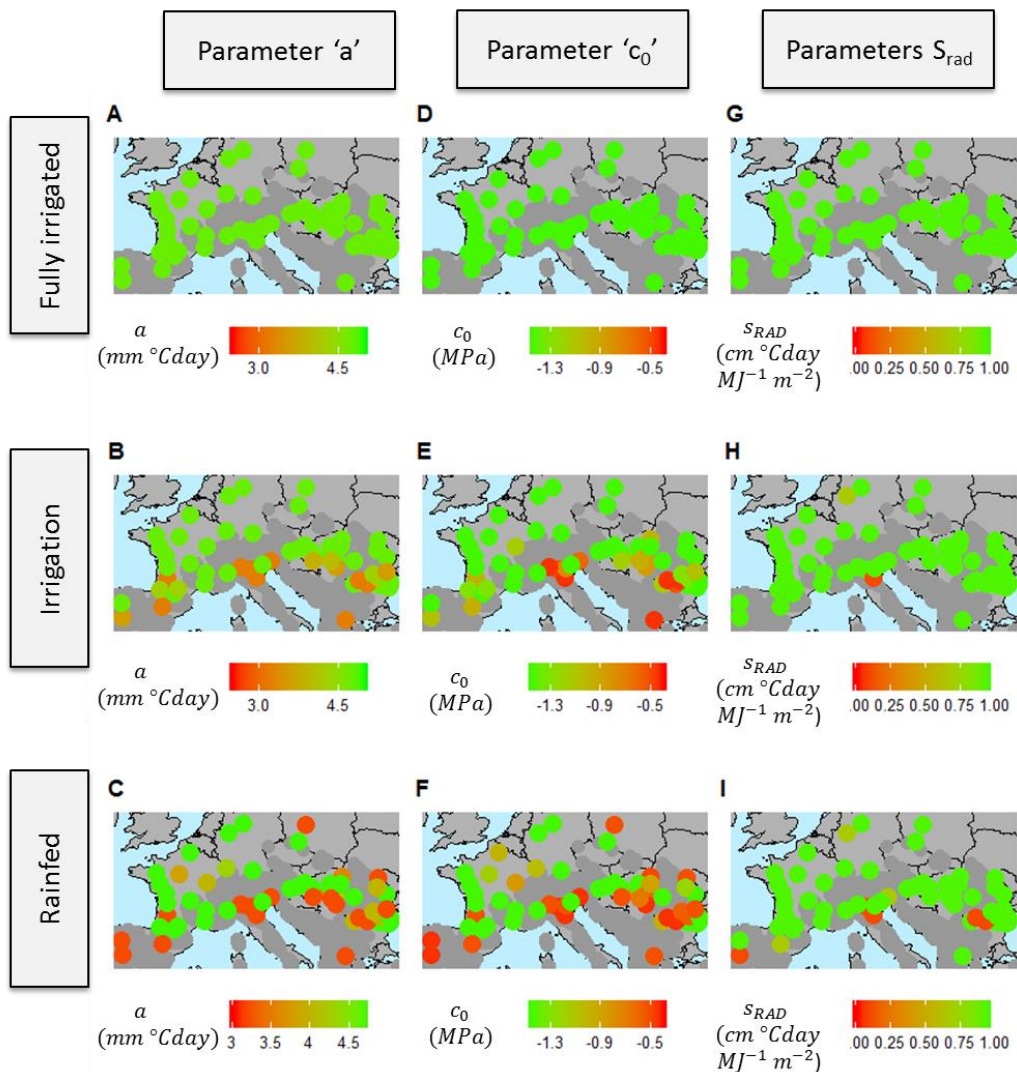
Unconstrained Phenotypic Space

Figure 5.5 : Best parameter value calculated for each site in the three watering regimes, using a grid of parameters values (unconstrained phenotypic space). The set of best parameter values maximises mean yield over the 36 years of simulation in each site.

120

In fully irrigated conditions, the best sets of parameter values were similar in all sites (Fig. 5.4: A, D,G), with highest maximum elongation rates (a = 4.73 mm°Cd^{-1}), low sensitivities to water deficit and evaporative demand (c$_0$ = -1.4 MPa) and high sensitivities of leaf width to intercepted light (s$_r$ = 0.94 cm °Cday MJ^{-1} m^{-2}). A strategy with high use of resources was therefore always beneficiary in the absence of water constraints. Conversely, in southern sites with rainfed conditions, the best ideotypes were those with lowest maximum elongation rate and highest sensitivity to water deficit and evaporative demand (Fig. 5.4, B,E,H). Although maximum sensitivity of leaf width to intercepted light was most often beneficial, the opposite result was observed in some southern sites. An intermediate pattern between full irrigation and rainfed conditions was observed in optimised irrigation regimes.

When sites, year and irrigation regimes were analysed jointly, a clear relationship was observed between best parameter values and the supply / demand ratio (Fig.5.6). For the three parameters, those resulting in highest leaf area resulted in best yields in the absence of water deficit (S/D from 0.8 to 1). This involved highest values of maximum leaf elongation rate, minimum sensitivity (elongation continuing till -1.5 MPa) and maximum leaf width in high intercepted light. Conversely, low elongation rates, highest sensitivities to water deficit and lowest leaf width resulted in the highest yields under severe water deficit (S/D from 0.5 to 0.65).
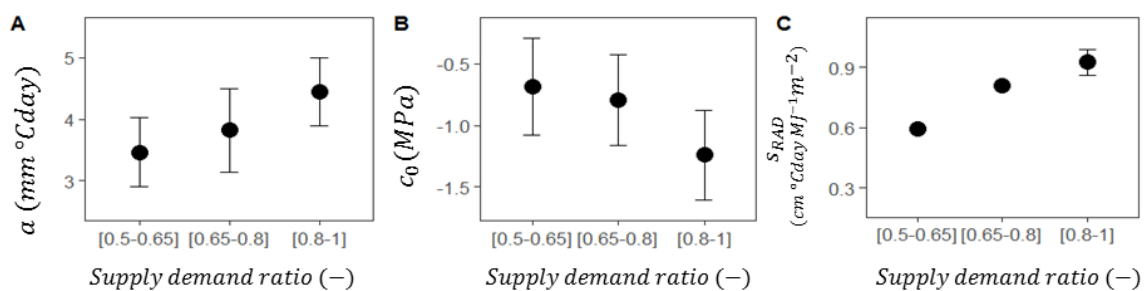

Figure 5.6 : Set of best parameter values for three classes of mean supply/demand ratio for all sites, using a grid of parameters values. Mean supply demand ratio is calculated in a window of 100 °Cd before and after flowering.

We have then analysed these results per drought scenario, for each of the four patterns of water deficit determined by clustering, namely (i) no water deficit, observed in all sites for the well-watered treatment, but also in northern sites in rainfed conditions (Fig.5.1); (ii) early terminal stress, with water deficit occurring before flowering and continuing during grain filling, mostly observed in southern sites in rainfed conditions (Fig.5.1), (iii) late water deficit occurring after flowering time and (iv) water deficit with recovery during grain filling. The last two scenarios were mainly observed in rainfed conditions at intermediate latitudes. Simulated yields were the highest in the "no stress" scenario (Fig. 5.7: from 7.8 to 12.3 tha^{-1}) and the lowest in the early stress scenario, ranging from 5.4 to 5.8 t ha^{-1}. Intermediate values were simulated in the other two scenarios, with yield ranging from 6.8 to 7.4 tha^{-1} for the 'recovery' scenario and from 6.9 to 7.7 tha^{-1} for the 'late stress' scenario.

121
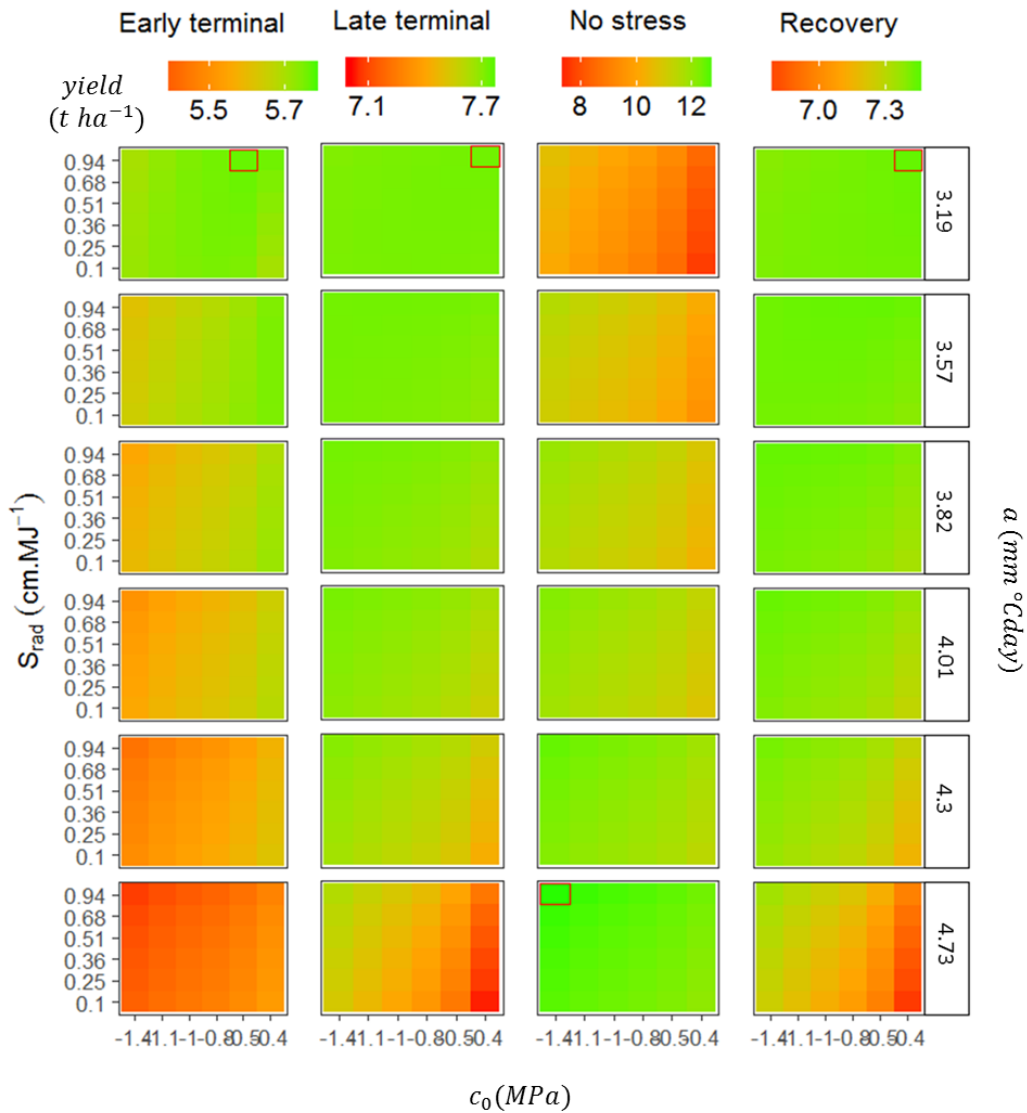
Unconstrained Phenotypic Space

Figure 5.7 : Heatmap of the effects on yield of the three studied parameters in the four drought scenarios x-axis : parameter 'c_0' ; y-axis : parameter 's_{rad}' ; rows : three classes for parameter 'a' ; columns : drought scenarios. Simulation were performed using genotypes defined by a grid of parameters values (unconstrained phenotypic space). Green to red, yield levels. The maximum yield in each cluster is displayed by a red hollow rectangle.

Four classes of maximum leaf elongation rate are presented in rows of Fig. 5.7, and scenarios are presented in columns. In each panel, all combinations of S_{rad} and c_0 are presented, with highest yields in green. In the 'no stress' scenario, the best ideotype was the one with the highest maximum leaf elongation rate (a = 4.73 mm °Cd⁻¹) and the lowest value of sensitivity to soil water deficit. Results were opposite in the other three scenarios with the best ideotypes showing the lowest values of parameter a (3.19 mm °Cd⁻¹) and c_0 being within the two highest sensitivities. A high sensitivity of leaf width to plant intercepted radiation was positive in nearly all cases when considering the best set of parameters for the two other parameters. However, in the "late terminal" and "recovery" scenarios, a low sensitivity to intercepted radiation was positive when combined with highest values of maximum leaf elongation rate.

122

Overall, these results show a clear pattern, with the ideotype in well-watered conditions maximising light interception via highest values of elongation rate, the highest sensitivity of leaf width to intercepted light and the lowest sensitivity to water deficit. In all scenarios of water deficit, 'conservative' ideotypes resulted in highest yields, with lowest maximum elongation rate and maximum sensitivity to water deficit. Noteworthy, a small interaction was observed between the sensitivity of leaf width to intercepted light and the other two parameters.

Best ideotypes identified within the unconstrained phenotypic space were not available within the observed genetic variability, although tendencies remained similar in observed and unconstrained phenotypic spaces.

We have then analysed the behaviour of virtual hybrids presenting existing combinations of parameter values in the panel of 254 maize hybrids. Some combinations of parameter values did not exist within this panel. For example the correlation between maximum leaf elongation rate (a) and sensitivity to evaporative demand and water deficit (c_0, Fig.5.3A, R^2 = 0.38) results in the fact that there is no hybrid presenting both a high maximum leaf elongation rate and a low sensitivity to water deficit. The same appears for hybrids with low maximum leaf elongation rate and high sensitivity. Conversely, there was no correlation of these two parameters with the sensitivity to intercepted radiation so all combinations were possible (Fig. 5.3 BC).

Best ideotypes (Fig. 5.8, A to I) showed a pattern with latitude and water deficit that was consistent with the analysis of unconstrained phenotypic space. In fully irrigated conditions (Fig. 5.8, ADG), the best genotype was the same in all sites, with the highest measured maximum leaf elongation rates (5.1 mmdd^{-1}), a moderate value of sensitivity of elongation rate to water deficit (-0.91 MPa) and a high sensitivity of width to intercepted radiation (0.64 cm.MJ^{-1}). With lower irrigation regimes, ideotypes with lowest maximum elongation rate performed the best, as above (Fig. 5.9 A), but the optimum sensitivity to water deficit was essentially similar at all levels of water deficit (Fig. 5.9 B).
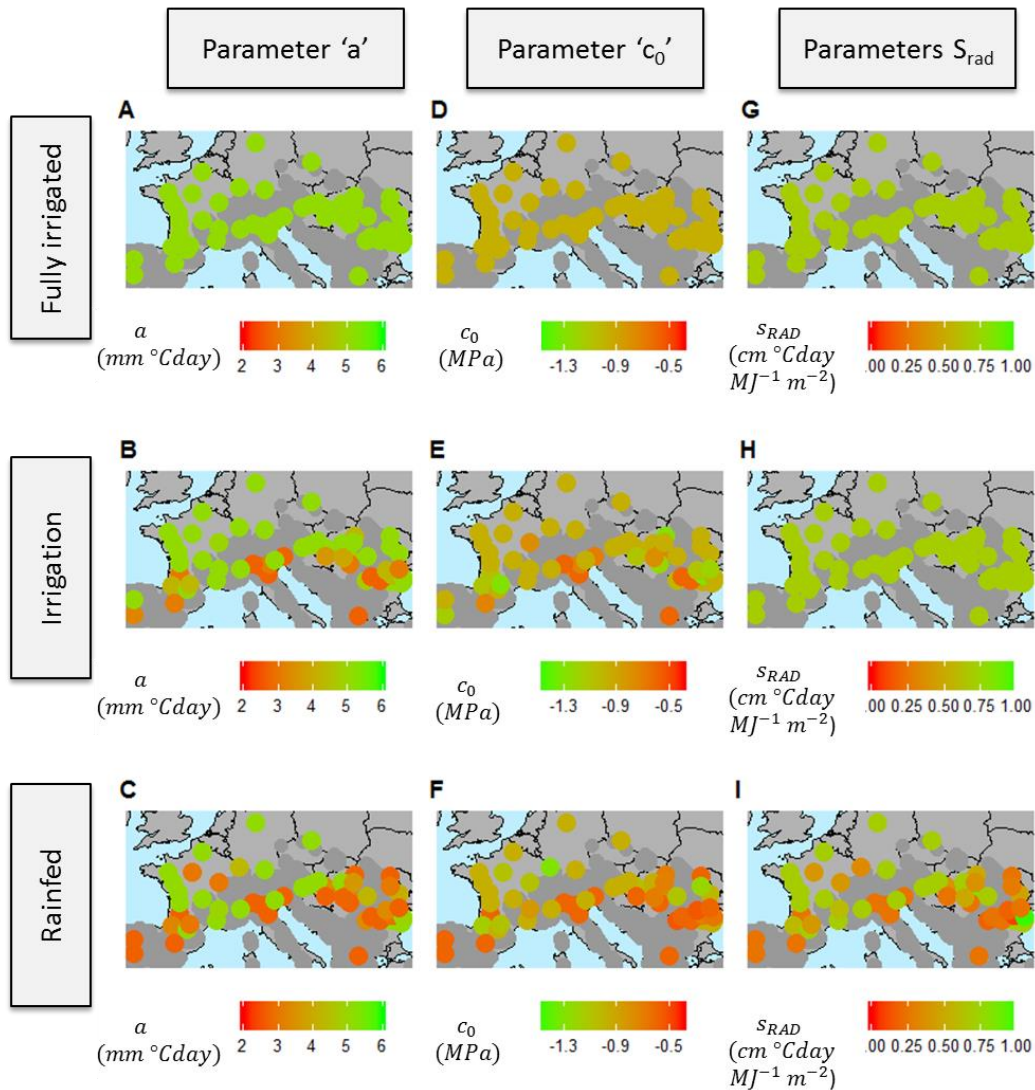
Observed Phenotypic Space

Figure 5.8 : Best parameter value calculated for each site in the three watering regimes using the parameter values measured in the 254 hybrids (observed phenotypic space). The set of best parameter values maximises mean yield over the 36 years of simulation in each site.
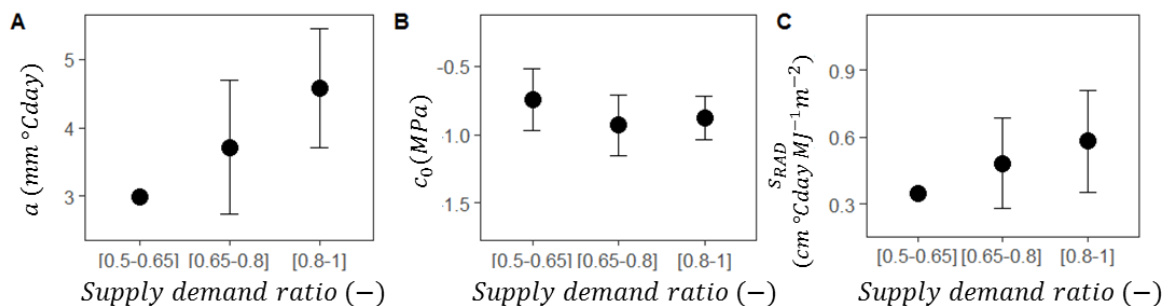

Figure 5.9 : Set of best parameter values for three classes of mean supply/demand ratio for all sites, using measured parameters in 254 hybrids (observed phenotypic space). Mean supply demand ratio is calculated in a window of 100 °Cd before and after flowering.
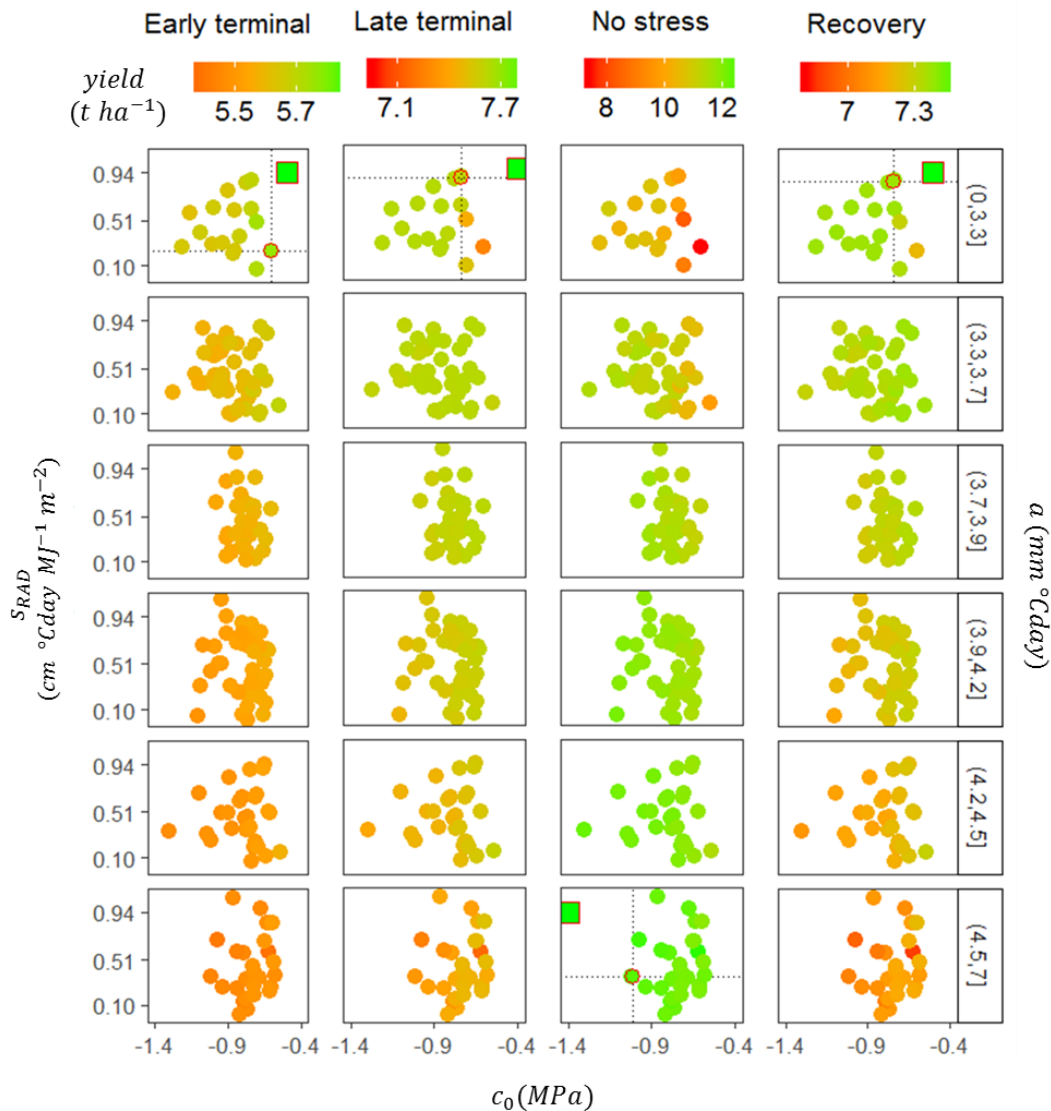
Observed Phenotypic Space

Figure 5.10 : Scatterplot of the effects on yield of the three studied parameters in the drought scenarios. x-axis : parameter 'c_0' ; y-axis : parameter 's_{rad}' ; rows, classes of parameter 'a' ; columns, drought scenarios. Simulation were performed using genotypes with observed parameter values (observed phenotypic space). Circles : mean yield of each genotype (set of observed parameter values). The best genotype in each cluster is represented as a circle with a red surround. The best genotype from unconstrained phenotypic space is represented as a square with a red contour.

Hence, we have observed appreciable differences in results between un-constrained and constrained strategies for identification of best ideotypes. Broadly, the trends were similar in both approaches with water-saving strategies and maximisation of leaf area growth resulting in highest yield in water deficit and well-watered scenarios, respectively. This difference in result can be observed in Fig. 5.10 that presents heat maps similar to those of Fig. 5.7, but in the observed phenotypic space. In well-watered conditions, the best ideotype within the observed phenotypic space had a lower response of width to intercepted light compared to that in the unconstrained space (Table 5.1 : 0.36 compared to 0.94 cmMJ^{-1}) and a higher sensitivity to water deficit (Table 5.1 : -1.02 compared to -1.4 MPa). The yield of the best ideotype was also lower than with an unconstrained phenotypic space (-2.8%). In intermediate scenarios (late terminal and recovery) the best ideotype in the observed and

125

unconstrained phenotypic space had the lowest maximum leaf elongation rate (Table 5.1: respectively 3.23 and 3.19 mm°Cd^{-1}) and highest response to intercepted radiation (Table 5.1: respectively 0.86 and 0.94 mm°Cd^{-1}) but the best ideotype did not reach the low values of sensitivity to water deficit as those determined within the unconstrained phenotypic space (Table 5.1: respectively -0.74 and -1.44 MPa). This led to an average yield loss of -3.2% and -4.2% compared to the ideotype with unconstrained phenotypic space. Finally, in the highest level of water deficit (early terminal), maximum leaf elongation rate and sensitivity to water deficit had similar values with the two approaches (Table 5.1: respectively 3.23 and 3.19 mm°Cd^{-1} and -0.74 and -1.44 MPa), but the main difference was on the sensitivity to intercepted radiation, lower for the ideotype of the observed phenotypic space (Table 5.1: 0.24 and 0.94), with an average difference in yield reaching 3.9%.

Overall, while similar trends were identified for the two approaches, the best ideotypes found within the unconstrained phenotypic space were not available within the observed genetic diversity in any of the four environment types, resulting in yield losses from 2.8 to 4.2 % in average.

Table 5.1 : Parameter values and end of season yield of the best ideotype in the constrained and unconstrained phenotypic space in each cluster of water stress over the network of sites.

Cluster of environment	Unconstrained				Observed				Yield difference
	a	c_0	s_{RAD}	Yield (t ha^{-1})	a	c_0	s_{RAD}	Yield (t ha^{-1})	
Early terminal	3.19	-0.5	0.94	5.86	2.68	-0.6	0.24	5.64	3.9%
Late terminal	3.19	-0.4	0.94	7.78	3.23	-0.74	0.86	7.54	3.2%
No stress	4.73	-1.4	0.94	12.28	6.01	-1.02	0.36	11.95	2.8%
Recovery	3.19	-0.4	0.94	7.45	3.23	-0.74	0.86	7.15	4.2%

Relative yield difference is calculated as the relative change in yield from the both ideotypes.

Discussion

Predicting G x E interaction via crop models including genetic diversity.

Predicting when and where a trait value would lead to yield benefit is of particular importance in rainfed environments because drought scenarios can highly vary between years and cause large G x E interaction on yield. Indeed, depending on the pattern of the drought scenarios, any trait value can have positive or negative effects on crop production (Tardieu, 2012). This is particularly true for traits linked to leaf expansion and transpiration because of the trade-off between water saving and carbon acquisition. However, to our knowledge, there is no available study testing where and when it should be positive to select genotypes with combinations of high elongation rate, high width and low sensitivity to water deficit. The model used for simulation in this study (Lacube et al., 2017) uses formalisms that describe leaf growth with several environmental effects (radiation, evaporative demand and soil water deficit), and integrates genotypic variability on these parameters. It therefore gives the possibility to predict genotypic effects in new environments for which the model was not directly developed, and overall in a virtual network which would never be available with conventional field trials.

Simulation showed the large variability of trait values maximising yields depending on year, site, and watering scenario. In particular, traits related to a rapid growth (both high maximum elongation rate and low sensitivity to water deficit) had a positive effect on yield in non-water limiting environments whereas they both affect yield negatively in drought related environments. Those mechanisms appearing as emergent properties of the model (Wang et al., 2002) are well-known avoidance mechanisms, limiting transpiration early in the season and allowing higher water availability during the critical phases of grain filling (Schoppach and Sadok, 2012). A non-expected result was that this strategy was positive in the three tested drought pattern tested here. The corollary effect was that limiting growth in optimal conditions through a low potential growth and a high sensitivity to water deficit limits intercepted light and biomass accumulation, leading to lower yields. By contrast, responses of leaf growth to intercepted light showed less genotype x environment interaction. Knowing that the stress indices in the crop model APSIM are based on a ratio between supply (uptake of the roots from the soil) and demand (transpiration from conversion of intercepted light into biomass) for water, the limiting factor in the studied set of environments was always water availability in the soil compared to incident radiation.

Overall, these G x E interactions as emergent properties of the simulations confirmed that a favourable trait in one environment can have deleterious effects in another. It highlights the importance of future crop model improvements to be focused on the integration of measurable genotypic parameters (Hoogenboom et al., 2004), and show that traits related to leaf growth mechanisms can affect final grain yield in optimal and drought conditions and have a relevant place in crop improvement programs.

Simulating the effect of available phenotypic space rather than sensitivity analysis on crop parameter to test future genetic gain.

Ideotyping with crop models is probably one of the paths to study potential crop improvements to maintain crop yields in a changing environment (Hammer et al., 2002; Casadebaig et al., 2011; Tardieu and Hammer, 2012). Recent studies pointed out that in some cases, the optimisation of target traits could even increase yield in the future for several crops including maize (Rötter et al., 2015), with relative yield gain as much as 7%. In this study, we show how new ideotypes of leaf expansion could lead to yield gains in both optimal and stressed conditions, from 3 to 5%. Moreover,

as climate change does not change the patterns of stress but rather the frequencies of occurrence of each stress in a specific site (Harrison et al., 2014), the study can be translated to future climatic conditions under climate change.

However, an approach based on the existing genetic variability of parameter values presents marked differences with that in an unconstrained phenotypic space. Indeed, in the process of ideotyping, studying more than one trait imposes that these traits have to be taken into account together in the model (Denison, 2015; Sadras and Denison, 2016). We show in this study that two different approaches with a constrained (observed) and non-constrained phenotypic space could give different results due to the correlations between parameters or traits. Correlations between traits that limit the phenotypic space were handled with two different strategies in the model.

– Strong correlations between measured traits were directly taken into account by the model and therefore cannot be considered independently in sensitivity analyses. For example, the sensitivity of leaf expansion to evaporative demand is common for several leaves and a unique parameter summarises behaviours for all leaves (Lacube et al., 2017). In the same way, the sensitivity of leaf growth to soil water deficit and evaporative demand are closely related in several crops such as rice and maize (REF) and as such, they were link together in the model leading to a unique parameter.

-Other correlations were analysed here but parameters could still be considered individually. For example, the correlation between maximum leaf elongation rate and sensitivity to water deficit for crops has been previously observed in various mapping populations of maize (Welcker et al., 2011) and was also observed here in the panel of maize hybrids. Without being directly inserted into formalisms, this correlation was taken into account by considering observed sets of parameters in a large panel maximising the genetic diversity of maize hybrids.

By considering both types of correlation, we assume that parameters are not independent and are either constrained by evolution and/ or physiological processes. Particularly, we showed that no set of measured traits (in the studied panel) could meet the requirements of a high potential leaf growth while having a low sensitivity of growth to water stress and a high response to intercepted radiation. If the aim was to analyse the model by itself (sensitivity analysis) or test hypothetical gain in a virtual genetic diversity, the first approach would have been sufficient, but with the aim of offering keys to breeders for future crop improvement, it was important to test whether ideotypes exist within the known genetic variability. From a practical point of view, building of elite material from virtual ideotypes requires that the corresponding genetic variability exists and is exploitable for breeding. It is possible that the 'missing ideotypes' exist within a larger genetic variability (e.g. flint or tropical lines), but this remains to be demonstrated. Actually, the correlation between maximum leaf elongation rate and sensitivity to water deficit was also observed in flint and tropical genetic material (Welcker et al 2011).

References

Asseng S, Ewert F, Martre P, Rötter RP, Lobell DB, Cammarano D, Kimball BA, Ottman MJ, Wall GW, White JW, Reynolds MP, Alderman PD, Prasad PVV, Aggarwal PK, Anothai J, Basso B, Biernath C, Challinor AJ, De Sanctis G, Doltra J, Fereres E, Garcia-Vila M, Gayler S, Hoogenboom G, Hunt LA, Izaurralde RC, Jabloun M, Jones CD, Kersebaum KC, Koehler AK, Müller C, Naresh Kumar S, Nendel C, O'Leary G, Olesen JE, Palosuo T, Priesack E, Eyshi Rezaei E, Ruane AC, Semenov MA, Shcherbak I, Stöckle C, Stratonovitch P, Streck T, Supit I, Tao F, Thorburn PJ, Waha K, Wang E, Wallach D, Wolf J, Zhao Z, Zhu Y (2014) Rising temperatures reduce global wheat production. Nature Climate Change **5:** 143-147

Bindi M, Olesen JE (2011) The responses of agriculture in Europe to climate change. Regional Environmental Change **11:** 151-158

Casadebaig P, Debaeke P, Lecoeur J (2008) Thresholds for leaf expansion and transpiration response to soil water deficit in a range of sunflower genotypes. European Journal of Agronomy **28:** 646-654

Casadebaig P, Guilioni L, Lecoeur J, Christophe A, Champolivier L, Debaeke P (2011) SUNFLO, a model to simulate genotype-specific performance of the sunflower crop in contrasting environments. Agricultural and Forest Meteorology **151:** 163-178

Challinor AJ, Watson J, Lobell DB, Howden SM, Smith DR, Chhetri N (2014) A meta-analysis of crop yield under climate change and adaptation. Nature Clim. Change **4:** 287-291

Chapman SC, Chakraborty S, Dreccer MF, Howden SM (2012) Plant adaptation to climate change—opportunities and priorities in breeding. Crop and Pasture Science **63:** 251-268

Chenu K, Porter JR, Martre P, Basso B, Chapman SC, Ewert F, Bindi M, Asseng S (2017) Contribution of Crop Models to Adaptation in Wheat. Trends in Plant Science **22:** 472-490

Denison RF (2015) Evolutionary tradeoffs as opportunities to improve yield potential. Field Crops Research **182:** 3-8

Gouache D, Bogard M, Pegard M, Thepot S, Garcia C, Hourcade D, Paux E, Oury F-X, Rousset M, Deswarte J-C, Le Bris X (2017) Bridging the gap between ideotype and genotype: Challenges and prospects for modelling as exemplified by the case of adapting wheat (Triticum aestivum L.) phenology to climate change in France. Field Crops Research **202:** 108-121

Hammer GL, Kropff MJ, Sinclair TR, Porter JR (2002) Future contributions of crop modelling—from heuristics and supporting decision making to understanding genetic regulation and aiding crop improvement. European Journal of Agronomy **18:** 15-31

Hammer GL, van Oosterom E, McLean G, Chapman SC, Broad I, Harland P, Muchow RC (2010) Adapting APSIM to model the physiology and genetics of complex adaptive traits in field crops. Journal of Experimental Botany **61:** 2185-2202

Harrison MT, Tardieu F, Dong Z, Messina CD, Hammer GL (2014) Characterizing drought stress and trait influence on maize yield under current and future conditions. Glob Chang Biol **20:** 867-878

Hoogenboom G, White JW, Messina CD (2004) From genome to crop: integration through simulation modeling. Field Crops Research **90:** 145-163

Jeuffroy M-H, Casadebaig P, Debaeke P, Loyce C, Meynard J-M (2014) Agronomic model uses to predict cultivar performance in various environments and cropping systems. A review. Agronomy for Sustainable Development **34:** 121-137

Lacube S, Fournier C, Palaffre C, Millet EJ, Tardieu F, Parent B (2017) Distinct controls of leaf widening and elongation by light and evaporative demand in maize. Plant, Cell & Environment**:** n/a-n/a

Marcaida M, Li T, Angeles O, Evangelista GK, Fontanilla MA, Xu J, Gao Y, Li Z, Ali J (2014) Biomass accumulation and partitioning of newly developed Green Super Rice (GSR) cultivars under drought stress during the reproductive stage. Field Crops Research **162:** 30-38

Martre P, Quilot-Turion B, Luquet D, Memmah M-MO-S, Chenu K, Debaeke P (2015) Chapter 14 - Model-assisted phenotyping and ideotype design A2 - Sadras, Victor O. *In* DF Calderini, ed, Crop Physiology (Second Edition). Academic Press, San Diego, pp 349-373

Parent B, Tardieu F (2014) Can current crop models be used in the phenotyping era for predicting the genetic variability of yield of plants subjected to drought or high temperature? J Exp Bot **65:** 6179-6189

Perego A, Sanna M, Giussani A, Chiodini ME, Fumagalli M, Pilu SR, Bindi M, Moriondo M, Acutis M (2014) Designing a high-yielding maize ideotype for a changing climate in Lombardy plain (northern Italy). Sci Total Environ **499:** 497-509

Reynolds MP, Quilligan E, Aggarwal PK, Bansal KC, Cavalieri AJ, Chapman SC, Chapotin SM, Datta SK, Duveiller E, Gill KS, Jagadish KSV, Joshi AK, Koehler A-K, Kosina P, Krishnan S, Lafitte R, Mahala RS, Muthurajan R, Paterson AH, Prasanna BM, Rakshit S, Rosegrant MW, Sharma I, Singh RP, Sivasankar S, Vadez V, Valluru R, Vara Prasad PV, Yadav OP (2016) An integrated approach to maintaining cereal productivity under climate change. Global Food Security **8:** 9-18

Rötter RP, Tao F, Höhn JG, Palosuo T (2015) Use of crop simulation modelling to aid ideotype design of future cereal cultivars. Journal of Experimental Botany **66:** 3463-3476

Sadras VO, Denison RF (2016) Neither crop genetics nor crop management can be optimised. Field Crops Research **189:** 75-83

Schoppach R, Sadok W (2012) Differential sensitivities of transpiration to evaporative demand and soil water deficit among wheat elite cultivars indicate different strategies for drought tolerance. Environmental and Experimental Botany **84:** 1-10

Tao F, Rötter RP, Palosuo T, Díaz-Ambrona CGH, Mínguez MI, Semenov MA, Kersebaum KC, Nendel C, Cammarano D, Hoffmann H, Ewert F, Dambreville A, Martre P, Rodríguez L, Ruiz-Ramos M, Gaiser T, Höhn JG, Salo T, Ferrise R, Bindi M, Schulman AH (2017) Designing future barley ideotypes using a crop model ensemble. European Journal of Agronomy **82:** 144-162

Tardieu F (2012) Any trait or trait-related allele can confer drought tolerance: just design the right drought scenario. Journal of Experimental Botany **63:** 25-31

Tardieu F, Cabrera-Bosquet L, Pridmore T, Bennett M (2017) Plant Phenomics, From Sensors to Knowledge. Current Biology **27:** R770-R783

Tardieu F, Hammer G (2012) Designing crops for new challenges. European Journal of Agronomy **42:** 1-2

Townsend TJ, Roy J, Wilson P, Tucker GA, Sparkes DL (2017) Food and bioenergy: Exploring ideotype traits of a dual-purpose wheat cultivar. Field Crops Research **201:** 210-221

Wang E, Robertson MJ, Hammer GL, Carberry PS, Holzworth D, Meinke H, Chapman SC, Hargreaves JNG, Huth NI, McLean G (2002) Development of a generic crop model template in the cropping system model APSIM. European Journal of Agronomy **18:** 121-140

Welcker C, Sadok W, Dignat G, Renault M, Salvi S, Charcosset A, Tardieu F (2011) A Common Genetic Determinism for Sensitivities to Soil Water Deficit and Evaporative Demand: Meta-Analysis of Quantitative Trait Loci and Introgression Lines of Maize. Plant Physiology **157:** 718-729

Wright IJ, Reich PB, Cornelissen JH, Falster DS, Groom PK, Hikosaka K, Lee W, Lusk CH, Niinemets Ü, Oleksyn J (2005) Modulation of leaf economic traits and trait relationships by climate. Global Ecology and Biogeography **14:** 411-421

Yin X, Stam P, Kropff MJ, Schapendonk AHCM (2003) Crop Modeling, QTL Mapping, and Their Complementary Role in Plant Breeding Joint contrib. from Plant Res. Int. and the C.T. de Wit Graduate School for Prod. Ecol. and Resour. Conserv. Agronomy Journal **95:** 90-98

Conclusion and perspectives

The aims of this thesis were firstly to develop new formalisms for the simulation of maize leaf growth and sensitivity to environmental conditions, which integrate genetic variability of hundreds of genotypes, secondly to simulate the impact on yield of the genetic variability of resulting parameters in various environmental scenarios over Europe. An originality of this work was to undergo all steps, from the dissection of physiological responses to the environment, the choice of new formalisms to consider these new results, the parameterisation of a diversity panel, the development of a framework of simulation and the analysis of the impact of such diversity for different irrigation scenarios over Europe.

A new ecophysiological model for leaf elongation and widening in maize

The analysis of several datasets of leaf dimensions showed that leaf elongation only was not sufficient to explain the variability of leaf area observed in various environments, while only few studies focused on leaf width compared to leaf elongation (Lacube et al., 2017). The study has highlighted the dynamic effect of intercepted light on leaf widening, in contrast with the major effect of evaporative demand on leaf elongation. It has resulted in new formalisms integrating genetic the genetic variability of parameters to simulate individual leaf dimensions and leaf area. Both intercepted light and evaporative demand, related to carbon-driven and hydraulic-driven controls of leaf expansion, respectively, were considered independently to simulate leaf area in a set of environmental conditions. Leaf area influences plant intercepted radiation, biomass accumulation and future yield and improving the quality of leaf area simulation is an important step towards a better simulation of more integrated traits (Martre et al., 2015). Overall, the formalisms proposed in this thesis have improved the prediction of leaf area, but also allowed better analysis of the genetic variability of yields in various environmental conditions over Europe. In addition to improving our understanding of leaf growth and development, these new formalisms have the potential of better capturing and explaining the genotype by environment interaction of yield by inserting the new module in the APSIM model (Hammer et al., 2010).

A parsimonious leaf growth model adapted to simulate genotypic variability

The module of leaf development and expansion developed in this thesis presents improvement compared to the previous one developed by Chenu et al., 2008, 2009. First, parameters were tested on several dataset and different genotypes so we could state if they should be considered either as fixed at whole-species level or genotype-dependent. Fixed parameters were then optimised or measured for a reference genotype, whereas genotype-dependent parameters were measured for hundreds of genotypes. Here, 'measured' means that parameters were derived from measurable traits in platform or field experiments. Overall, this model is reasonably parsimonious:

- The model establishing leaf development stages uses three measurements to be fully parameterised: (i) the maximum number of leaves of the considered genotype, which can be measured after flowering time, (ii) the leaf appearance rate, which can be calculated from the time course of the number of appeared leaves during the vegetative stage and (iii) the ligulation rate, which can be calculated from the time course of the number of ligulated

leaves. The last two time courses are usually recorded jointly on the same plants. To our knowledge, they cannot be recorded automatically with sufficient precision by image analysis and 3-D plants reconstruction, so they require direct observations.

- The model of leaf elongation and widening needs three parameters : (i) the maximum elongation rate of a given leaf, which can be assessed with manual measurements at beginning and end of the night in well-watered conditions, with a platform involving displacement transducers or (after calibration) with a platform measuring whole-plant leaf area by image analysis (ii) the sensitivity of leaf growth to water deficit and evaporative demand which can be measured in the same two categories of platforms under fluctuating conditions of evaporative demand or soil water deficit, and (iii) the response of leaf width to intercepted light, by growing plants under contrasting light levels (either field or controlled environment).

The resulting model of leaf growth and development has been successfully implemented and tested (Chapter 2) as a module of the crop model APSIM (note that this adapted APSIM model is not implemented in the current released APSIM version). While it has been extensively used here within APSIM, it has been thought and developed as an independent module that can be used in different. contexts. For example, it can be implemented in the modelling platform 'BioMa'[8], a software framework that has been designed and developed to parameterise and run modelling solutions in different models. It can therefor work as an independent module which shares input and outputs variables with other components/modules, and that can be switched with other canopy growth simulation models to compare results. If used in this framework of simulation, the possible applications of the module developed can become wider.

Processes involved in leaf growth and development have been shown to have similarities between various monocotyledons such as sorghum (Bernstein et al., 1993) or rice (Parent et al., 2010) , even if parameter values such as the duration of steady and non-steady elongation phases largely differs between species (Parent et al., 2009). Several adaptations of the module are needed, but this module might be used for other monocotyledon species.

In parallel with this thesis, studies have been published on maize grain abortion under water deficit (Oury et al., 2015; Oury et al., 2016). Abortion rates along the ear are linked to the effect of water deficit on silk elongation, which is closely related to its effect on leaf elongation both environmentally and genetically (Turc et al., 2016). A genotype with a high sensitivity of leaf growth to water deficit is therefore more sensitive to abortion in case of water deficit around flowering. A module of grain number via the simulation of silk growth, and individual kernel fertilisation was developed by the Australian team of APSIM in Toowoomba (Greg Mc. Lean) and Pioneer (Carlos Messina), in collaboration with LEPSE. The module is still in the process of being tested but I have implemented the formalisms in a working version of APSIM. Considering the genetical and biological parallelism between silk and leaf growth, parameters representing sensitivities to water status were linked together in the model. This module could therefore be used together with the leaf model for further analysis of ideotypes in contrasted environments.

---

[8] http://bioma.jrc.ec.europa.eu/

A link between phenotyping platform and crop modelling

A strong effort in this thesis was to adapt formalisms in order to consider parameters which are measurable for hundreds of genotypes. Indeed, recent development of high-throughput phenotyping gives the possibility of measuring traits at plant scale, for hundreds of genotypes in one experiment. A large part of this thesis was therefore dedicated to the coupling of phenotyping experiments and analyses with the estimation of parameters linked to leaf growth and development. Firstly, the sensitivity of leaf growth to soil water deficit and evaporative demand was estimated both from whole plant leaf area and individual leaf sizes in several platform experiments. This work was done in close collaboration with Santiago Alvarez Prado (LEPSE). Results showed that both measurements could be linked together, and that sensitivity could be estimated form hundreds of genotype with measurements of leaf area from image analyses in the high throughput phenotyping platform *PhenoArch* (INRA-LEPSE, Montpellier, France). Secondly, the responses of leaf widening to intercepted light were calculated from the relationships between measured end of season width in platform and field conditions. In the near future, this response will be calculated in a more automatic way, in phenotyping platforms, by the development of image analysis pipelines which would allow the dynamic measurement of leaf width in response to environmental conditions. This work has started at LEPSE and should be available within the next two years. Plants are currently imaged every day, reconstructed in three dimensions and segmented to measure traits at organ level. These developments could potentially allow estimation of leaf width and its response to environmental conditions.

The panel of genotypes used in this thesis was used in 3 platform experiments from which several parameters of the model, not belonging to the module presented here, will be available:

- Most crop model such as APSIM do not consider photosynthesis but use the concept of Radiation Use Efficiency, which summarises the capacity of a genotype to convert intercepted radiation into biomass. This parameter is now measured automatically in the platform (Cabrera Bosquet et al 2016) via estimations of intercepted light and biomass accumulation.
- Transpiration Efficiency (TE), which is used to either calculate the potential biomass production from the potential supply of water, or, in case of limiting light, calculate the plant transpiration from the biomass produced with light interception. Estimations of plant transpiration are currently being processed and analysed from platform experiments, as well as its response to evaporative demand. This should result in an automatic pipeline of analyses which would allow the direct calculation of TE and relative sensitivities to environmental conditions for hundreds of genotypes.

This work shows that phenotyping and modelling can be linked in order to simulate large number of genotypes or consider large sets of parameter values within the observed genetic diversity. For example, leaf expansion parameters measured in phenotyping platforms are needed in models in order to simulate leaf area and light interception. In turn, light interception is needed in phenotyping analysis pipelines to calculate parameters of radiation use efficiency or the response of leaf widening to intercepted radiation. In fact, both areas have rapidly progressed in the last ten years, phenotyping platforms through the evolution of robotics, cameras and image analysis technologies, and crop modelling through the increasing power for simulations and development of modelling frameworks. With these continuous improvements, we expect an increasing inter-relationship between new phenotyping and modelling developments.

A potential pathway linking genetic analysis and crop model simulation

Several authors highlighted the importance of using crop models to follow the path from gene-to-phenotype (Chenu et al., 2017). Such a model, integrating genotype-dependent parameters could be combined with genetic analyses. Parameters representing traits could be calculated through the effects of alleles at quantitative traits loci (QTLs analysis). Such exercises have been already tried, but most often on simpler traits such as the prediction of heading date (Bogard et al.,2014). Only few studies tested this approach on more integrated traits such as yield, as the work of Chenu et al. (2008) on the impact of the sensitivity of leaf growth to water deficit in Australian environments. The model developed in my thesis integrates the genetic variability of a larger number of parameters/traits measurable in phenotyping platforms.

This new APSIM version integrates genetic parameters/traits that are in most cases more heritable than integrated variables such as leaf area or yield, and the model takes into account the G x E interactions. A potential avenue is now to use genomic prediction to calculate the vector of parameters defining a genotype in the model, with an approach allowing dissection of the various processes that lead to yield. This is the project of Santiago Alvarez-Prado in LEPSE, so the crop models that I have developed will be used from now on for simulations of yield by using genomic prediction of parameters.

References:

Bernstein N, Silk WK, Läuchli A (1993) Growth and development of sorghum leaves under conditions of NaCl stress. Planta **191:** 433-439

Chenu K, Chapman SC, Hammer GL, McLean G, Salah HB, Tardieu F (2008) Short-term responses of leaf growth rate to water deficit scale up to whole-plant and crop levels: an integrated modelling approach in maize. Plant Cell Environ **31:** 378-391

Chenu K, Porter JR, Martre P, Basso B, Chapman SC, Ewert F, Bindi M, Asseng S (2017) Contribution of Crop Models to Adaptation in Wheat. Trends in Plant Science **22:** 472-490

Hammer GL, van Oosterom E, McLean G, Chapman SC, Broad I, Harland P, Muchow RC (2010) Adapting APSIM to model the physiology and genetics of complex adaptive traits in field crops. Journal of Experimental Botany **61:** 2185-2202

Lacube S, Fournier C, Palaffre C, Millet EJ, Tardieu F, Parent B (2017) Distinct controls of leaf widening and elongation by light and evaporative demand in maize. Plant, Cell & Environment**:** n/a-n/a

Martre P, Wallach D, Asseng S, Ewert F, Jones JW, Rotter RP, Boote KJ, Ruane AC, Thorburn PJ, Cammarano D, Hatfield JL, Rosenzweig C, Aggarwal PK, Angulo C, Basso B, Bertuzzi P, Biernath C, Brisson N, Challinor AJ, Doltra J, Gayler S, Goldberg R, Grant RF, Heng L, Hooker J, Hunt LA, Ingwersen J, Izaurralde RC, Kersebaum KC, Muller C, Kumar SN, Nendel C, O'Leary G, Olesen JE, Osborne TM, Palosuo T, Priesack E, Ripoche D, Semenov MA, Shcherbak I, Steduto P, Stockle CO, Stratonovitch P, Streck T, Supit I, Tao F, Travasso M, Waha K, White JW, Wolf J (2015) Multimodel ensembles of wheat growth: many models are better than one. Glob Chang Biol **21:** 911-925

Oury V, Caldeira CF, Prodhomme D, Pichon J-P, Gibon Y, Tardieu F, Turc O (2016) Is change in ovary carbon status a cause or a consequence of maize ovary abortion in water deficit during flowering? Plant Physiology

Oury V, Tardieu F, Turc O (2015) Ovary apical abortion under water deficit is caused by changes in sequential development of ovaries and in silk growth rate in maize. Plant Physiology

Parent B, Conejero G, Tardieu F (2009) Spatial and temporal analysis of non-steady elongation of rice leaves. Plant Cell Environ **32:** 1561-1572

Parent B, Suard B, Serraj R, Tardieu F (2010) Rice leaf growth and water potential are resilient to evaporative demand and soil water deficit once the effects of root system are neutralized. Plant Cell Environ **33:** 1256-1267

Turc O, Bouteillé M, Fuad-Hassan A, Welcker C, Tardieu F (2016) The growth of vegetative and reproductive structures (leaves and silks) respond similarly to hydraulic cues in maize. New Phytologist **212:** 377-388

Acknowledgments